ONTARIO GEOLOGICAL SURVEY

Geophysical Data Set 1079

Ontario Airborne Geophysical Surveys
Magnetic and Electromagnetic Data
Kabinakagami Lake Area

by

Ontario Geological Survey

2015

Ontario Geological Survey
Ministry of Northern Development and Mines
Willet Green Miller Centre, 933 Ramsey Lake Road,
Sudbury, Ontario P3E 6B5 Canada

Contents

FIGURES

TABLES

CREDITS

List of accountabilities and responsibilities:

- Jack Parker, Senior Manager, Earth Resources and Geoscience Mapping Section, Ontario Geological Survey (OGS), Ministry of Northern Development, Mines (MNDM) – accountable for the airborne geophysical survey projects, including contract management
- Edna Mueller-Markham, Senior Consulting Geophysicist, Paterson, Grant and Watson Limited (PGW), Toronto, Ontario, Geophysicist under contract to MNDM, responsible for the airborne geophysical survey project management, quality assurance (QA) and quality control (QC)
- Tom Watkins, Manager, Publication Services Unit, GeoServices Section, Ontario Geological Survey, MNDM – managed the project-related hard-copy products
- Desmond Rainsford, Geophysicist, Earth Resources and Geoscience Mapping Section, Ontario Geological Survey – responsible for final quality assurance (QA), quality control (QC) of published digital products
- Geotech Limited, Aurora, Ontario – data acquisition and data compilation.

DISCLAIMER

To enable the rapid dissemination of information, this digital data has not received a technical edit. However, every possible effort has been made to ensure the accuracy of the information presented in this report and the accompanying data; however, the Ontario Ministry of Northern Development and Mines does not assume liability for errors that may occur. Users should verify critical information.

CITATION

Parts of this publication may be quoted if credit is given. It is recommended that reference to this publication be made in the following form:

Ontario Geological Survey 2015. Ontario airborne geophysical surveys, magnetic and electromagnetic data, grid and profile data (ASCII format) and vector data, Kabinakagami Lake area; Ontario Geological Survey, Geophysical Data Set 1079a.

Ontario Geological Survey 2015. Ontario airborne geophysical surveys, magnetic and electromagnetic data, grid and profile data (Geosoft® format) and vector data, Kabinakagami Lake area; Ontario Geological Survey, Geophysical Data Set 1079b.

NOTE

Users of OGS products are encouraged to contact those Aboriginal communities whose traditional territories may be located in the mineral exploration area to discuss their project.

1. INTRODUCTION

This report describes a helicopter-borne combined aeromagnetic and electromagnetic survey carried out by Geotech Limited for the Ministry of Northern Development and Mines (MNDM) performed as part of the Ontario Geological Survey (OGS) geoscience program in the Kabinakagami Lake area in northwestern Ontario.

The airborne survey contracts were awarded through a Request for Proposal and Contractor Selection process. The system and contractor selected for each survey area were judged on many criteria, including the following:

- applicability of the proposed system to the local geology and potential deposit types
- aircraft capabilities and safety plan
- experience with similar surveys
- QA/QC plan
- capacity to acquire the data and prepare final products in the allotted time
- price-performance.

2. SURVEY LOCATION AND SPECIFICATIONS

2.1. SURVEY LOCATION

Geotech Ltd. conducted a helicopter-borne geophysical survey over the Kabinakagami Lake area in northern Ontario (Figure 1 and Figure 2).

The geophysical surveys consisted of a combined helicopter-borne electromagnetic (EM) survey using the versatile time-domain electromagnetic (VTEM®Plus) system with Z-component measurements and an aeromagnetic survey using a cesium magnetometer. A total of 15 970 line-kilometres of geophysical data were acquired during the survey.

The crew was based out of Tatnall, Brunswick Lake camp and Hearst (*see* Figure 2) for the acquisition phase of the survey. The survey was flown between July 18 and October 22, 2014.

The survey area is located at Kabinakagami Lake approximately 148 km west of Timmins, Ontario. The outline of the survey area and the flight path layout is shown in Figure 2 below.

Figure 1. Location map of the Kabinakagami Lake area geophysical survey.

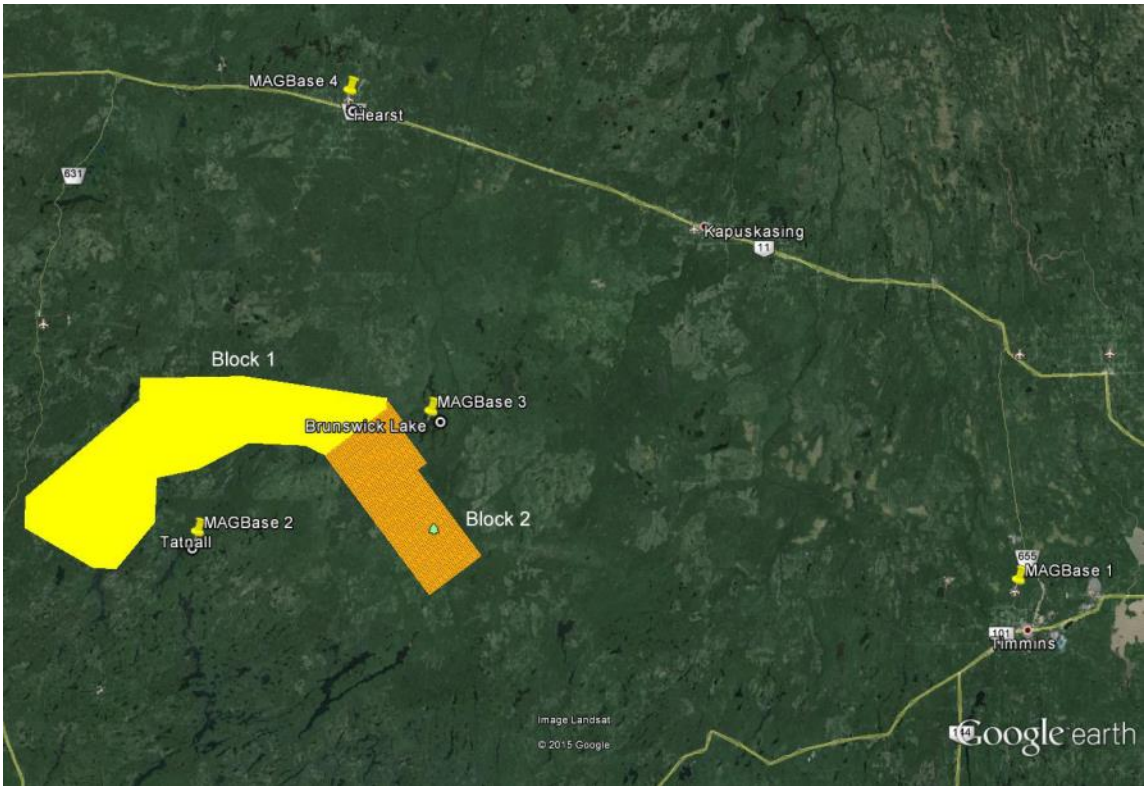

Figure 2. Flight path and magnetic base station (MAGBase) locations displayed on Google Earth™ image.

2.2. TOPOGRAPHIC RELIEF AND CULTURAL FEATURES

Topographically, the block exhibits a shallow relief with an elevation ranging from 265 to 506 m above mean sea level over an area of 2 799 km^2 (Figure 3).

The survey block has various rivers and streams running through the survey area which connect various lakes and wetlands. The most notable lake is Kabinakagami Lake located in the middle of Block 1. There are visible signs of culture, such as roads, railways and towns, located in the survey area.

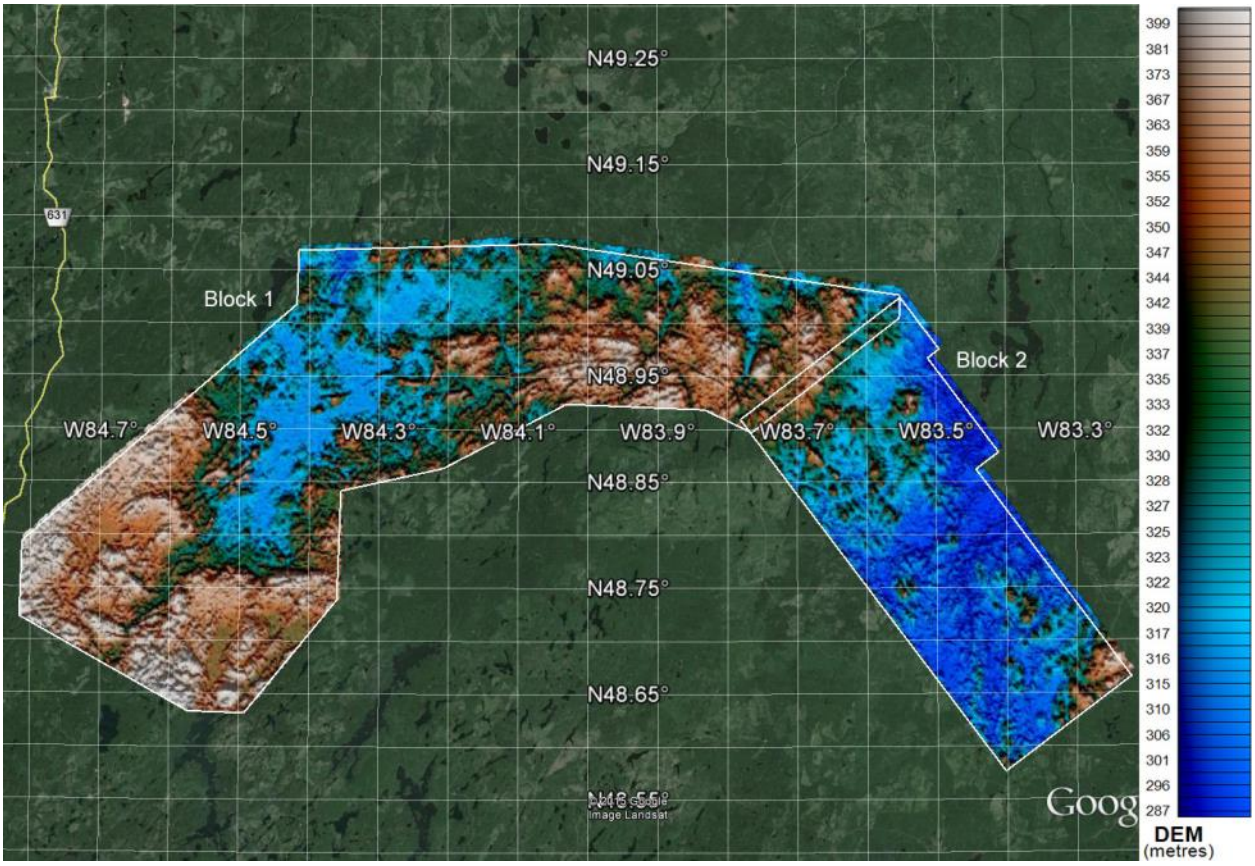

Figure 3. Digital Elevation Model (DEM) over Google Earth™ Image.

2.3. SURVEY AND SYSTEM SPECIFICATIONS

Data quality control and quality assurance, and preliminary data processing were carried out on a daily basis during the acquisition phase of the project. Final data processing followed immediately after completion of the survey. Final reporting, data presentation and archiving were completed at Geotech's Aurora office in November 2014.

Block 1 was flown in a south to north (N 0° E azimuth) direction, with traverse line spacing of 200 metres as depicted in Figure 2. Tie lines were flown perpendicular to the traverse lines (N 90° E azimuth) at a spacing of 1500 metres. Block 2 was flown in a southwest to northeast (N 55° E azimuth) direction, with traverse line spacing of 200 metres as depicted in Figure 3. Tie lines were flown perpendicular to the traverse lines (N 145° E azimuth) at a spacing of 1500 metres respectively. For more detailed information on the flight spacing and direction see Table 1.

2.4. DATA ACQUISITION

2.4.1. FLIGHT LINE SPECIFICATIONS

The survey block (*see* Figure 2) and general flight specifications are as follows.

Table 1. Flight line specifications

Survey block	Traverse Line spacing (m)	Area (Km^2)	Planned[1] Line-km	Actual Line-km	Flight direction	Line numbers
Block 1	Traverse: 200	1956	9682.7	9900	N 0° E / N 180° E	L1000 – L5570
	Tie: 1500		1494.3	1516	N 90° E / N 270° E	T6000 – T6430
Block 2	Traverse: 200	843	4192	4300	N 55° E / N235° E	L7000-L9310
	Tie: 1500		601	607	N 145° E / N 325° E	T10000-T10140
TOTAL		2799	15970	16323		

Survey block boundary co-ordinates are provided in Appendix H.

2.4.2. SURVEY OPERATIONS

Survey operations were based out of Tatnall Camp, Ontario from July 18 to September 4th, 2014 and Brunswick Lake Camp from September 5th to October 22nd, 2014. The flight schedule for the survey is outlined in Table 2 below.

Table 2. Survey flight schedule

Date	Flight #	Flown km	Block	Crew location	Comments
18-Jul-2014				Ottawa, Ontario	Crew arrived in Ottawa
19-Jul-2014				Ottawa, Ontario	System assembly & heli install
20-Jul-2014				Ottawa, Ontario	Testing
21-Jul-2014				Ottawa, Ontario	Approval of calibration test
22-Jul-2014				Ottawa, Ontario	Mobilized to Timmins
23-Jul-2014				Timmins, Ontario	System assembly & local logistics
24-Jul-2014				Timmins, Ontario	Testing
25-Jul-2014				Timmins, Ontario	Testing
26-Jul-2014				Timmins, Ontario	Testing
27-Jul-2014				Timmins, Ontario	Test flight and system adjustments
28-Jul-2014				Timmins, Ontario	Test flight and system adjustments
29-Jul-2014				Timmins, Ontario	Test flight and system adjustments
30-Jul-2014				Timmins, Ontario	Test flight and system adjustments
31-Jul-2014				Timmins, Ontario	Test flight and system adjustments
1-Aug-2014				Timmins, Ontario	Test flight and system adjustments
2-Aug-2014				Timmins, Ontario	Test flight and system adjustments
3-Aug-2014				Timmins, Ontario	Test flight and system adjustments
4-Aug-2014				Timmins, Ontario	Test flight and system adjustments
5-Aug-2014				Timmins, Ontario	Flew Reid-Mahaffey test

[1] Note: Actual Line kilometres represent the total line kilometres in the final database. These line-km normally exceed the planned line-km, as indicated in the survey NAV files.

Date	Flight #	Flown km	Block	Crew location	Comments
6-Aug-2014				Timmins, Ontario	Reid-Mahaffey test submitted
7-Aug-2014				Timmins, Ontario	Waiting for client approval
8-Aug-2014				Timmins, Ontario	Testing & Mobilized to Tatnall Camp
9-Aug-2014				Tatnall Camp, Ontario	Testing
10-Aug-2014	1	196	B1	Tatnall Camp, Ontario	196 km Flown
11-Aug-2014	2,3,4	425	B1	Tatnall Camp, Ontario	425 km flown
12-Aug-2014				Tatnall Camp, Ontario	No production due to weather
13-Aug-2014	5	25	B1	Tatnall Camp, Ontario	25 km flown limited due to weather
14-Aug-2014	6,7	445	B1	Tatnall Camp, Ontario	445 km flown
15-Aug-2014	8,9,10	536	B1	Tatnall Camp, Ontario	536 km flown
16-Aug-2014				Tatnall Camp, Ontario	No production due to weather
17-Aug-2014	11,12	433	B1	Tatnall Camp, Ontario	433 km flown
18-Aug-2014	13,14,15, 16	810	B1	Tatnall Camp, Ontario	810 km flown
19-Aug-2014				Tatnall Camp, Ontario	No production due to weather
20-Aug-2014				Tatnall Camp, Ontario	No production due to weather
21-Aug-2014				Tatnall Camp, Ontario	No production due to weather
22-Aug-2014	17,18	418	B1	Tatnall Camp, Ontario	418 km flown
23-Aug-2014	19,20,21	567	B1	Tatnall Camp, Ontario	567 km flown
24-Aug-2014	22,23,24	647	B1	Tatnall Camp, Ontario	647 km flown
25-Aug-2014				Tatnall Camp, Ontario	No production due to weather
26-Aug-2014	25,26,27	452	B1	Tatnall Camp, Ontario	452 km flown
27-Aug-2014	28,29	374	B1	Tatnall Camp, Ontario	374 km flown
28-Aug-2014	30,31,32	669	B1	Tatnall Camp, Ontario	669 km flown
29-Aug-2014	33,34,35	589	B1	Tatnall Camp, Ontario	589 km flown
30-Aug-2014				Tatnall Camp, Ontario	No production due to weather
31-Aug-2014	36,37,38	653	B1	Tatnall Camp, Ontario	653 km flown
1-Sep-2014				Tatnall Camp, Ontario	No production due to weather
2-Sep-2014	39,40,41	530	B1	Tatnall Camp, Ontario	530 km flown
3-Sep-2014	42,43	292	B1	Tatnall Camp, Ontario	292 km flown
4-Sep-2014				Tatnall Camp, Ontario	No production due to weather
5-Sep-2014				Brunswick Lake, Ontario	No production due to weather
6-Sep-2014	44,45	203	B1	Brunswick Lake, Ontario	203 km flown
7-Sep-2014	46,47,48	370	B1	Brunswick Lake, Ontario	370 km flown
8-Sep-2014	49,50,51, 52	190	B1	Brunswick Lake, Ontario	190 km flown
9-Sep-2014				Brunswick Lake, Ontario	No production due to weather
10-Sep-2014				Brunswick Lake, Ontario	No production due to weather
11-Sep-2014				Brunswick Lake, Ontario	No production due to weather
12-Sep-2014	53,54,55	490	B1	Brunswick Lake, Ontario	490 km flown
13-Sep-2014	56,57	195	B1	Brunswick Lake, Ontario	195 km flown
14-Sep-2014	58,59	166	B1	Brunswick Lake, Ontario	166 km flown
15-Sep-2014	60,61	247	B1	Brunswick Lake, Ontario	247 km flown
16-Sep-2014	62	22	B1	Brunswick Lake, Ontario	22 km flown – limited due to weather

Date	Flight #	Flown km	Block	Crew location	Comments
17-Sep-2014				Brunswick Lake, Ontario	No production due to weather
18-Sep-2014	63,64,65, 66	710	B1	Brunswick Lake, Ontario	710 km flown
19-Sep-2014				Brunswick Lake, Ontario	No production due to weather
20-Sep-2014				Brunswick Lake, Ontario	No production due to weather
21-Sep-2014				Brunswick Lake, Ontario	No production due to weather
22-Sep-2014	67,68,69	332	B1	Brunswick Lake, Ontario	332 km flown
23-Sep-2014	70,71	282	B1	Brunswick Lake, Ontario	282 km flown
24-Sep-2014	72,73	451	B2	Brunswick Lake, Ontario	451 km flown
25-Sep-2014	74,75	328	B2	Brunswick Lake, Ontario	328 km flown
26-Sep-2014	76,77	297	B2	Brunswick Lake, Ontario	297 km flown
27-Sep-2014	78,79	312	B2	Brunswick Lake, Ontario	312 km flown
28-Sep-2014	80	179	B2	Brunswick Lake, Ontario	179 km flown
29-Sep-2014				Brunswick Lake, Ontario	No production due to weather
30-Sep-2014	81,82,83,84	460	B2	Brunswick Lake, Ontario	460 km flown
1-Oct-2014	85,86,87	371	B2	Brunswick Lake, Ontario	371 km flown
2-Oct-2014				Brunswick Lake, Ontario	No production due to weather
3-Oct-2014				Brunswick Lake, Ontario	No production due to weather
4-Oct-2014	88	85	B2	Brunswick Lake, Ontario	85 km flown – limited due to weather
5-Oct-2014				Brunswick Lake, Ontario	No production due to weather
6-Oct-2014	89,90	84	B2	Brunswick Lake, Ontario	84 km flown – limited due to weather
7-Oct-2014	91	28	B2	Brunswick Lake, Ontario	28 km flown – limited due to weather
8-Oct-2014				Brunswick Lake, Ontario	No production due to weather
9-Oct-2014				Brunswick Lake, Ontario	No production due to weather
10-Oct-2014				Brunswick Lake, Ontario	No production due to weather
11-Oct-2014	92,93,94,95	515	B2	Brunswick Lake, Ontario	515 km flown
12-Oct-2014	96,97,98,99, 100	409	B2	Brunswick Lake, Ontario	409 km flown
13-Oct-2014	101	106	B2	Brunswick Lake, Ontario	106 km flown
14-Oct-2014				Brunswick Lake, Ontario	No production due to weather
15-Oct-2014	102,103,104, 105	390	B2	Brunswick Lake, Ontario	390 km flown
16-Oct-2014				Brunswick Lake, Ontario	No production due to the weather
17-Oct-2014				Brunswick Lake, Ontario	No production due to the weather
18-Oct-2014				Brunswick Lake, Ontario	No production due to the weather
19-Oct-2014	106,107,108	255	B2	Hearst, Ontario	255km flown
20-Oct-2014				Hearst, Ontario	No production due to the weather
21-Oct-2014	109	137	B2	Hearst, Ontario	137km flown
22-Oct-2014	110,111	294	B2	Hearst, Ontario	Remaining kms were flown – flying complete

3. SURVEY AREA GEOLOGY

The following description of the regional geology of the area is drawn partly from Wilson (1993). The area is largely underlain by the Archean Kabinakagami Lake greenstone belt which forms part of the Wawa Subprovince. The arcuate greenstone belt comprises primarily of mafic metavolcanic rocks to the west with intermediate to felsic metavolcanic rocks being dominant in the eastern part (Figure 4). Metasedimentary rocks outcrop along the southeastern shore of Kabinakagami Lake. The greenstone belt has undergone low to intermediate amphibolite grade metamorphism. The plutonic rocks surrounding the greenstone belt are typically biotite or biotite-hornblende granodiorite to trondhjemite along with gneissic tonalite. All units are cut by west-northwest- and northeast-trending diabase dikes.

A regional-scale deformation zone (Puskuta Lake shear zone) has been identified along the southwestern margin of the greenstone belt in the eastern part of the area. Two former producing gold mines (Shenango and Hiawatha) are located in the central and western parts of the greenstone belt. These small operations were only in production for a few years and closed around the time of the Second World War.

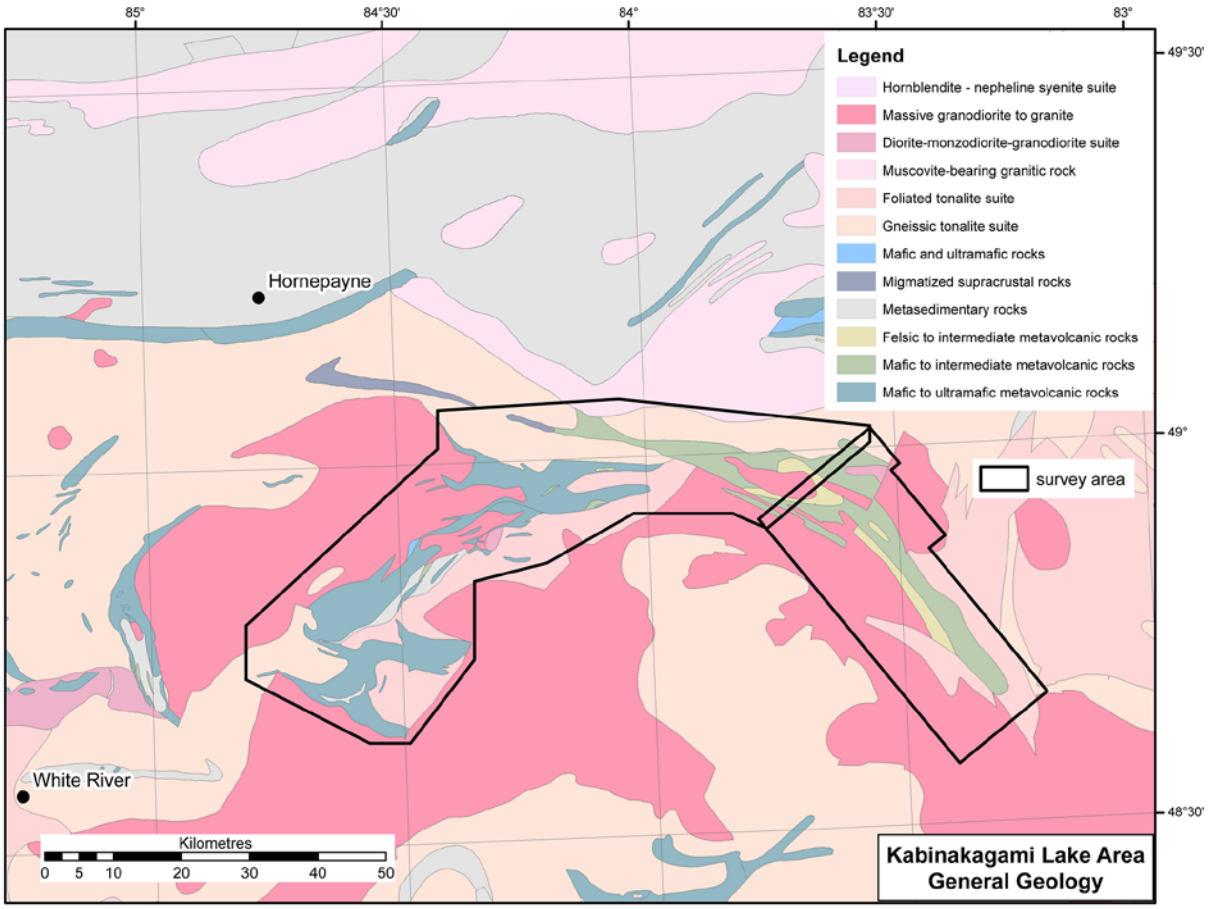

Figure 4. Kabinakagami Lake survey area, simplified bedrock geology with superimposed survey outline (*from* Ontario Geological Survey 2011).

4. AIRCRAFT, EQUIPMENT AND PERSONNEL

4.1. FLIGHT LOGISTICS

During the survey, the helicopter was maintained at a mean altitude of 92 m above the ground with an average survey speed of 80 km/hour. This allowed for an average EM bird terrain clearance of 46 m and a magnetic sensor clearance of 59 m.

The on-board operator was responsible for monitoring the system integrity. He also maintained a detailed flight log during the survey, tracking the times of the flight as well as any unusual geophysical or topographic features.

Upon return to base camp, the survey data were transferred from a compact flash card (PCMCIA) to the data processing computer. The data were then uploaded via ftp to the Geotech office in Aurora for daily quality assurance and quality control by qualified personnel.

4.2. AIRCRAFT AND EQUIPMENT

4.2.1. SURVEY AIRCRAFT

The survey was flown using a Eurocopter Aerospatiale (Astar) 350 B3 helicopter, registration C-GEOC. The helicopter is owned and operated by Geotech Aviation. Installation of the geophysical and ancillary equipment was carried out by Geotech Ltd crew.

4.2.2. ELECTROMAGNETIC SYSTEM

The electromagnetic system was a Geotech Time Domain EM (VTEM®Plus) with full receiver-waveform streamed data recording at 192 kHz. The full waveform VTEM system uses the streamed half-cycle recording of transmitter and receiver waveforms to obtain a complete system response calibration throughout the entire survey flight. VTEM with the Serial number 31 had been used for the survey. The configuration is as indicated in Figure 6.

The VTEM Receiver and transmitter coils were in concentric-coplanar and Z-direction oriented configuration. The receiver system for the project also included coincident-coaxial X-direction and Y-direction coils to measure the in-line and off-line dB/dt, respectively, and calculate B-Field responses. The EM bird was towed at a mean distance of 47 m below the aircraft as shown in Figure 6 and Figure 7. The VTEM transmitter current waveform is shown diagrammatically in Figure 5. The receiver decay recording scheme is shown in Table 3.

The VTEM decay sampling scheme is shown in Table 3 below. Forty-three time measurement gates were used for the final data processing in the range from 0.021 to 8.083 msec. Zero time for the off-time sampling scheme is equal to the current pulse width and is defined as the time near the end of the turn-off ramp where the dI/dt waveform falls to 1/2 of its peak value.

Table 3. Off-time decay sampling scheme

VTEM Decay Sampling Scheme				
index	**Start**	**End**	**Middle**	**Width**
Milliseconds				
4	0.018	0.023	0.021	0.005
5	0.023	0.029	0.026	0.005
6	0.029	0.034	0.031	0.005

VTEM Decay Sampling Scheme				
index	Start	End	Middle	Width
Milliseconds				
7	0.034	0.039	0.036	0.005
8	0.039	0.045	0.042	0.006
9	0.045	0.051	0.048	0.007
10	0.051	0.059	0.055	0.008
11	0.059	0.068	0.063	0.009
12	0.068	0.078	0.073	0.010
13	0.078	0.090	0.083	0.012
14	0.090	0.103	0.096	0.013
15	0.103	0.118	0.110	0.015
16	0.118	0.136	0.126	0.018
17	0.136	0.156	0.145	0.020
18	0.156	0.179	0.167	0.023
19	0.179	0.206	0.192	0.027
20	0.206	0.236	0.220	0.030
21	0.236	0.271	0.253	0.035
22	0.271	0.312	0.290	0.040
23	0.312	0.358	0.333	0.046
24	0.358	0.411	0.383	0.053
25	0.411	0.472	0.440	0.061
26	0.472	0.543	0.505	0.070
27	0.543	0.623	0.580	0.081
28	0.623	0.716	0.667	0.093
29	0.716	0.823	0.766	0.107
30	0.823	0.945	0.880	0.122
31	0.945	1.086	1.010	0.141
32	1.086	1.247	1.161	0.161
33	1.247	1.432	1.333	0.185
34	1.432	1.646	1.531	0.214
35	1.646	1.891	1.760	0.245
36	1.891	2.172	2.021	0.281
37	2.172	2.495	2.323	0.323
38	2.495	2.865	2.667	0.370
39	2.865	3.292	3.063	0.427
40	3.292	3.781	3.521	0.490
41	3.781	4.341	4.042	0.560
42	4.341	4.987	4.641	0.646
43	4.987	5.729	5.333	0.742
44	5.729	6.581	6.125	0.852
45	6.581	7.560	7.036	0.979
46	7.560	8.685	8.083	1.125

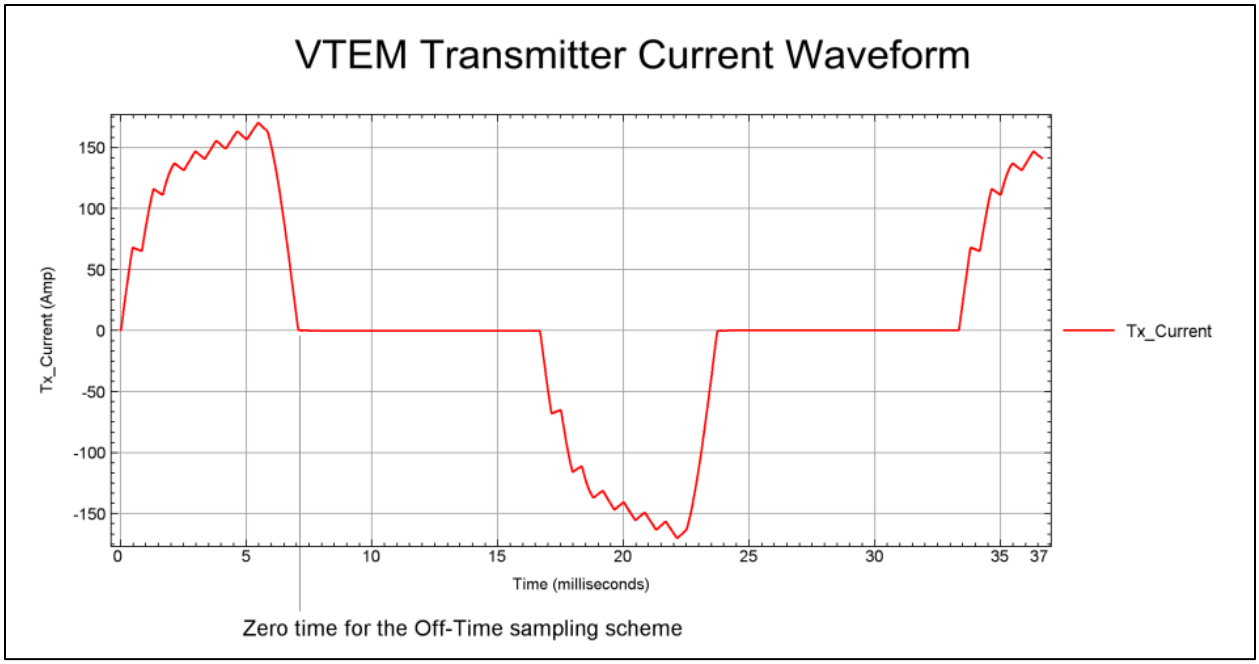

Figure 5. VTEM current waveform.

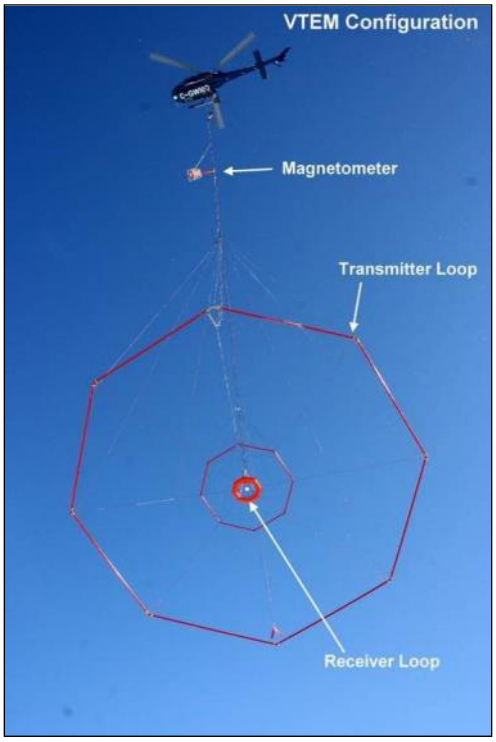

Figure 6. VTEM®Plus configuration, with magnetometer.

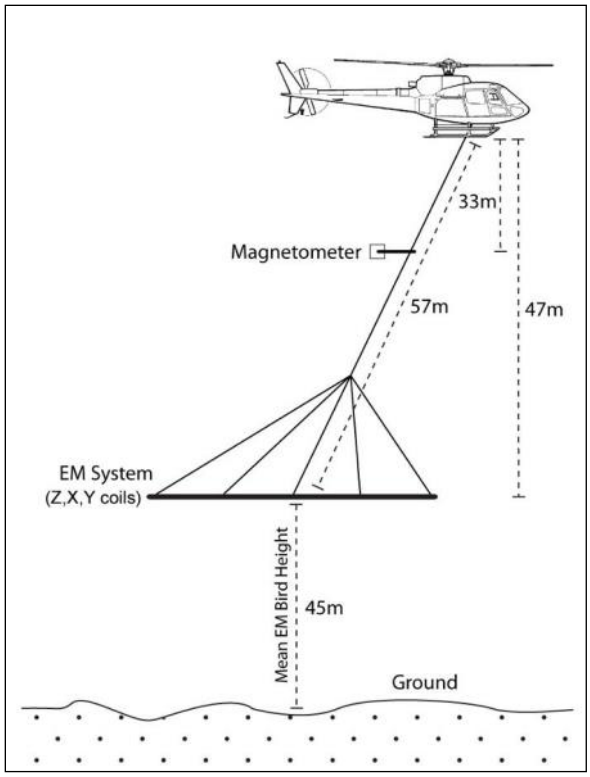

Figure 7. VTEM®Plus system configuration (not to scale).

4.2.3. VTEM®PLUS SYSTEM SPECIFICATION

Transmitter

- Transmitter loop diameter: 26 m
- Effective transmitter loop area: 2123.7 m^2
- Number of turns: 4
- Transmitter base frequency: 30 Hz
- Peak current: 183 A
- Pulse width: 7.078 ms
- Wave form shape: trapezoid
- Peak dipole moment: 388,640 nIA
- Average EM Bird terrain clearance: 46 m above the ground

Receiver

- X and Y Coil diameter: 0.32 m
- Number of turns: 245
- Effective coil area: 19.69 m^2
- Z-Coil diameter: 1.2 m
- Number of turns: 100
- Effective coil area: 113.04 m^2

4.2.4. AIRBORNE MAGNETOMETER

The magnetic sensor utilized for the survey was a Geometrics® Model G823A optically pumped cesium-vapour magnetic field sensor mounted 33 m below the helicopter, as shown in Figure 7. The sensitivity of the magnetic sensor is 0.02 nanoTesla (nT) at a sampling interval of 0.1 seconds.

4.2.5. RADAR ALTIMETER

A Terra TRA 3000/TRI 40 radar altimeter was used to record terrain clearance. The antenna was mounted beneath the bubble of the helicopter cockpit (Figure 7).

4.2.6. DIGITAL ACQUISITION SYSTEM

A Geotech data acquisition system recorded the digital survey data on an internal compact flash card. Data are displayed on an LCD screen as traces to allow the operator to monitor the integrity of the system. The data type and sampling interval as provided in Table 4.

Table 4. Acquisition sampling rates

Data Type	Sampling
TDEM	0.1 sec
Magnetometer	0.1 sec
GPS Position	0.1 sec
Radar Altimeter	0.2 sec

4.2.7. BASE STATION MAGNETOMETER

A dedicated computer connected to a high sensitivity Geometrics® G822B cesium magnetometer and integrated GPS unit, for the accurate time synchronization, was employed to record magnetic activity. The magnetometer had a sensitivity of better than 0.01 nT at a sampling interval of 0.1 s. Digital data from the base station magnetometer were recorded at all times during the survey. The digital data included the date, an absolute magnetic value, and GPS time with accurate synchronization to the aircraft data acquisition system.

The Tatnall base station magnetometer sensor was installed in the east side of camp (48°41.8232 N, 84°13.1407 W), Brunswick Lake (48°58.5334 N, 83°24.3848 W) and Hearst (49°42.6196 N, 83°41.5860 W) away from electric transmission lines and moving metal (iron) objects such as motor vehicles. The base station data were backed-up to the data processing computer at the end of each survey day.

4.2.8. GPS GROUND BASE STATION

A dedicated Novatel® ProPak™-V3 TR20 GPS receiver and ground-based GPS antenna was used with a 0.1 s raw GPS data recording interval. Post-flight differential GPS data processing, utilizing Novatel® GrafNav 8.3 software, was used to produce sub-meter accuracy of the airborne system location at 10 Hz sampling interval. The GPS ground base station was positioned at each survey base of operations and setup in the same vicinity as the base station magnetometer.

4.2.9. GPS NAVIGATION SYSTEM

The navigation system used a Geotech PC104 based navigation system utilizing NovAtel's WAAS (Wide Area Augmentation System) enabled GPS receiver, Geotech navigate software, a full screen display with controls in front of the pilot to direct the flight and a NovAtel GPS antenna mounted on the helicopter tail (Figure 6). As many as 11 GPS and 2 WAAS satellites may be monitored at any one time. The positional accuracy or circular error probability (CEP) is 1.8 m, with WAAS active, it is 1.0 m. The co-ordinates of the regional AEM survey were set-up prior to the survey and the information was fed into the airborne navigation system.

4.3. PERSONNEL

The following personnel were involved with the survey.

Field

Project Manager:	Darren Tuck (Office)
Data QC:	Neil Fiset (Office)
	Nick Venter (Office)
Crew chief:	Colin Lennox
	Gavin Boege
Operator:	Paul Taylor
Pilot:	Walter Zec
	Brad MacRae
	Bruno Prieur
Mechanical Engineer:	Tyler McLellan
	Chris Ward

The survey pilot and the mechanical engineer were employed directly by the helicopter operator – Geotech Aviation.

Office

Preliminary Data Processing:	Neil Fiset
	Nick Venter
Interim Data Processor:	Shaolin Lu
	Marta Orta
	Keeme Mokubung
Supervisor of Data QC:	Geoffrey Plastow
Reporting/Mapping:	Wendy Acorn

The data acquisition phase was carried out under the supervision of Andrei Bagrianski, *P. Geo.*, Chief Operating Officer. The processing and interpretation phase was under the supervision of Geoffrey Plastow, *P. Geo*. Customer relations were looked after by Mandy Long.

5. DATA PROCESSING

Data compilation and processing were carried out using Geosoft® OASIS montaj™ and programs proprietary to Geotech Ltd.

5.1. FLIGHT PATH

The flight path, recorded by the data acquisition program as WGS 84 latitude/longitude datum and co-ordinate system, was converted to NAD83, UTM Zone 16 and 17 North co-ordinate system in Oasis montaj™.

The flight path was drawn using linear interpolation between x, y positions from the navigation system. Positions are updated every second and expressed as UTM easting (x) and UTM northing (y).

5.2. ELECTROMAGNETIC DATA

As the data were acquired by the data acquisition system on the helicopter, they go through a digital filter to reject major sferic events and are stacked to further reduce system noise. Afterward, the streamed data are processed by applying a system response correction, B-field integration, time window binning, compensation, filtering, and leveling.

The Full Waveform EM specific data processing operations included:

- Half cycle stacking (performed at time of acquisition);
- System response correction;
- Parasitic and drift removal

The digital filtering process is a three stage filter used to reject major sferic events and reduce system noise. Local sferic activity can produce sharp, large amplitude events that cannot be removed by conventional filtering procedures. Smoothing or stacking will reduce their amplitude but leave a broader residual response that can be confused with geological phenomena. To avoid this possibility, a computer algorithm searches out and rejects the major sferic events. The data was then stacked using 15 half cycles, 0.3 seconds, to create a stacked half-cycle waveform at 0.1 second intervals. The stacking coefficients are tapered with a shape that approximates a Gaussian function.

During post-flight processing, the streamed data have a sensor response correction applied which corrects the receiver channels and current monitor to a common impulse response based on the Full Waveform Calibration. The B-field data are calculated by integrating the dB/dt cycles from the 192 kHz streamed data. The streamed data are then converted into a set of time window channels to reduce noise levels further.

The data have noise levels reduced further by the use of an EM compensation procedure which removes characteristic noise from each fiducial determined by the difference between the transmitter and bucking loop fields at the receiver during the flight. This is achieved by a statistical correlation between each time window channel and primary field measurement taken during the on-time.

Next, filtering of the electromagnetic data was performed in 2 steps. The first is a 4 fiducial wide non-linear filter to eliminate any large spikes remaining in the dataset. The second filter is a low pass symmetric linear digital filter that has zero phase shift which prevents any lag or peak displacement from occurring, and it suppresses only variations with a wavelength less than about 1 second or 25 metres.

The VTEM system has 3 receiver coil orientations: X, Y and Z. Generalized modelling results of the VTEM system are shown in Appendix I.

A parallax correction was applied to the EM data to account for the distance by which the EM transmitter-receiver loop lags behind GPS. In this parallax correction the EM data are adjusted by the nearest integer number of fiducials that it would take to travel the horizontal distance from the center of the loop to the GPS.

The Z-axis receiver coil was oriented parallel with the transmitter coil axis and both were horizontal to the ground. The Z-component data produce double peak type anomalies for “thin” sub vertical targets and single peak anomalies for “thick” targets. The limits and changeover of “thin-thick” depends on dimensions of the TEM system (Appendix I, Figure I-17).

The X-axis coil is oriented parallel with the ground and along the line-of-flight. The Y-axis coil is oriented parallel with the ground and perpendicular to the line-of-flight. The combination of the X and Z coils configuration provides information on the position, depth, dip and thickness of a conductor.

The X-component data produce cross-over type anomalies: from “+ to – ” in flight direction of flight for “thin” sub vertical targets and from “- to +” in direction of flight for “thick” targets.

Because the X component polarity is under line-of-flight, convolution Fraser Filter (FF) (middle panel in Figure 8) is applied to X component data to represent axes of conductors in the form of grid map. In this case, positive FF anomalies always correspond to “plus-to-minus” X data crossovers independent of the flight direction.

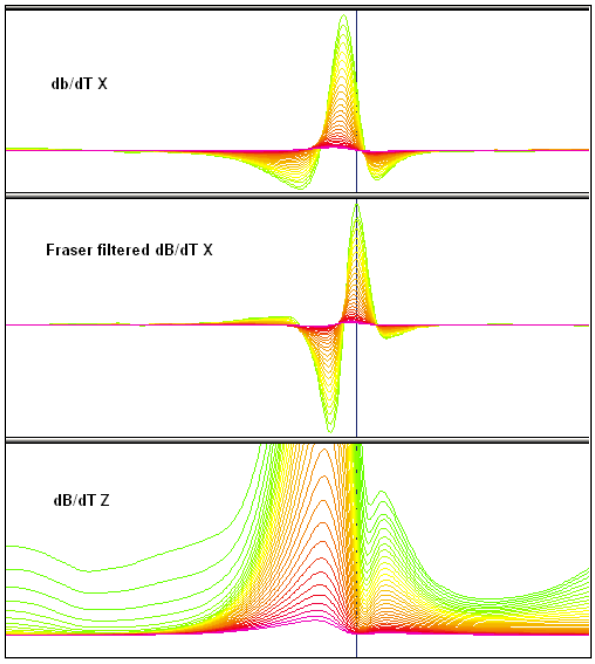

Figure 8. Z, X and Fraser filtered X (FFx) components for “thin” target.

5.3. CONDUCTIVITY DEPTH IMAGING (CDI)

A set of conductivity depth images (CDI) were generated using Geotech in-house CDI algorithm, developed by Geotech Ltd. A total of 44 dB/dt Z component channels, starting from channel 4 (21 µsec) to channel 46 (8685 µsec), were used for the CDI calculation for the data.

The used CDI algorithm is based on scheme of the apparent resistivity transform of Maxwell (A.Meju 1998)[2] and TEM response from conductive half-space. The software was developed by Geotech and depth calibrated based on forward plate modelling for VTEM system configuration. For more information on the CDI algorithm please refer to Appendix K.

The apparent conductivity and depth information for the survey area was visualized in 3-D space in the form of a Geosoft Voxel. The apparent conductivity Voxel has its depth relative to surface of the earth and increases down (negative). Apparent conductivity depth-slices were extracted from the voxel with intervals every 100 m for 4 levels of depth below ground level (0 m, -100 m, -200 m and -300 m).

5.4. ANOMALY SELECTION

The EM data were subjected to an anomaly recognition process using all the channels of the dBz/dt profiles. The resulting EM anomaly picks are presented as overlays on the maps and correspond to the approximate position of the conductors' centres projected to surface.

Each individual conductor pick is represented by an anomaly symbol classified according to the calculated conductance[3]. Identified anomalies were classified into one of six categories, as presented in Figure 9. The anomaly symbol is accompanied by postings denoting the number of Channels Deflected (upper-right), the dBz/dt Apparent Conductance (lower-right), the Apparent Depth (lower-left) and the Identification of the Anomaly (upper left), a unique number to each flight line.

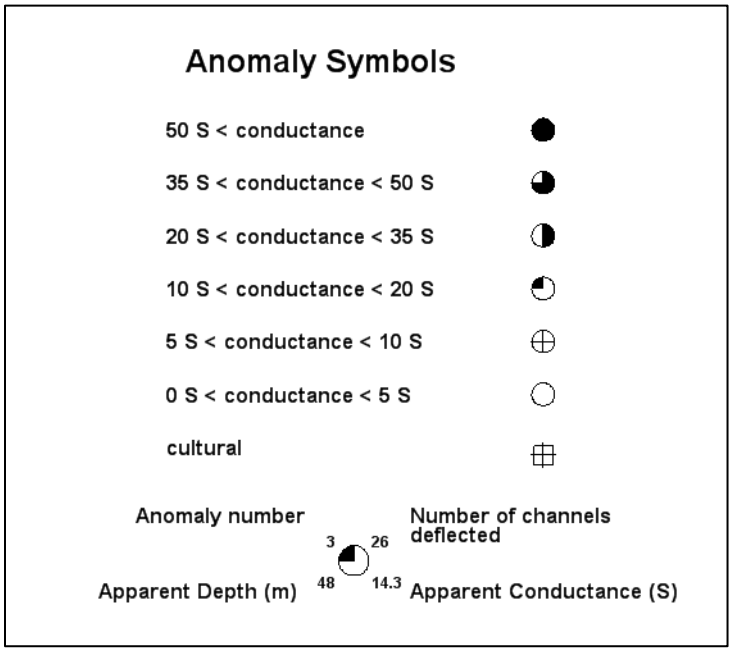

Figure 9. EM anomaly symbols.

The anomalous responses have been picked, reviewed and edited by an interpreter on a line-by-line basis to discriminate between bedrock, overburden and culture conductors. The accepted channels are provided in a Geosoft database.

[2] Meju, M.A. 1998. Short Note: A simple method of transient electromagnetic data analysis, Geophysics, **63**, 405–410.

[3] Note: Conductance values were obtained from the dBz/dt and B-Field EM time constants (Tau) whose relationships to Tau were calculated using the oblate spheroid model of McNeill (1980).

5.5. MAGNETIC MICROLEVELLING

Microlevelling is the process of removing residual flight line noise that remains after conventional levelling using control lines. It has become increasingly important as the resolution of aeromagnetic surveys has improved and the requirement of interpreting subtle geophysical anomalies has increased.

To isolate and remove this noise, the following procedure was employed. An elliptical reject filter, aligned with the flight lines, was first applied to the levelled total magnetic field grid. This filter removes features with a long wavelength in the flight line direction, but a short wavelength in the transverse direction. While removing the unwanted residual levelling errors, it also significantly distorts higher amplitude anomalies.

In order to minimize the effect on real anomalies, the flight path was ‘threaded’ through the filtered grid and a database profile channel was created from the grid. The difference between the control line levelled magnetic profile and this filtered profile was calculated. The difference profile was clipped to the amplitude of the observed noise in the grid. A half cosine roll-off filter was then applied to this channel and a final correction profile was derived with wavelengths longer than 1 km. This microlevel correction profile was applied to the levelled magnetic profile and a final magnetic profile channel was created.

5.6. KEATING CORRELATION COEFFICIENTS

Possible kimberlite targets are recognized from the residual magnetic intensity data, based on the identification of roughly circular anomalies. This procedure is automated by using a known pattern recognition technique (Keating 1995), which consists of computing, over a moving window, a first-order regression between a vertical cylinder model anomaly and the gridded magnetic data. Only the results, where the absolute value of the correlation coefficient is above a threshold of 75%, were retained. On the magnetic maps, the results are depicted as circular symbols, scaled to reflect the correlation value. The most favourable targets are those that exhibit a cluster of high amplitude solutions. Correlation coefficients with a negative value correspond to reversely magnetized sources.

The cylinder model parameters are as follows:

- Cylinder diameter: 200 m
- Cylinder length: infinite
- Overburden thickness: 6.6 m
- Magnetic inclination: 74.18° N
- Magnetic declination: -8.45° W
- Magnetization scale factor: 100
- Model window size: 13 x 13 cells (520 m x 520 m)
- Model window grid cell size: 40 m

It is important to be aware that other magnetic sources may correlate well with the vertical cylinder model, whereas some kimberlite pipes of irregular geometry may not. The user should study the magnetic anomaly that corresponds with the Keating symbols, to determine whether it does resemble a kimberlite pipe signature, reflects some other type of source or even noise in the data e.g., boudinage (beading) effect of the bi-cubic spline gridding. All available geological information should be incorporated into kimberlite pipe target selection.

5.7. GEOLOGICAL SURVEY OF CANADA DATA LEVELLING

In 1989, as part of the requirements for the contract with the Ontario Geological Survey (OGS) to compile and level all existing Geological Survey of Canada (GSC) aeromagnetic data (flown prior to 1989) in Ontario, PGW developed a robust method to level the magnetic data of various base levels to a common datum provided by the GSC as 812.8 m grids. The essential theoretical aspects of the levelling methodology were fully discussed in Gupta et al. (1989) and Reford et al. (1990). The method was later applied to the remainder of the GSC data across Canada and the high-resolution, combined aeromagnetic and EM (AMEM) surveys flown by the OGS. It has since been applied to all newly acquired OGS aeromagnetic surveys.

5.7.1. TERMINOLOGY

The Master grid refers to the 200 m Ontario magnetic grid compiled and levelled to the 812.8 m magnetic datum from the Geological Survey of Canada.

GSC levelling is the process of levelling profile data to a master grid, first applied to GSC data.

Intrasurvey levelling or microlevelling refers to the removal of residual line noise described earlier in this chapter; the wavelengths of the noise removed are usually shorter than tie line spacing.

Intersurvey levelling or GSC levelling refers to the level adjustments applied to a block of data; the adjustments are the long wavelength (in the order of tens of kilometres) differences with respect to a common datum, in this case, the 200 m Ontario master grid, which was derived from all pre-1989 GSC magnetic data and adjusted, in turn, by the 812.8 m GSC Canada wide grid.

5.7.2. THE GSC LEVELLING METHODOLOGY

The GSC levelling methodology is described below, using the Vickers survey flown for OGS as an example.

Several data processing procedures are assumed to be applied to the survey data prior to levelling, such as microlevelling, IGRF calculation and removal. The final levelled data are gridded at 1/5 of the line spacing. If a survey was flown as several distinct blocks with different flight directions, then each block is treated as an independent survey.

The steps in the GSC levelling process are as follows:

1. Create an upward continuation of the survey grid to 305 m

Almost all recent surveys (1990 and later) to be compiled were flown at a nominal terrain clearance of 100 m or less. The first step in the levelling method is to upward continue the survey grid to 305 m, the nominal terrain clearance of the Ontario Master Grid (Figure 10). The grid cell size for the survey grids is set at 100 m. Since the wavelengths of level corrections will be greater than 10 to 15 km, working with 100 m or even 200 m grids at this stage will not affect the integrity of the levelling method. Only at the very end, when the level corrections are imported into the databases, will the level correction grids be re-gridded to 1/5 of line spacing.

The unlevelled 100 m grid is extended by at least 2 grid cells beyond the actual survey boundary, so that, in the subsequent processing, all data points are covered.

2. Create a difference grid between the survey grid and the Ontario master grid.

The difference between the upward continued survey grid and the Ontario master grid, re-gridded at 100 m, is computed (Figure 11). The short wavelengths represent the higher resolution of the survey grid. The long wavelengths represent the level difference between the two grids.

3. Rotate difference grid so that flight line direction is parallel with grid column or row, if necessary.

4. Apply the first pass of a non-linear filter (Naudy and Dreyer, 1968) of wavelength on the order of 15 to 20 km along the flight line direction. Reapply the same non-linear filter across the flight line direction.

5. Apply the second pass of a non-linear filter of wavelength on the order of 2000 to 5000 m along the flight line direction. Reapply the same non-linear filter across the flight line direction.

6. Rotate the filtered grid back to its original (true) orientation (Figure 12).

7. Apply a low pass filter to the non-linear filtered grid.

Streaks may remain in the non-linear filtered grid, mostly caused by edge effects. They must be removed by a frequency-domain, low pass filter with the wavelengths in the order of 25 km (Figure 13).

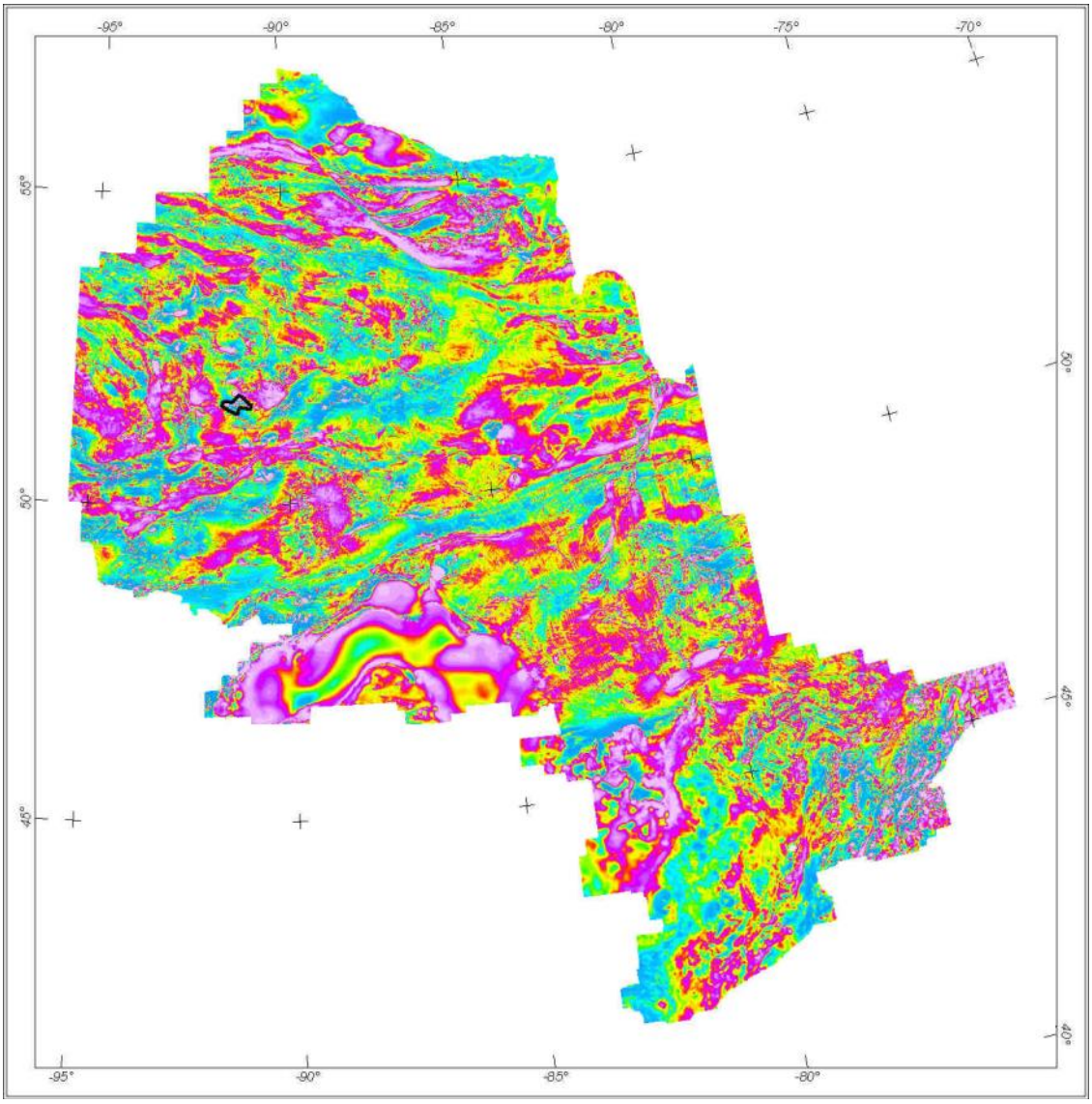

Figure 10. The Ontario Master Aeromagnetic Grid (Ontario Geological Survey 1999). The outline for the sample data set to be levelled (Vickers) is shown.

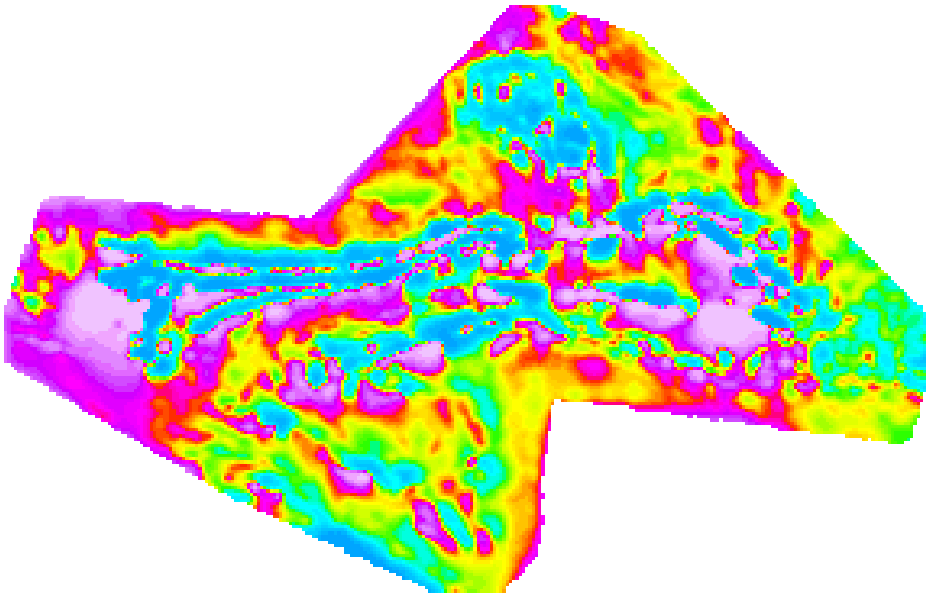

Figure 11. Difference grid (difference between survey grid and master grid), Vickers survey (Ontario Geological Survey 2002).

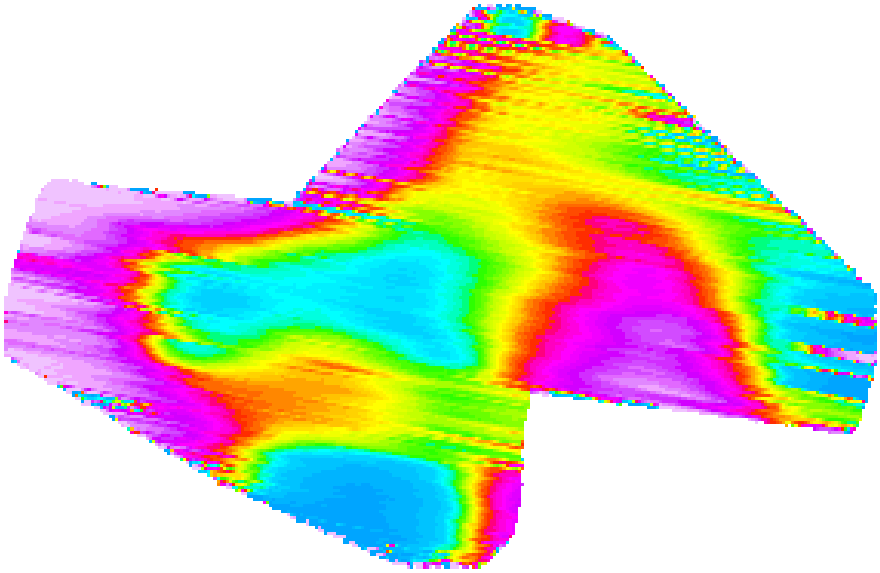

Figure 12. Difference grid after application of non-linear filtering and rotation, Vickers Survey.

8. Re-grid to 1/5 line spacing and import level corrections into database.

9. Subtract the level correction channel from the un-levelled channel to obtain the level corrected channel.

10. Make final grid using the gridding algorithm of choice with grid cell size at 1/5 of line spacing.

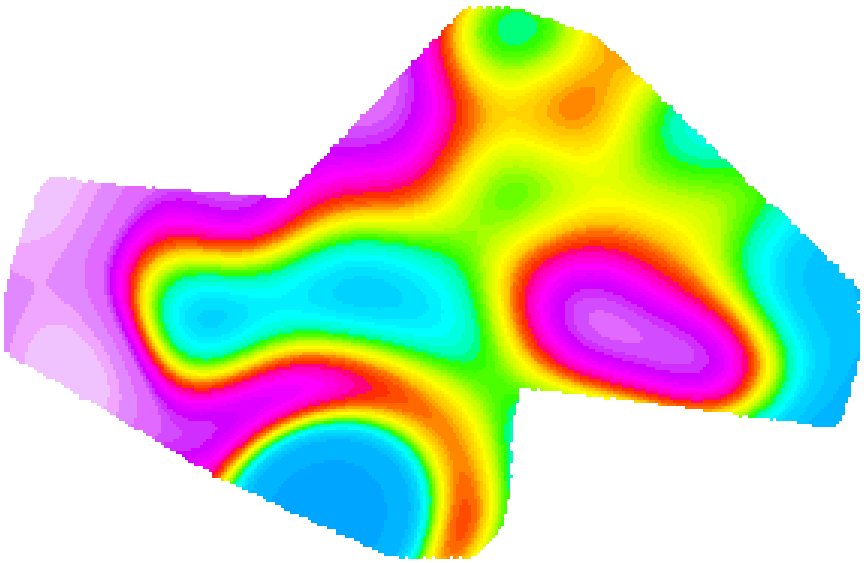

Figure 13. Level correction grid, Vickers survey.

Survey Specific Parameters

The following GSC levelling parameters were used in the Kabinakagami Lake survey:

- Upward continuation of 245.3m for Block 1 and 244.8 for Block 2
- OGS 200 m grid regridded to 100 m (Ontario-wide TMI grid)
- Residual grid regridded to 100 m
- Calculate difference grid between OGS_100 and Residual_100
- Difference grid of Block 2 rotated to N-S; no need to rotate grid of Block 1
- Difference grid filtered with *regrid.gx* using LP=15,000m (1st pass) and 2 000 m (2nd pass)
- Difference grid of block 2 rotated back to survey azimuth; no need to rotate grid of block 1
- Magmap filtered with LP=25 000 m
- Difference grid regridded to 40 m cell size
- Sampled back to database (lev_corr)
- Correction subtracted from residual magnetic intensity channel

6. FINAL PRODUCTS

The following products were delivered to MNDM.

6.1. PROFILE AND ANOMALY DATABASES

The following databases are provided in both Geosoft® GDB and ASCII format.

- Magnetic and electromagnetic profile database
- EM anomaly database
- Keating correlation coefficient database
- Waveform database
- CDI database

6.2. GRIDDED DATA

The following data, gridded from co-ordinates in UTM Zone 16 and 17 N, NAD83 datum, are provided in both Geosoft® GRD and GXF formats.

- digital elevation model
- GSC levelled residual magnetic field
- calculated second vertical derivative of the GSC levelled residual magnetic field
- TDEM decay constant Z-component
- apparent conductivity depth slices

6.3. MAPS

Final maps were produced at a scale of 1:20 000 and 1:50 000 for best representation of the survey size and line spacing. The co-ordinate and/or projection system used was NAD83 Datum, UTM Zone 16 North. The following maps were created.

Digital 1:20 000 scale maps in Geosoft® MAP format, with a topographic layer, of the following:

- residual magnetic field contours with electromagnetic anomalies, Keating coefficients and flight lines, maps 82 738 to 82 753 (inclusive)

Digital 1:50 000 scale maps in Geosoft® MAP format, with a topographic layer, of the following:

- colour-filled contours of the residual magnetic field, electromagnetic anomalies and flight lines, maps 82 754 and 82 757

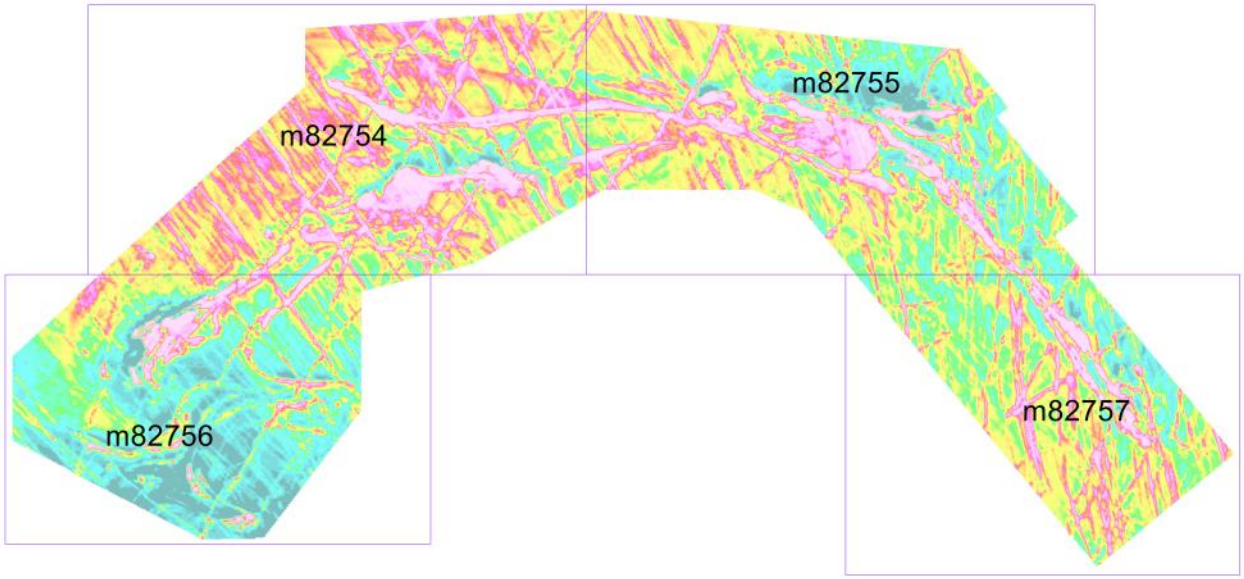

- shaded colour image of the second vertical derivative of the residual magnetic field, Keating coefficients and flight lines, maps 82 758 to 82 761

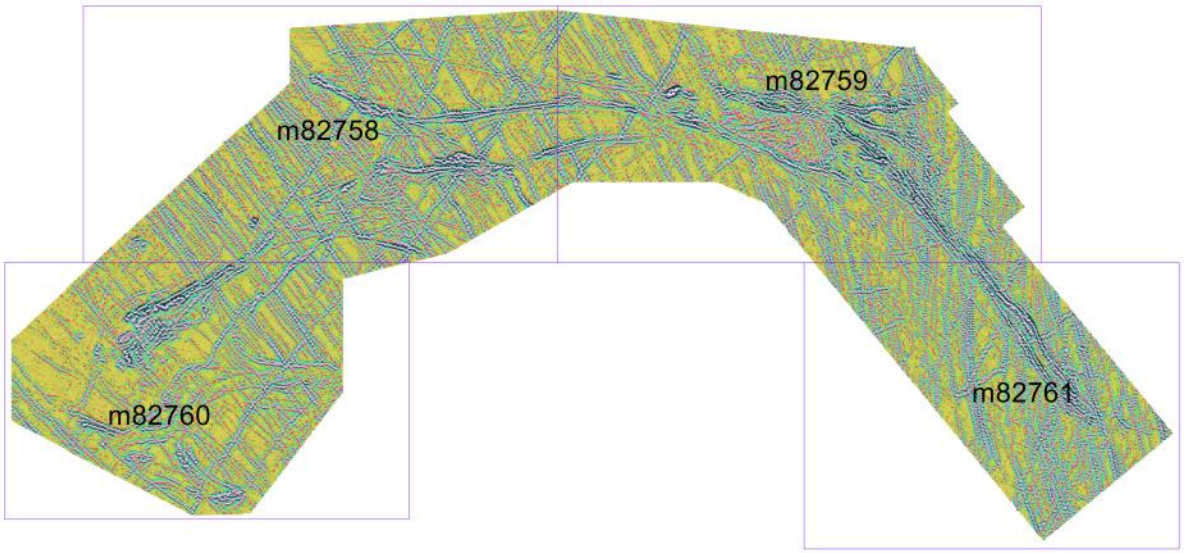

- colour-filled contours of the EM decay constant, electromagnetic anomalies and flight lines, maps 82 762 to 82 765

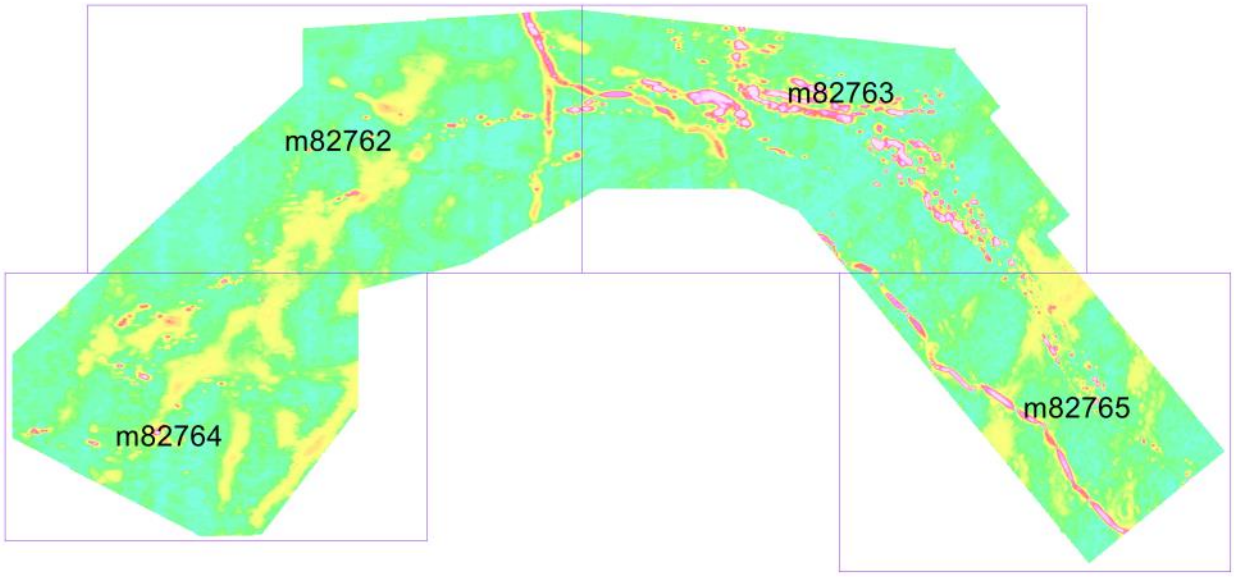

- colour-filled contours of the apparent conductance, electromagnetic anomalies and flight lines, maps 82 766 to 82 769

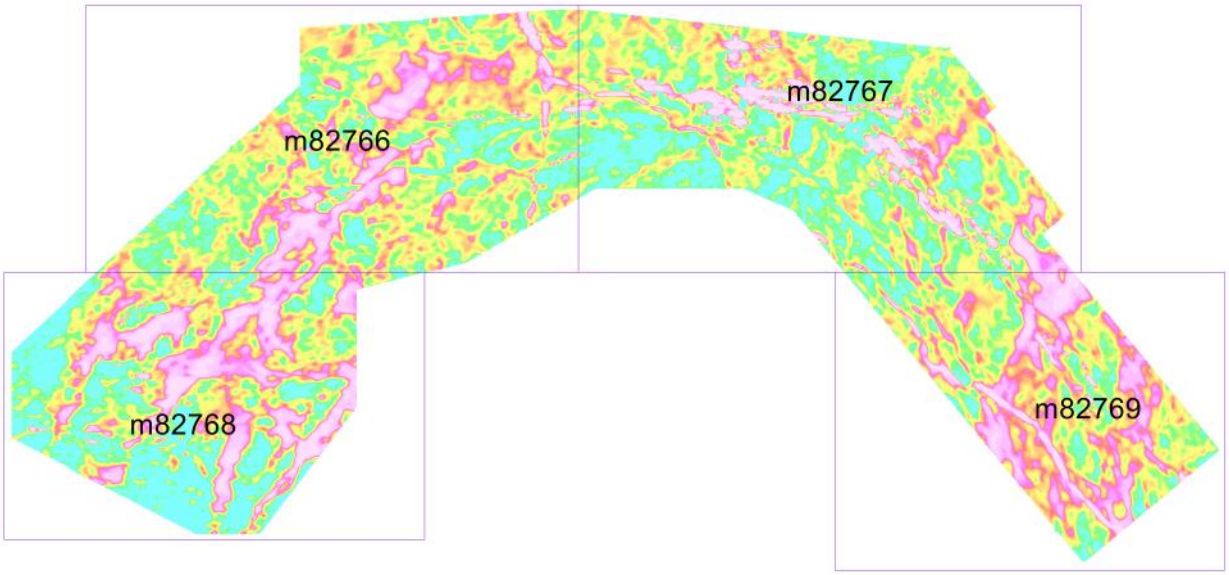

6.4. PROJECT REPORT

The survey report describes the data acquisition, processing, and final presentation of the survey results. The survey report is provided only digitally, in portable document format (*.pdf*).

6.5. FLIGHT VIDEOS

The digitally recorded video from each survey flight are provided in a compressed binary format on an external disc drive. Flight videos were delivered to the MNDM but are not part of the published Geophysical Data Set.

6.6. VECTOR FILES

Vector graphic files store the lines, shapes and colours that make up an image as mathematical formula; as a result they can be resized without losing detail or clarity.

They are created in Geosoft by exporting the selected layer as a dxf file. See Appendix A for the list of vector files provided

6.7. GEO-REFERENCED IMAGE FILES

A GeoTIFF file has georeferenced information embedded in it such as projection and coordinates which allows the TIFF file to be spatially referenced.

They are created in Geosoft by exporting the selected layer as a geoTIFF file. See Appendix A for the list of GeoTIFFS provided.

6.8. VTEM STREAMED DATA

The VTEM streamed data is recorded at 192 kHz and is described in section 5.2 of this report.

Files containing stream data have extension ".c" and are provided in a separate hard-drive due to their large size. A flight usually contains several ".c" files recorded every ten (10) minutes and stored in binary format.

A typical ".c" file name is "vvv yy.mm.dd hh.mm.ss.c"

Where:

vvv: VTEM system serial number
yy: year
mm: month
dd: day
hh: hour
mm: minute
ss: second

VTEM streamed data were delivered to the MNDM but are not part of the published Geophysical Data Set.

7. QUALITY ASSURANCE AND QUALITY CONTROL

Quality assurance and quality control (QA/QC) were undertaken by the survey contractor, Geotech Ltd., PGW (QA/QC Geophysicist), and MNDM. Stringent QA/QC was emphasized throughout the project so that the optimal geological signal was measured, archived and presented. The quality control procedures are summarized below.

7.1. PREPRODUCTION CALIBRATION AND TESTING

Test surveys were flown at the Bourget and Reid–Mahaffey test sites to calibrate the magnetometer and TDEM systems respectively. These tests are presented in Appendix L.

In addition the following tests were carried out on the survey site:

1. Polarity Test – performed prior to the survey commencing. This test was designed to ensure that the polarity of the system is correct.
2. Aluminium Plate Test – performed prior to the survey commencing and at the end of every week. The test checked the sensitivity of the system during the survey period and ensured that the system was calibrated properly at all times.
3. Radar Altimeter Test – performed prior to survey commencing or if a new radar altimeter was installed. The test was performed to ensure the accuracy of the radar altimeter.
4. Full Waveform VTEM Calibration – performed prior to the survey commencing. This calibration is performed on the complete VTEM system installed in and connected to the helicopter, using special calibration equipment. The procedure takes half-cycle files acquired and calculates a calibration file consisting of a single stacked half-cycle waveform. The purpose of the stacking is to attenuate natural and man-made magnetic signals, leaving only the response to the calibration signal.

7.2. DAILY CALIBRATIONS AND PRE-FLIGHT PRECAUTIONS

The TDEM system and magnetometer were sufficiently warmed up before each survey day to minimize temperature-related system drifting.

- Timing and synchronization of all recording instruments was checked for correct operation.
- Each flight included 2 background pre-flight and post-flight measurements for background and assessment of noise levels. The aircraft climbed to 500 m AGL (Above Ground Level) and maintained straight and level flight for one (1 minute or 5 km). A 'background check' was conducted at the beginning of each flight and repeated approximately every hour and after completing the last survey line of the flight.
- Each flight included 2 background measurements; pre-flight and post-flight for TDEM compensation and collection of the reference waveform.
- A test line of a minimum of 5 km long, with a variety of conductive responses, was flown daily at survey height.

7.3. DAILY FIELD QUALITY CONTROL

7.3.1. GENERAL

- Check that all the files are on the server as expected.
- Download and unzip the files. Make sure they were complete and not corrupted.
- Check the header of the airborne raw data files to ensure the system was configured properly.
- Preprocess and then import the data into the Geosoft® software.
- Plot the flight path in Google Earth and Geosoft to verify that the data are complete and properly located and that the lines, as described in the flight logs, were flown.
- Check the flight path for crossing lines or lines that did not maintain proper separation.
- Plot the final flight path and look for problems, such as gaps and GPS busts.

7.3.2. ELECTROMAGNETIC DATA

- Visual check for shifts, excessive spiking, drift, etc.
- Correct/compensate the EM data.
- Identify the backgrounds and measure/log the EM noise levels including original and compensated channels. Ensure they are within specification

- Filter the EM data and check for drift or offsets
- After splitting the GDB into lines, check again

7.3.3. MAGNETIC DATA AND MAGNETIC BASE STATION

- Check the start and end time of base station record and ensure that it covers the full survey data.
- Check the base station for cultural noise and diurnal activity. Ensure the diurnal is within specifications.
- Check the airborne magnetic data for gaps, dropouts, or excessive noise

7.3.4. ALTITUDE

- Visually check the altitude particularly at the start and ends of lines.
- Calculate the average helicopter altitude and ensure that it meets specifications.

7.4. QUALITY CONTROL IN THE OFFICE

Data verification was performed by experienced geophysicists in the processing centre or on-site using a work station that is capable of reading, analysing and duplicating the data on a daily basis. This system was available to MNDM (QA/QC geophysicist) to monitor data acquisition and verification.

The work flow diagram provided below (Figure 14) shows the tests and checks on data applied during the course of the survey and subsequent processing. The red lines represent feedback loops that will send data back to be reprocessed or even re-flown so as to correct for any deficiencies detected either in the field during QA/QC or at the Data Processing centre where senior staff review incoming data sets.

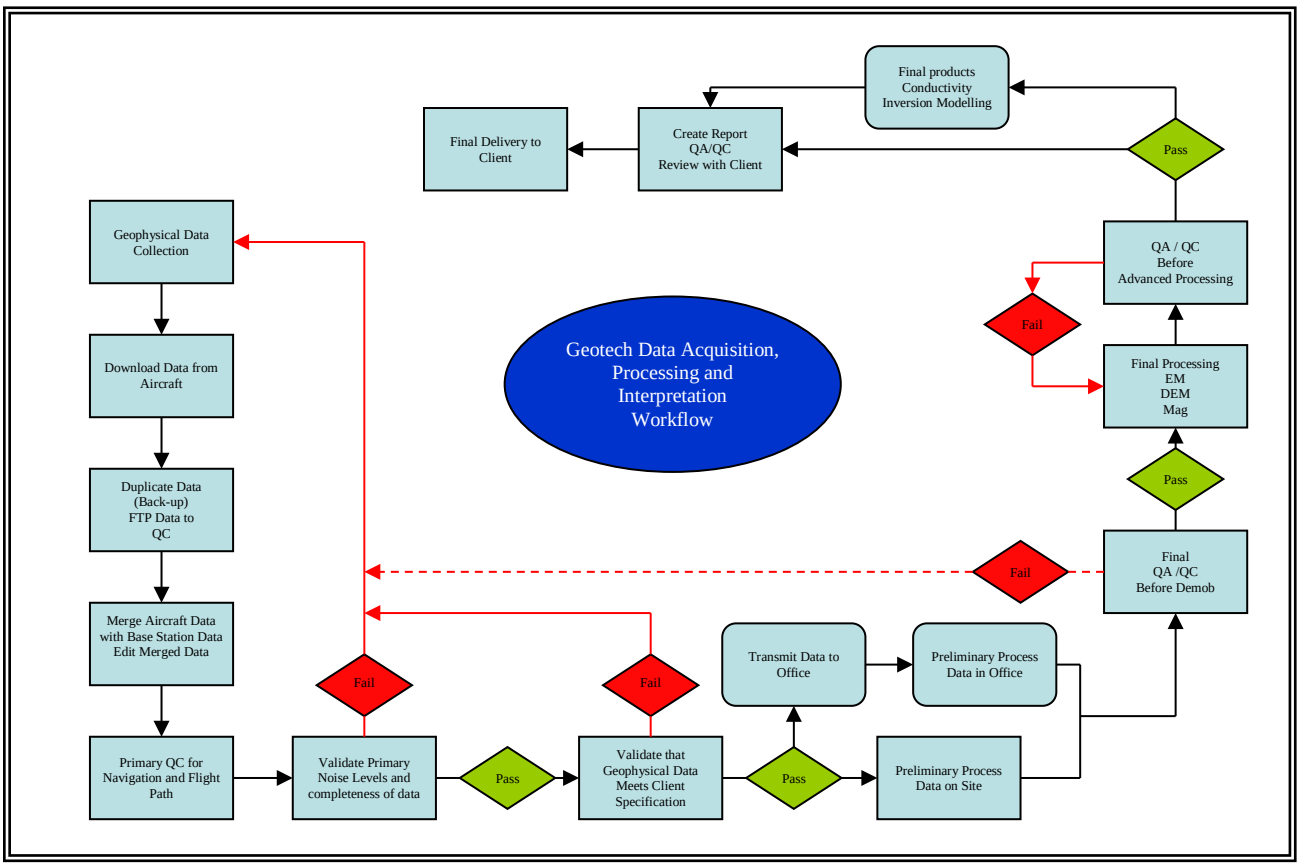

Figure 14. Data acquisition, data processing and interpretation workflow.

8. REFERENCES

Gupta, V., Paterson, N., Reford, S., Kwan, K., Hatch, D. and MacLeod, I. 1989. Single master aeromagnetic grid and magnetic colour maps for the province of Ontario; *in* Summary of Field Work and Other Activities 1989, Ontario Geological Survey, Miscellaneous Paper 146, p.244-250.

Keating, P.B. 1995. A simple technique to identify magnetic anomalies due to kimberlite pipes; Exploration and Mining Geology, v.4, no.2, p.121-125.

McNeill, J.D. 1980. Applications of transient electromagnetic techniques, Technical Note 7, Geonics Ltd., Mississauga, Ontario.

Meju, M.A. 1998. Short Note: A simple method of transient electromagnetic data analysis, Geophysics, 63, p.405–410.

Naudy, H. and Dreyer, H. 1968. Essai de filtrage nonlinéaire appliqué aux profiles aeromagnétiques; Geophysical Prospecting, v.16, p.171-178.

Ontario Geological Survey 1999. Single master gravity and aeromagnetic data for Ontario; Ontario Geological Survey, Geophysical Data Set 1036.

———2003. Ontario airborne geophysical surveys, magnetic and electromagnetic data, Vickers area; Ontario Geological Survey, Geophysical Data Set 1106-revised.

———2011. 1:250 000 scale bedrock geology of Ontario; Ontario Geological Survey, Miscellaneous Release—Data 126–Revision 1.

Reford, S.W., Gupta, V.K., Paterson, N.R., Kwan, K.C.H. and Macleod, I.N. 1990. Ontario master aeromagnetic grid: A blueprint for detailed compilation of magnetic data on a regional scale; in Expanded Abstracts, Society of Exploration Geophysicists, 60th Annual International Meeting, San Francisco, v.1, p.617-619.

Wilson, A.C. 1993. Geology of the Kabinakagami Lake greenstone belt; Ontario Geology Survey, Open File Report 5787, 80p.

Appendix A. GEOPHYSICAL DATA FILE LAYOUT

The files for the Kabinakagami Lake Survey, Geophysical Data Set 1079, are archived on 2 three-volume sets of DVDs and are sold as separate products as follows:

ASCII format	Geophysical Data Set (GDS) 1079a volumes 1 to 3
Geosoft® binary format	Geophysical Data Set (GDS) 1079b volumes 1 to 3

The content of the ASCII and Geosoft® binary file types are identical. They are provided in both forms to suit the user's available software. The survey data are divided as follows:

Geophysical Data Set 1079a (DVD)

- Profile data
  - Profile database of electromagnetic and magnetic data (10 Hz sampling) in ASCII (XYZ) format
- Gridded data in ASCII (GXF) format:
  - total (residual) field magnetics
  - second vertical derivative of the total field magnetics
  - decay constant
  - apparent conductivity at -100m depth
  - digital elevation model
- EM anomaly database in ASCII (CSV) format
- Keating correlation coefficient database in ASCII (CSV) format
- Vector files in DXF format:
  - flight path
  - EM anomalies
  - Keating correlation (kimberlite) anomalies
  - total field magnetic contours
  - decay constant contours
  - apparent conductivity contours
- GEOTIFF images
  - colour total field magnetics with base map
  - colour shaded relief of second vertical derivative with base map
  - colour decay constant with base map
  - apparent conductivity at -100m depth with base map
- Waveform database in ASCII (XYZ) format
- Conductivity Depth Imaging (CDI) data:
  - CDI database in Geosoft® Binary GDB format
  - Plotted CDI sections in portable document format, PDF
- Survey report in Adobe® Acrobat® PDF format

Geophysical Data Set 1079b (DVD)

- Profile data
  - Profile database of electromagnetic and magnetic data (10 Hz sampling) in Geosoft® Binary GDB format
- Gridded data in Geosoft® Binary (GRD) format:
  - total (residual) field magnetics
  - second vertical derivative of the total field magnetics
  - decay constant
  - apparent conductivity at -100m depth
  - digital elevation model
- EM anomaly database in Geosoft® Binary GDB format
- Keating correlation coefficient database in Geosoft® Binary GDB format
- Vector files in DXF format:
  - flight path
  - EM anomalies
  - Keating correlation (kimberlite) anomalies
  - total field magnetic contours
  - decay constant contours
  - apparent conductivity contours
- GEOTIFF images
  - colour total field magnetics with base map
  - colour shaded relief of second vertical derivative with base map
  - colour decay constant with base map
  - apparent conductivity at -100m depth with base map
- Waveform database in Geosoft® GDB format
- Conductivity Depth Imaging (CDI) data:
  - CDI database in Geosoft® Binary GDB format
  - Plotted CDI sections in portable document format, PDF
- Survey report in Adobe® Acrobat® PDF formats

Appendix B. PROFILE ARCHIVE DEFINITION

The profile data are provided in two formats, one binary and one ASCII.

ASCII XYZ and Geosoft® OASIS montaj™ binary database file (no compression) of electromagnetic, magnetic and ancillary data, sampled at 10 Hz

KL1MAGEM.XYZ (ASCII) for Block 1
KL1MAGEM.GDB (Binary) for Block 1
KL2MAGEM.XYZ (ASCII) for Block 2
KL2MAGEM.GDB (Binary) for Block 2

The contents of *.GDB/*.XYZ (both file types contain the same set of data channels) are summarized as follows:

Magnetic/Electromagnetic/ Ancillary Line Data

In KL1MAGEM.XYZ and KL2MAGEM.XYZ the electromagnetic channel data are provided in individual channels with numerical indices (e.g., em_z_final_off[4] to em_z_final_off[46]) along with magnetic and ancillary channels. In KL1MAGEM.GDB and KL2MAGEM.GDB, the electromagnetic channel data are provided in array channels with 43 elements.

Table 5. Survey database channels

Channel name	Units	Description
gps_x_raw	metres	raw GPS X
gps_y_raw	metres	raw GPS Y
gps_z_raw	metres	raw GPS Z
gps_x_final	decimal-degrees	differentially corrected GPS X (NAD83 datum)
gps_y_final	decimal-degrees	differentially corrected GPS Y (NAD83 datum)
gps_z_final	metres ASL	differentially corrected GPS Z (NAD83 datum)
x_nad83	metres	easting in UTM co-ordinates using NAD83 datum
y_nad83	metres	northing in UTM co-ordinates using NAD83 datum
lon_nad83	decimal-degrees	longitude using NAD83 datum
lat_nad83	decimal-degrees	latitude using NAD83 datum
radar_raw	metres above terrain	raw radar altimeter
radar_final	metres above terrain	corrected radar altimeter
dem	metres ASL	digital elevation model
fiducial		Fiducial
flight		flight number
line_number		full flight line number(flight line and part numbers)
line		flight line number
time_utc	seconds	utc time
date	YYYY/MM/DD	local date
height_mag	metres above terrain	magnetometer height
mag_base_final	nanoteslas	corrected magnetic base station data
mag_raw	nanoteslas	raw magnetic field
mag_diurn	nanoteslas	diurnally-corrected magnetic field
mag_lev	nanoteslas	levelled magnetic field
igrf	nanoteslas	local IGRF field
mag_igrf	nanoteslas	IGRF-corrected magnetic field
mag_final	nanoteslas	diurnally and IGRF-corrected magnetic field
cvg	nanoteslas per metre	calculated magnetic vertical derivative from mag_final
mag_2vd	nanoteslas per square	calculated 2vd from mag_final

Channel name	Units	Description
	metre	
mag_gsclevel	nanoteslas	GSC levelled magnetic field
cvg_gscl	nanoteslas per metre	calculated magnetic vertical derivative from mag_gsclevel
mag_2vd_gscl	nanoteslas per square metre	calculated 2vd from mag_gsclevel
height_em	metres above terrain	electromagnetic receiver height
em_z_raw_off	(pV)/(A*m^4)	raw (stacked) dB/dt, Z-component, off-time channels 4 to 46
em_z_final_off	(pV)/(A*m^4)	filtered and leveled dB/dt, Z-component, off-time channels 4 to 46
em_bz_raw_off	(pV*ms)/(A*m^4)	raw (stacked) B-field, Z-component, off-time channels 4 to 46
em_bz_final_off	(pV*ms)/(A*m^4)	filtered and leveled B-field, Z-component, off-time channels 4 to 46
em_x_raw_off	(pV)/(A*m^4)	raw (stacked) dB/dT, X-component, off-time channels 20 to 46
em_x_final_off	(pV)/(A*m^4)	filtered and leveled dB/dT, X-component, off-time channels 20 to 46
em_sfxff_final_off	(pV)/(A*m^4)	Fraser filtered calculated from channel em_x_final_off, channels 20 to 46
em_bx_raw_off	(pV*ms)/(A*m^4)	raw (stacked) B-field, X-component, off-time channels 20 to 46
em_bx_final_off	(pV*ms)/(A*m^4)	filtered and leveled B-field, X-component, off-time channels 20 to 46
em_y_raw_off	(pV)/(A*m^4)	raw (stacked) dB/dT, Y-component, off-time channels 20 to 46
em_y_final_off	(pV)/(A*m^4)	filtered and leveled dB/dT, Y-component, off-time channels 20 to 46
em_by_raw_off	(pV*ms)/(A*m^4)	raw (stacked) B-field, Y-component, off-time channels 20 to 46
em_by_final_off	(pV*ms)/(A*m^4)	filtered and leveled B-field, Y-component, off-time channels 20 to 46
power	microvolts	60 Hz power line monitor
tau_bz	microseconds	decay constant (tau) for B-field Z-component
tau_z	microseconds	decay constant (tau) for dB/dt Z-component
nchan_bz		latest time channels of TAU calculation, B-field Z
nchan_z		latest time channels of TAU calculation, dB/dt Z
appcond	Siemens per metre	apparent conductivity

Appendix C. EM ANOMALY ARCHIVE DEFINITION

The electromagnetic anomaly data are provided in two formats, one ASCII and one binary:

KL1ANOMALY.csv – ASCII comma-delimited Excel® format for Block 1
KL1ANOMALY.gdb – Geosoft® OASIS montaj™ binary database file for Block 1
KL2ANOMALY.csv – ASCII comma-delimited Excel® format for Block 2
KL2ANOMALY.gdb – Geosoft® OASIS montaj™ binary database file for Block 2

Both file types contain the same set of data channels, summarized as follows:

Table 6. Anomaly database channels.

Channel name	Units	Description
x_nad83	metres	easting in UTM co-ordinates using NAD83 datum
y_nad83	metres	northing in UTM co-ordinates using NAD83 datum
lon_nad83	decimal-degrees	longitude using NAD83 datum
lat_nad83	decimal-degrees	latitude using NAD83 datum
dem	metres asl	digital elevation model
fiducial		Fiducial
flight		flight number
line		flight line number
time_utc	seconds	utc time
date	YYYY/MM/DD	local date
em_z_final_off	$(pV)/(A*m^4)$	filtered and leveled dB/dt, Z-component, off-time channels 4 to 46
em_bz_final_off	$(pV*ms)/(A*m^4)$	filtered and leveled B-field, Z-component, off-time channels 4 to 46
tau_z	microseconds	decay constant (tau) for dB/dt Z-component
conductivity	Siemens per metre	apparent conductivity
height_em	metres above terrain	electromagnetic receiver height
anomaly_no		nth anomaly along the survey line
anomaly_ID		Alpha identifier
anomaly_type_letter		anomaly classification, “thick” (K) or “thin” (N) anomaly
anomaly_type_no		anomaly classification (i.e. anomaly grade), 1 to 6 from the weakest to the strongest
conductance_dBdt	Siemens	apparent conductance, calculated from dB/dt data
conductance_bfield	Siemens	apparent conductance, calculated from B-filed data
depth_to_conductor	metres	Depth to conductor
heading	degrees	direction of flight
survey_number		Government survey number
nchan_z		Number of off-time channels deflected

Appendix D. KEATING CORRELATION ARCHIVE DEFINITION

The Keating kimberlite pipe correlation coefficient data are provided in 2 formats, one ASCII and one binary:

KL1KC.csv – ASCII comma-delimited format for Block 1
KL1KC.gdb – Geosoft® OASIS montaj™ binary database file for Block 1
KL2KC.csv – ASCII comma-delimited format for Block 2
KL2KC.gdb – Geosoft® OASIS montaj™ binary database file for Block 2

Both file types contain the same set of data channels, summarized as follows:

Table 7. Keating database channels.

Channel name	Units	Description
x_nad83	metres	easting in UTM co-ordinates using NAD83 datum
y_nad83	metres	northing in UTM co-ordinates using NAD83 datum
lon_nad83	decimal-degrees	longitude using NAD83 datum
lat_nad83	decimal-degrees	latitude using NAD83 datum
corr_coeff	percent	correction coefficient
pos_coeff	percent	positive correction coefficient
neg_coeff	percent	negative correction coefficient
norm_error	percent	standard error normalized to amplitude
amplitude	nanoteslas	peak-to-peak anomaly amplitude within window

Appendix E. GRID ARCHIVE DEFINITION

The gridded data are provided in 2 formats, one ASCII and one binary:

*.gxf - Geosoft® ASCII Grid eXchange Format (no compression)

*.grd - Geosoft® OASIS montaj™ binary grid file (no compression)

Grids are NAD83 UTM Zone 16 North for Block 1 and NAD83 UTM Zone 17 North for Block 2, with a grid cell size of 40 m x 40 m.

Grids in Geosoft GRD and GXF format, as follows:

The grids are summarized as follows:

- KL1MAG83: Total Magnetic Intensity (nT) for Block 1
- KL1MAGGSC83: GSC-Levelled Total Magnetic Intensity (nT) for Block 1
- KL12VD83: Second Calculated Vertical Derivative of TMI (nT/m^2) for Block 1
- LK12VDMAGGSC83: GSC-Levelled Second Calculated Vertical Derivative of TMI (nT/m^2) for Block 1
- KL1DEM83: Digital Elevation Model (metres) for Block 1
- KL1DCZ83: TDEM Decay Constant Z Component (µsec) for Block 1
- KL1CON83: TDEM Apparent Conductivity depth slice 100 m below surface (mS/m) for Block 1
- KL2MAG83: Total Magnetic Intensity (nT) for Block 2
- KL2MAGGSC83: GSC-Levelled Total Magnetic Intensity (nT) for Block 2
- KL22VD83: Second Calculated Vertical Derivative of TMI (nT/m^2) for Block 2
- LK22VDMAGGSC83: GSC-Levelled Second Calculated Vertical Derivative of TMI (nT/m^2) for Block 2
- KL2DEM83: Digital Elevation Model (metres) for Block 2
- KL2DCZ83: TDEM Decay Constant Z Component (µsec) for Block 2
- KL2CON83: TDEM Apparent Conductivity depth slice 100 m below surface (mS/m) for Block 2

A Geosoft .GRD file has a .GI metadata file associated with it, containing grid projection information.

Appendix F. GEOTIFF AND VECTOR ARCHIVE DEFINITION

GeoTIFF Images

Geographically referenced colour images, incorporating a planimetric base, are provided in GeoTIFF format for use in GIS applications:

- KLMAG83.TIF – Colour residual, GSC levelled, magnetic field grid plotted on a planimetric base
- KL2VD83.TIF – Shaded colour image of the second vertical derivative of the residual magnetic field on a planimetric base
- KLDCZ83.TIF – Colour decay constant on a planimetric base
- KLCON83.TIF – Colour apparent conductivity on a planimetric base100 m below surface

Vector Archives

Vector line work from the map is provided in DXF (v12) ASCII format using the following naming convention:

- KLPATH83_20K.DXF – flight path of the survey area from 1:20 000 scale maps
- KLPATH83_50K.DXF – flight path of the survey area from 1:50 000 scale maps
- KLKC83_20K.DXF – Keating correlation targets from 1:20 000 scale maps
- KLKC83_50K.DXF – Keating correlation targets from 1:50 000 scale maps
- KLMAG83_20K.DXF – contours of the GSC levelled, residual magnetic field in nT from 1:20 000 scale maps
- KLMAG83_50K.DXF – contours of the GSC levelled, residual magnetic field in nT from 1:50 000 scale maps
- KLDCZ83.DXF – contours of the Z coil decay constant in µsec
- KLAC83.DXF – contours of the apparent conductivity100 m below surface in (mS/m)
- KLEM83_20K.DXF – electromagnetic anomaly symbols from 1:20 000 scale maps
- KLEM83_50K.DXF – electromagnetic anomaly symbols from 1:50 000 scale maps

The layers within the DXF files correspond to the various object types found therein and have intuitive names.

Appendix G. WAVEFORM AND CONDUCTIVITY DEPTH IMAGE ARCHIVE DEFINITION

The databases of the transmitter reference waveform and the Conductivity Depth Image (CDI) are provided in binary format:

Transmitter Current Waveform

KLMAGEM_VTEM_Waveform.gdb – Geosoft® OASIS montaj™ binary database file

Conductivity Depth Image

KL1MAGEM_CDI.gdb – Geosoft® OASIS montaj™ binary database file for Block 1
KL2MAGEM_CDI.gdb – Geosoft® OASIS montaj™ binary database file for Block 2

Descriptions of the data channels are provided below.

Geosoft database for the VTEM waveform

Table 8. VTEM Waveform database channels.

Channel name	Description
Time:	Sampling rate interval, 5.2083 microseconds
Tx_Current:	Output current of the transmitter (amps)

Geosoft database for conductivity depth image (CDI) data format

Table 9. CDI database channels.

Channel name	Units	Description
x_nad83	metres	easting in UTM co-ordinates using NAD83 datum
y_nad83	metres	northing in UTM co-ordinates using NAD83 datum
dist	metres	distance from the beginning of the line
depth	metres	array channel, depth from the surface
z	metres	array channel, depth from sea level
appres	ohm.m	array channel, apparent resistivity
appcond	Siemens per metre	array channel, apparent conductivity
tr	metres	electromagnetic receiver height from sea level
topo	metres	digital elevation model
height_em	metres	electromagnetic receiver height
em_z_final_off	$pV/(A*m^4)$	array channel, filtered and leveled dB/dt, Z-component, off-time
mag_gsclevel	nanoteslas	GSC levelled magnetic field
cvg_gscl	nanoteslas per metre	calculated magnetic vertical derivative from mag_gsclevel
doi	metres	Depth of Investigation: a measure of VTEM depth effectiveness
power		60Hz power line monitor

In addition, PDF files of plotted CDI sections (one per flight line) are presented in the following files:

KL1MAGEM_CDI_Sections_All_Lines(mutliZONs) – CDI sections with individual colour schemes for Block 1

KL1MAGEM_CDI_Sections_All_Lines(singleZON) – CDI sections with common colour scheme for Block 1

KL2MAGEM_CDI_Sections_All_Lines(mutliZONs) – CDI sections with individual colour schemes for Block 2

KL2MAGEM_CDI_Sections_All_Lines(singleZON) – CDI sections with common colour scheme for Block 2

Appendix H. SURVEY BLOCK CO-ORDINATES

(WGS 84, UTM Zone 16 and 17 North)

Block 1	
WGS84 UTM Zone 16N	
X	Y
684900	5389800
678900	5389800
660800	5399100
660800	5407000
688850	5432900
688850	5438550
715400	5440250
752250	5436350
752250	5433950
737200	5421300
732150	5423500
717600	5423500
704900	5416250
694250	5413500
694250	5402050
684900	5389800

Block 2	
WGS84 UTM Zone 17N	
X	Y
296350	5421350
313650	5433500
317550	5427950
316300	5427050
323400	5416900
320950	5415200
336550	5392900
322950	5383400
296350	5421350

Appendix I. GENERAL MODELLING RESULTS OF THE VTEM SYSTEM

Introduction

The VTEM system is based on a concentric or central loop design, whereby, the receiver is positioned at the centre of a transmitter loop that produces a primary field. The wave form is a bipolar, modified square wave with a turn-on and turn-off at each end.

During turn-on and turn-off, a time varying field is produced (dB/dt) and an electromotive force (emf) is created as a finite impulse response. A current ring around the transmitter loop moves outward and downward as time progresses. When conductive rocks and mineralization are encountered, a secondary field is created by mutual induction and measured by the receiver at the centre of the transmitter loop.

Efficient modelling of the results can be carried out on regularly shaped geometries, thus yielding close approximations to the parameters of the measured targets. The following is a description of a series of common models made for the purpose of promoting a general understanding of the measured results.

A set of models has been produced for the Geotech VTEM®Plus system dB/dt Z and X components (see models I-1 to I-17). The Maxwell ™ modelling program (EMIT Technology Pty. Ltd. Midland, WA, AU) used to generate the following responses assumes a resistive half-space. The reader is encouraged to review these models, so as to get a general understanding of the responses as they apply to survey results. While these models do not begin to cover all possibilities, they give a general perspective on the simple and most commonly encountered anomalies.

As the plate dips and departs from the vertical position, the peaks become asymmetrical.

As the dip increases, the aspect ratio (Min/Max) decreases and this aspect ratio can be used as an empirical guide to dip angles from near 90º to about 30º. The method is not sensitive enough where dips are less than about 30º.

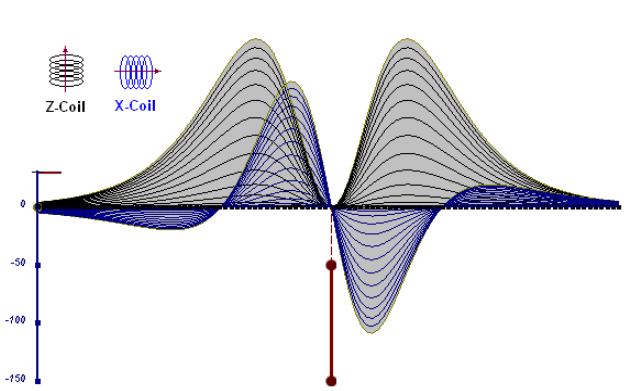

Figure I-1. vertical thin plate

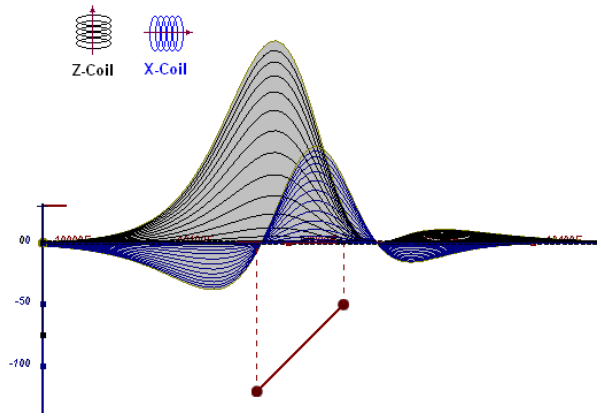

Figure I-2. inclined thin plate

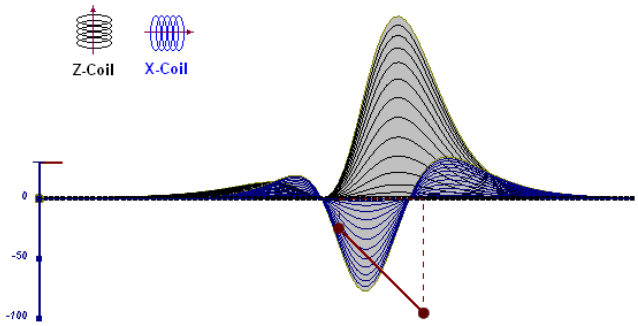

Figure I-3. inclined thin plate

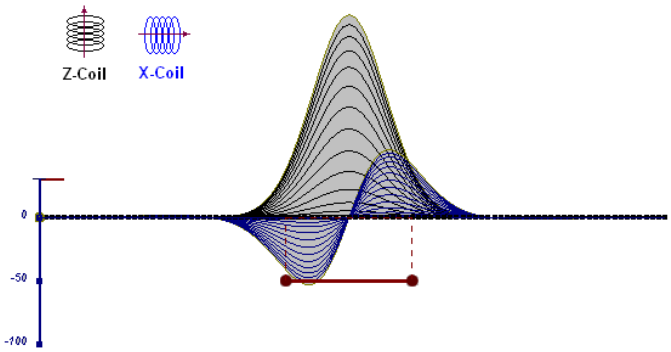

Figure I-4. horizontal thin plate

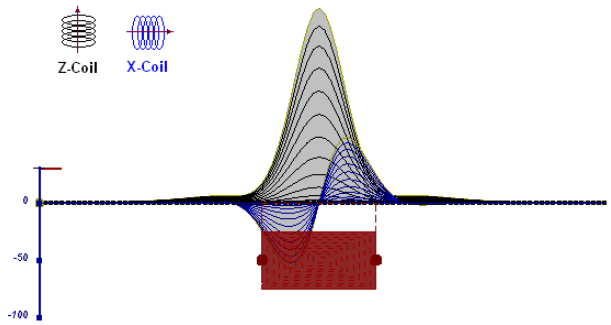

Figure I-5. horizontal thick plate (linear scale of the response)

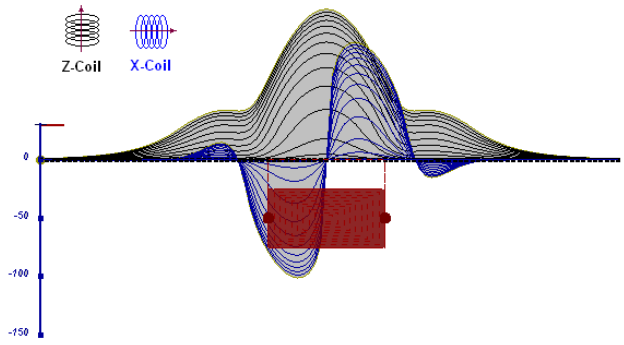

Figure I-6. horizontal thick plate (log scale of the response)

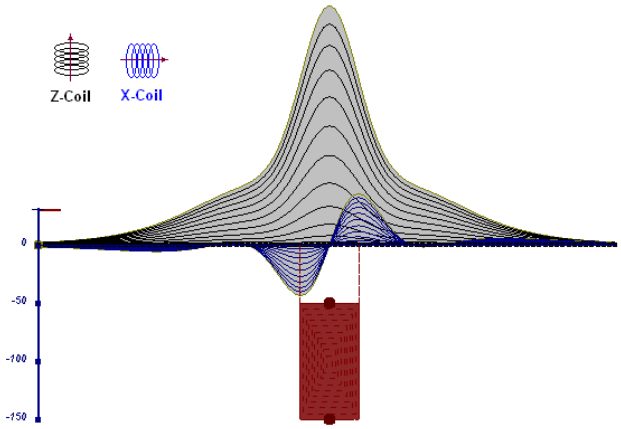

Figure I-7. vertical thick plate (linear scale of the response). 50 m depth

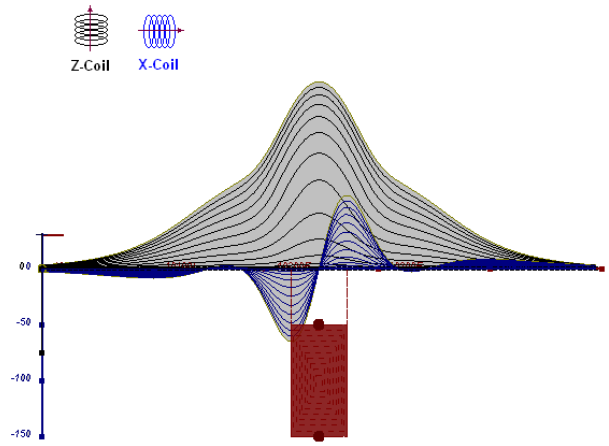

Figure I-8. vertical thick plate (log scale of the response). 50 m depth

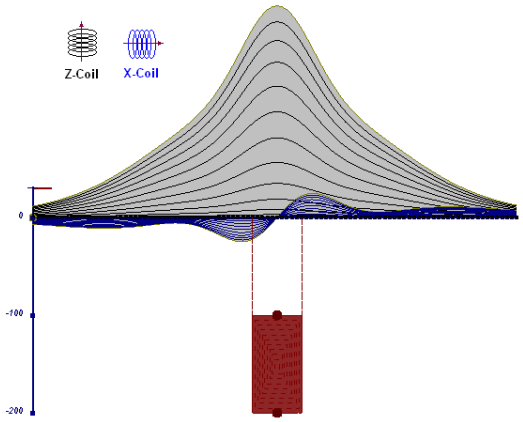

Figure I-9. vertical thick plate (linear scale of the response). 100 m depth

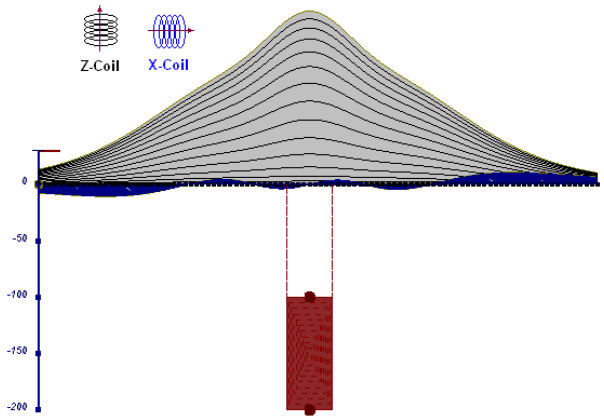

Figure I-10. vertical thick plate (linear scale of the response). Depth/hor.thickness=2.5

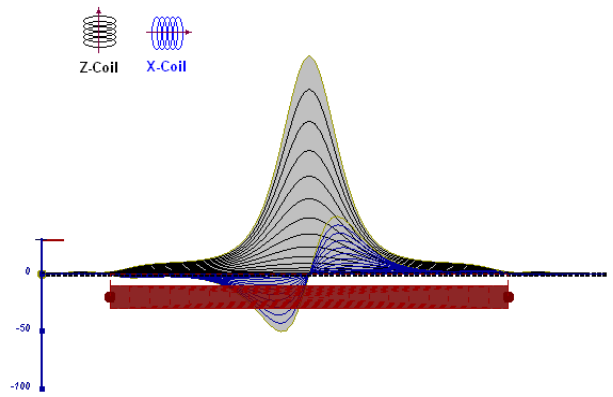

Figure I-11. horizontal thick plate (linear scale of the response)

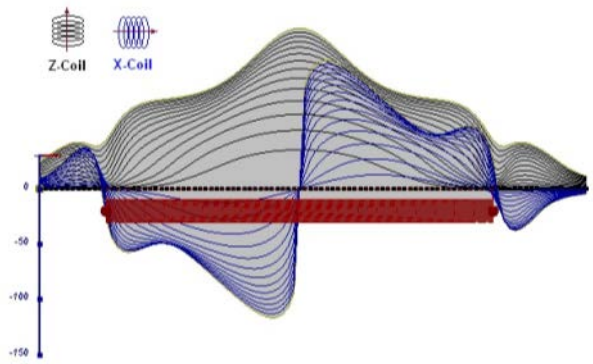

Figure I-12. horizontal thick plate (log scale of the response)

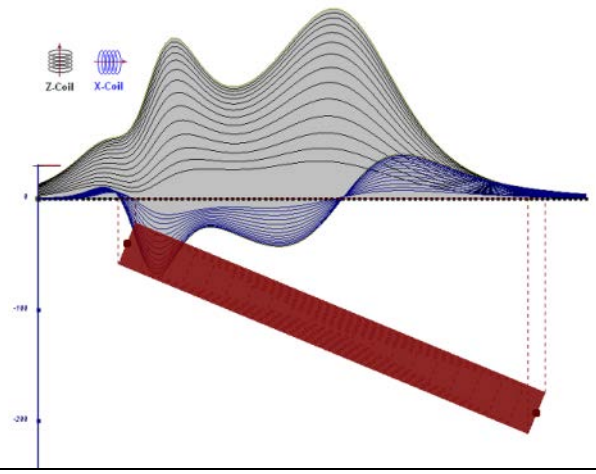

Figure I-13. inclined long thick plate

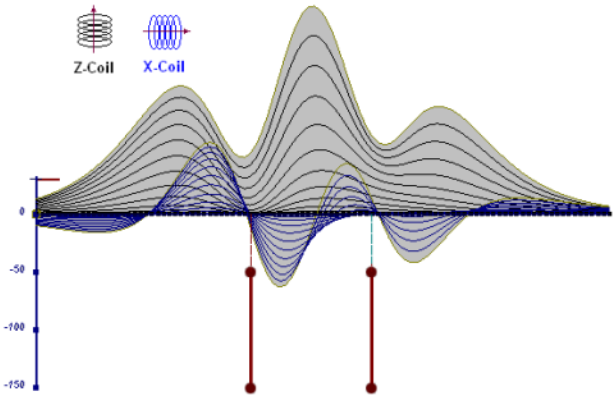

Figure I-14. two vertical thin plates

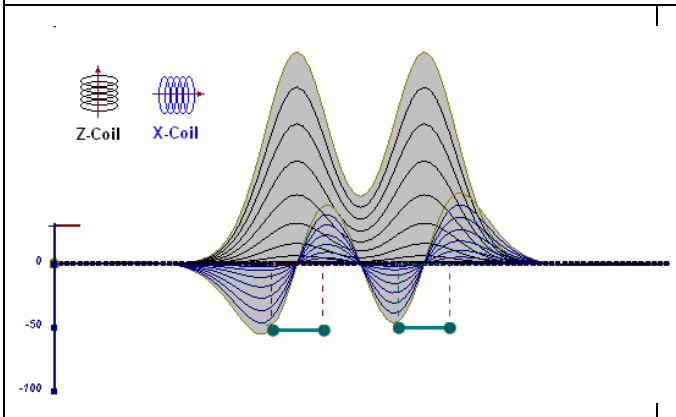

Figure I-15. two horizontal thin plates

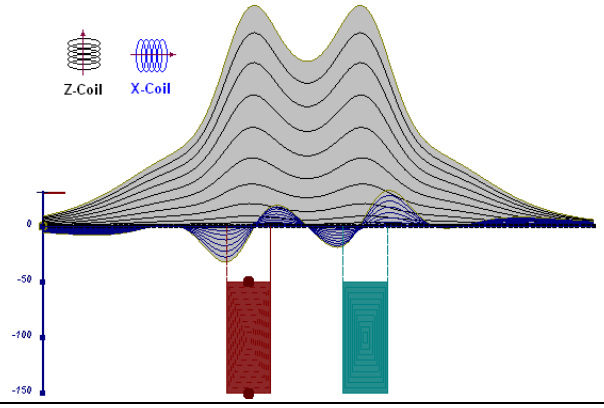

Figure I-16. two vertical thick plates

The same type of target but with different thickness, for example, creates different form of the response:

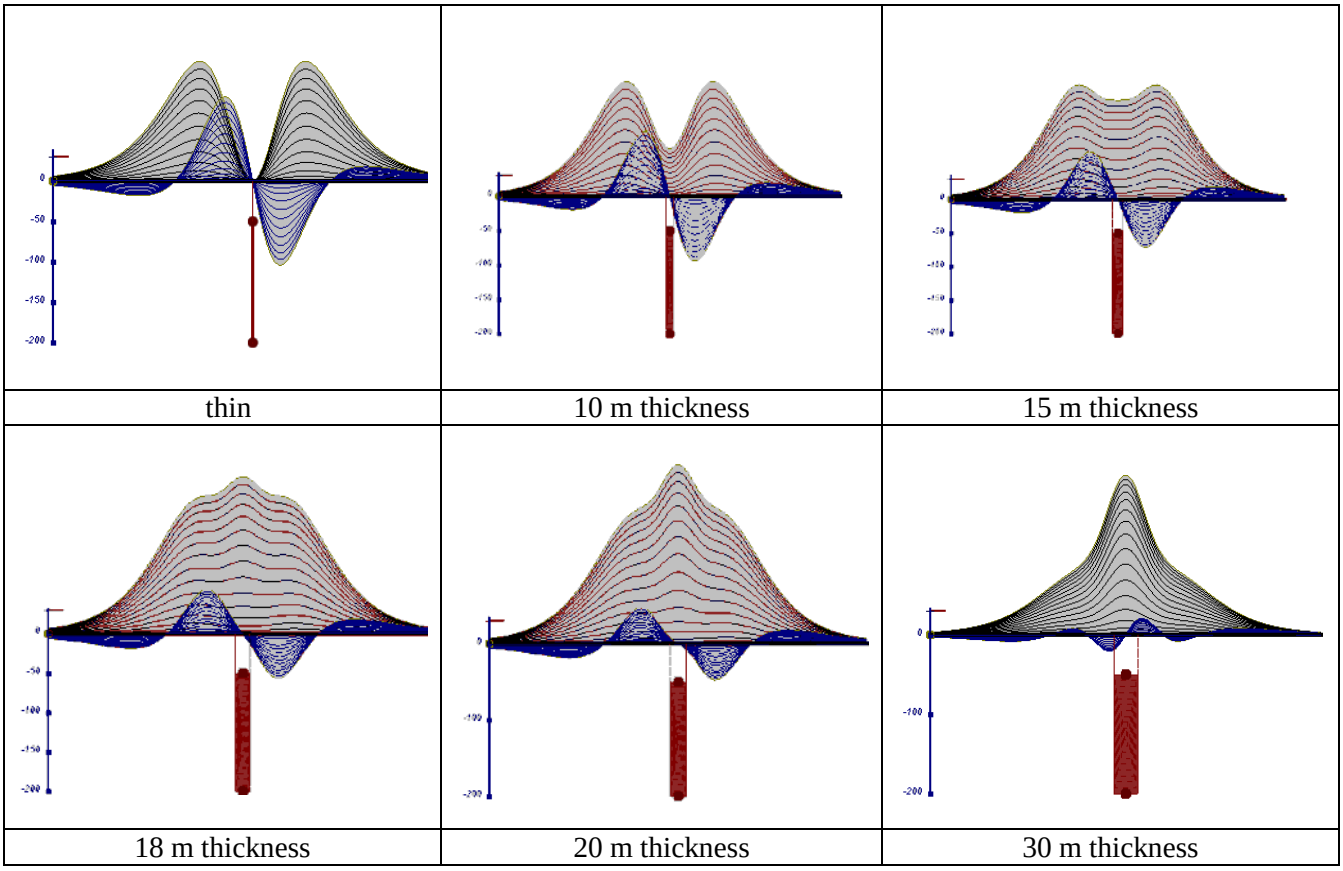

Figure I-17. Conductive vertical plate, depth 50 m, strike length 200 m, depth extend 150 m.

Alexander Prikhodko, PhD, *P.Geo*.
Geotech Ltd.
September 2010

Appendix J. EM TIME CONSTANT (TAU) ANALYSIS

Estimation of time constant parameter[4] in transient electromagnetic method is one of the steps toward the extraction of the information about conductances beneath the surface from TEM measurements.

The most reliable method to discriminate or rank conductors from overburden, background or one and other is by calculating the EM field decay time constant (TAU parameter), which directly depends on conductance despite their depth and accordingly amplitude of the response.

Theory

As established in electromagnetic theory, the magnitude of the electromotive force (emf) induced is proportional to the time rate of change of primary magnetic field at the conductor. This emf causes eddy currents to flow in the conductor with a characteristic transient decay, whose time constant (Tau) is a function of the conductance of the survey target or conductivity and geometry (including dimensions) of the target. The decaying currents generate a proportional secondary magnetic field, the time rate of change of which is measured by the receiver coil as induced voltage during the off time.

The receiver coil output voltage ($\mathbf{e_0}$) is proportional to the time rate of change of the secondary magnetic field and has the form,

$$e_0 \alpha (1 / \tau) e^{-(t/\tau)}$$

Where,
τ = L/R is the characteristic time constant of the target (TAU)
R = resistance
L = inductance

From the expression, conductive targets that have small value of resistance and hence large value of τ (tau) yield signals with small initial amplitude that decays relatively slowly with progress of time. Conversely, signals from poorly conducting targets that have large resistance value and small τ, have high initial amplitude but decay rapidly with time[4] (Figure J-1).

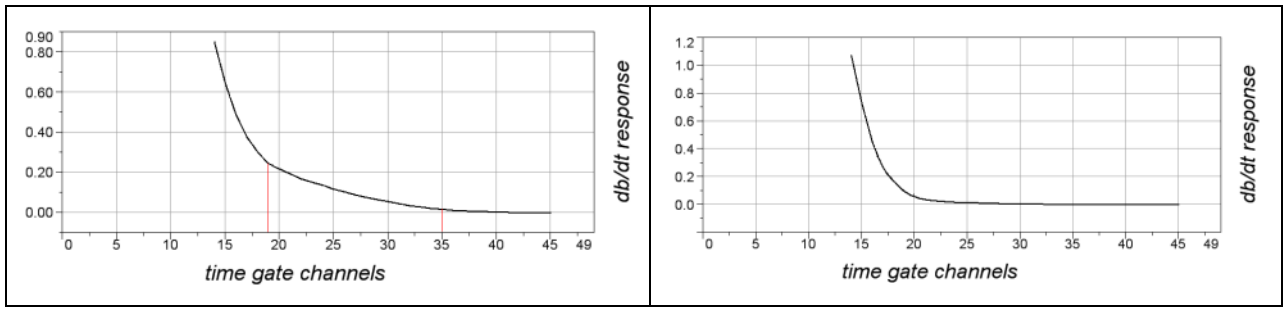

Figure J-1. Left – presence of good conductor, right – poor conductor.

[4] McNeill, JD, 1980, "Applications of Transient Electromagnetic Techniques", Technical Note TN-7 pg 5, Geonics Limited, Mississauga, Ontario.

EM Time Constant (Tau) Calculation

The EM Time-Constant (TAU) is a general measure of the speed of decay of the electromagnetic response and indicates the presence of eddy currents in conductive sources as well as reflecting the "conductance quality" of a source. Although TAU can be calculated using either the measured dB/dt decay or the calculated B-field decay, dB/dt is commonly preferred due to better stability (S/N) relating to signal noise. Generally, TAU calculated on base of early time response reflects both near surface overburden and poor conductors whereas, in the late ranges of time, deep and more conductive sources, respectively. For example early time TAU distribution in an area that indicates conductive overburden is shown in Figure J-2. In Figure J-3, the full time range is displayed, showing the expression of a deep, highly-conductive target in the left side of the image.

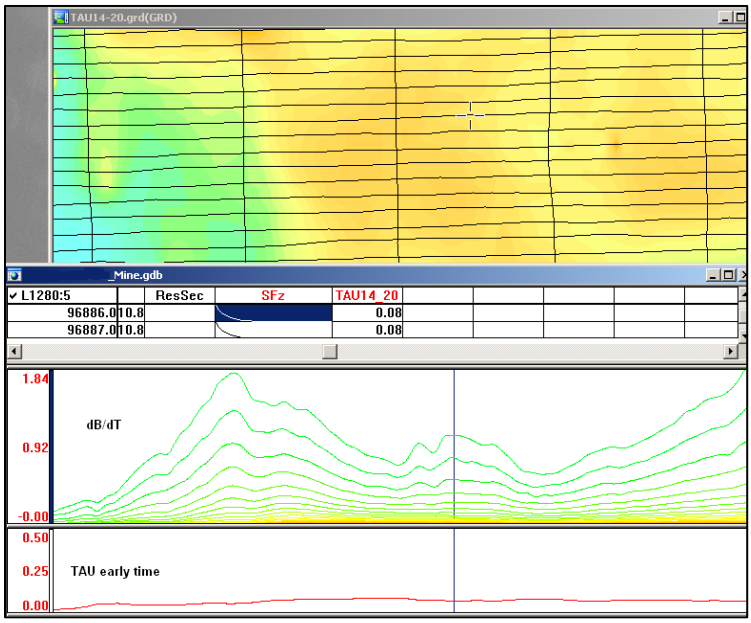

Figure J-2. Map of early time TAU. Area with overburden conductive layer and local sources.

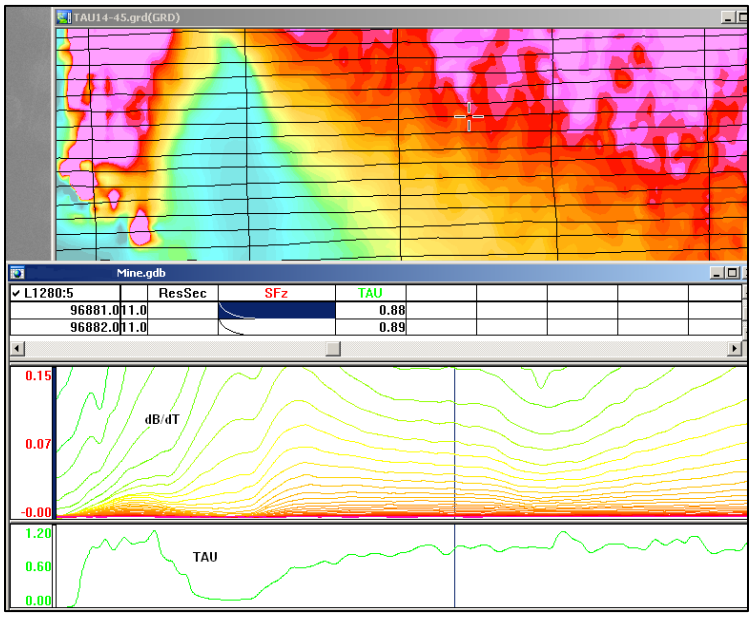

Figure J-3. Map of full time range TAU with EM anomaly due to deep highly conductive target.

There are many advantages of TAU maps:

- TAU depends only on one parameter (conductance) in contrast to response magnitude;
- TAU is integral parameter, which covers time range and all conductive zones and targets are displayed independently of their depth and conductivity on a single map.
- Very good differential resolution in complex conductive places with many sources with different conductivity.
- Signs of the presence of good conductive targets are amplified and emphasized independently of their depth and level of response accordingly.

In the example shown in figures J-4 and J-5, 3 local targets are defined, each of them with a different depth of burial, as indicated on the resistivity depth image (RDI). All are very good conductors but the deeper target (number 2) has a relatively weak dB/dt signal yet also features the strongest total TAU (Figure J-4). This example highlights the benefit of TAU analysis in terms of an additional target discrimination tool.

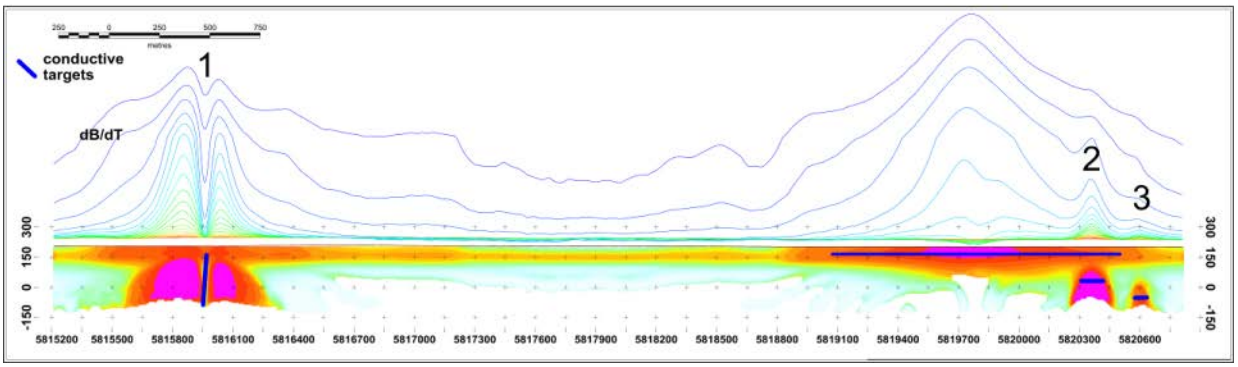

Figure J-4. dB/dt profile and RDI with different depths of targets.

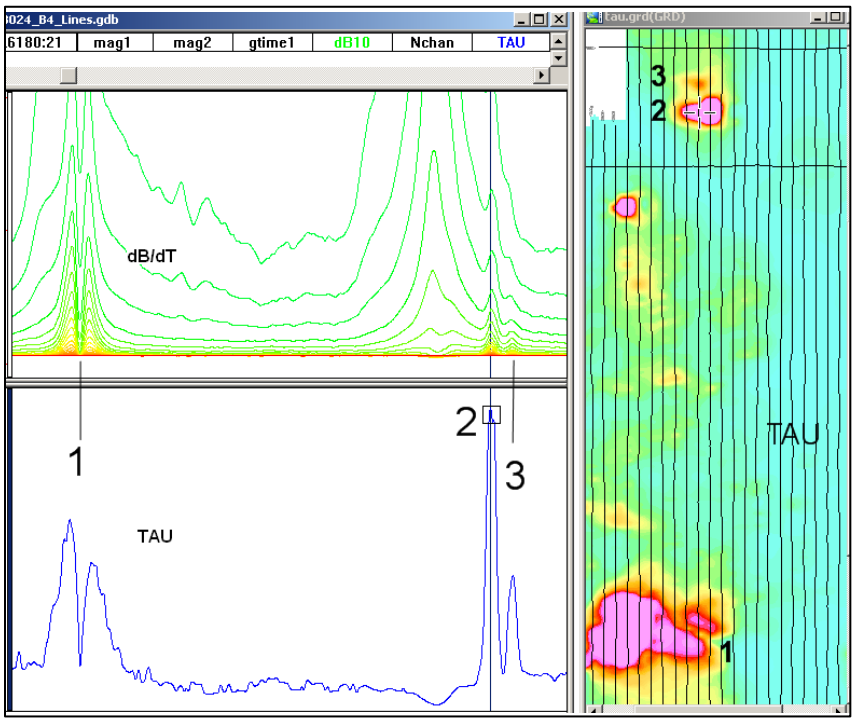

Figure J-5. Map of total TAU and dB/dt profile.

The EM Time Constants for dB/dt and B-field were calculated using the "sliding Tau" in-house program developed at Geotech[5]. The principle of the calculation is based on using of time window (4 time channels) which is sliding along the curve decay and looking for latest time channels which have a response above the level of noise and decay. The EM decays are obtained from all available decay channels, starting at the latest channel. Time constants are taken from a least square fit of a straight-line (log/linear space) over the last 4 gates above a preset signal threshold level (Figure J-6). Threshold settings are pointed in the "label" property of TAU database channels. The sliding Tau method determines that, as the amplitudes increase, the time-constant is taken at progressively later times in the EM decay. Conversely, as the amplitudes decrease, Tau is taken at progressively earlier times in the decay. If the maximum signal amplitude falls below the threshold, or becomes negative for any of the 4 time gates, then Tau is not calculated and is assigned a value of "dummy" by default.

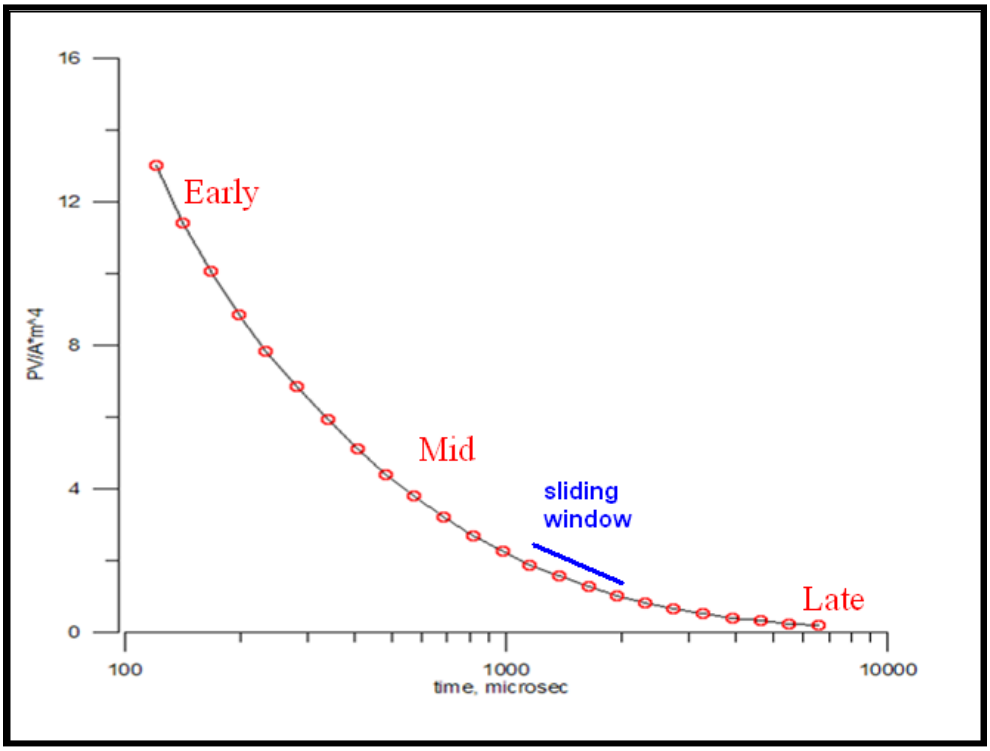

Figure J-6. Typical dB/dt decays of VTEM data.

Alexander Prikhodko, PhD, *P.Geo.*
Geotech Ltd.
September 2010

[5] Geotech Ltd. internal report by A.Prikhodko

Appendix K. TEM RESISTIVITY DEPTH IMAGING (RDI)

Resistivity depth imaging (RDI) is technique used to rapidly convert EM profile decay data into an equivalent resistivity versus depth cross-section, by deconvolution of the measured TEM data. The used RDI algorithm of Resistivity-Depth transformation is based on scheme of the apparent resistivity transform of Maxwell A.Meju (1998)[6] and TEM response from conductive half-space. The program was developed by Alexander Prikhodko and depth calibrated based on forward plate modelling for VTEM system configuration (Figures K-1 to 11).

RDIs provide reasonable indications of conductor relative depth and vertical extent, as well as accurate 1D layered-earth apparent conductivity/resistivity structure across VTEM flight lines.

Approximate depth of investigation of a TEM system, image of secondary field distribution in half space, effective resistivity, initial geometry and position of conductive targets is the information obtained on base of the RDIs.

Maxwell forward modelling with RDI sections from the synthetic responses (VTEM system)

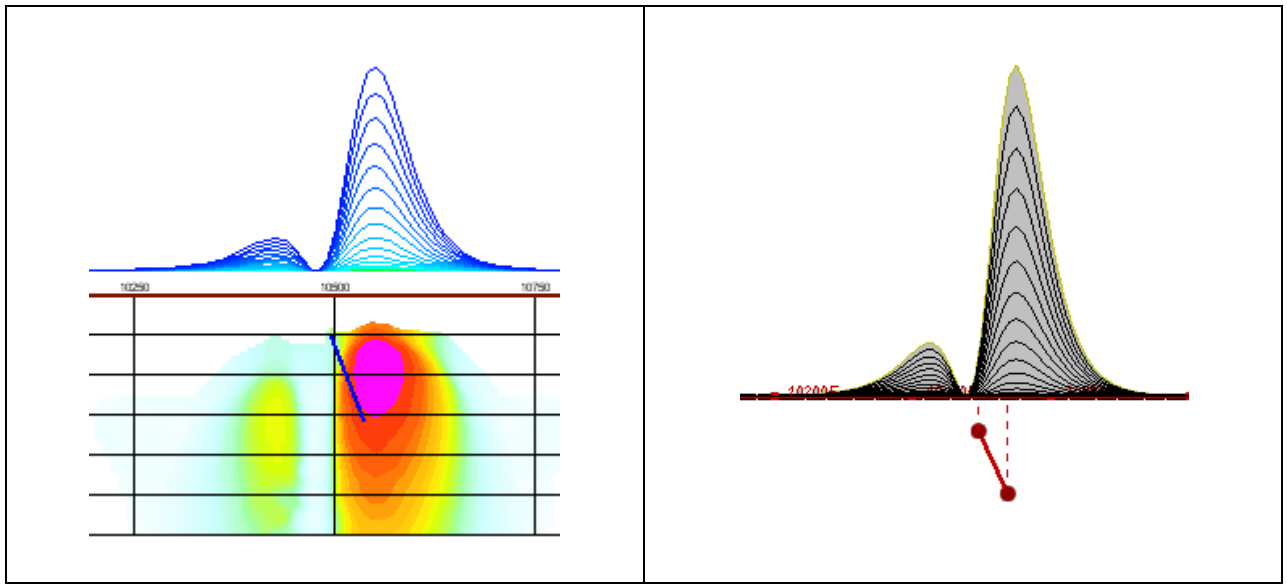

Figure K-1. Maxwell plate model and RDI from the calculated response for conductive “thin” plate (depth 50 m, dip 65 degree, depth extend 100 m).

[6] Meju, M.A. 1998. Short Note: A simple method of transient electromagnetic data analysis, Geophysics, **63**, 405–410.

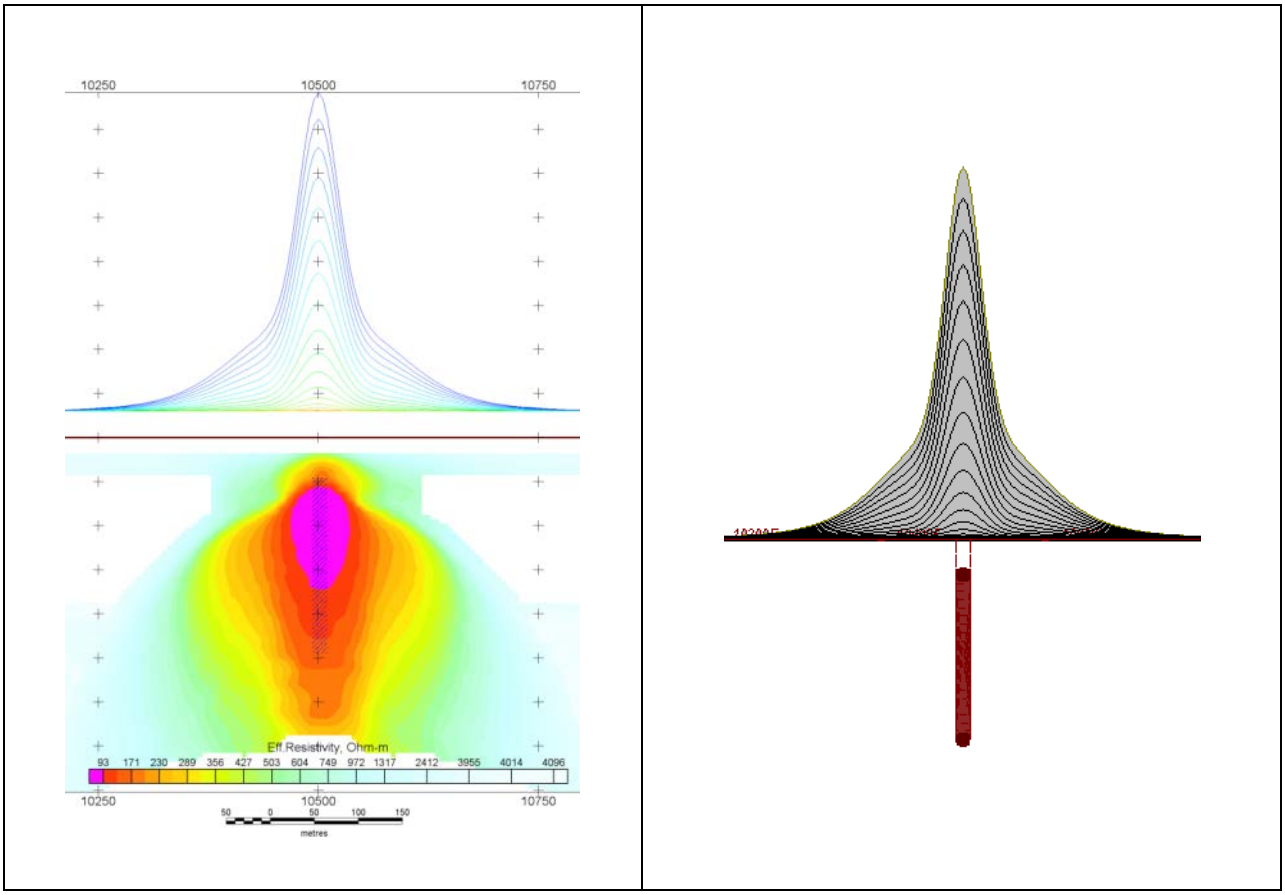

Figure K-2. Maxwell plate model and RDI from the calculated response for "thick" plate 18 m thickness, depth 50 m, depth extend 200 m).

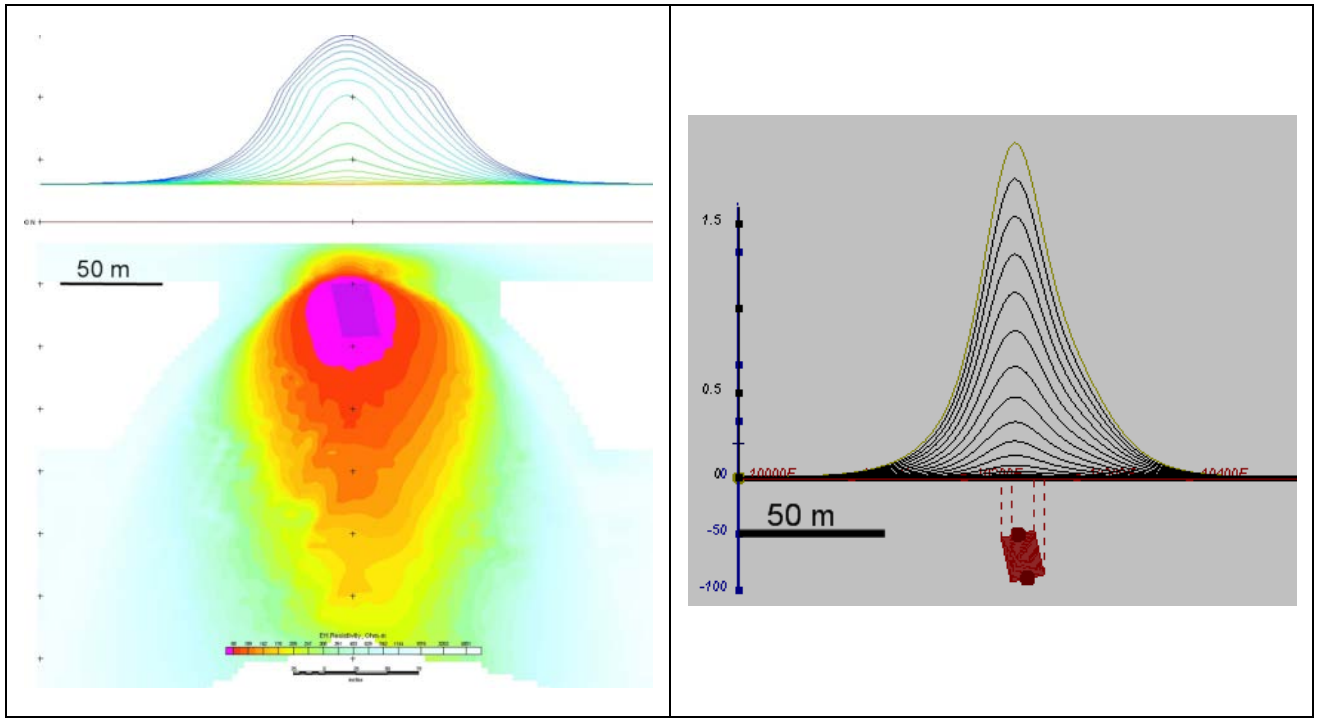

Figure K-3. Maxwell plate model and RDI from the calculated response for bulk ("thick") 100 m length, 40 m depth extend, 30 m thickness.

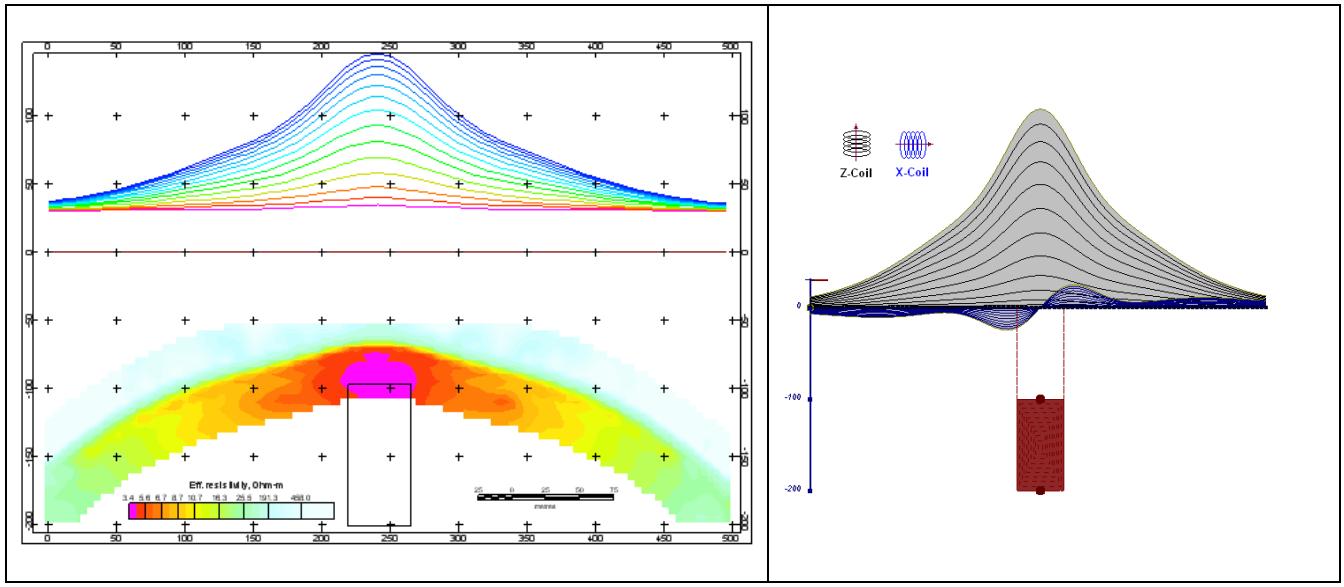

Figure K-4. Maxwell plate model and RDI from the calculated response for "thick" vertical target (depth 100 m, depth extend 100 m). 19-44 channels.

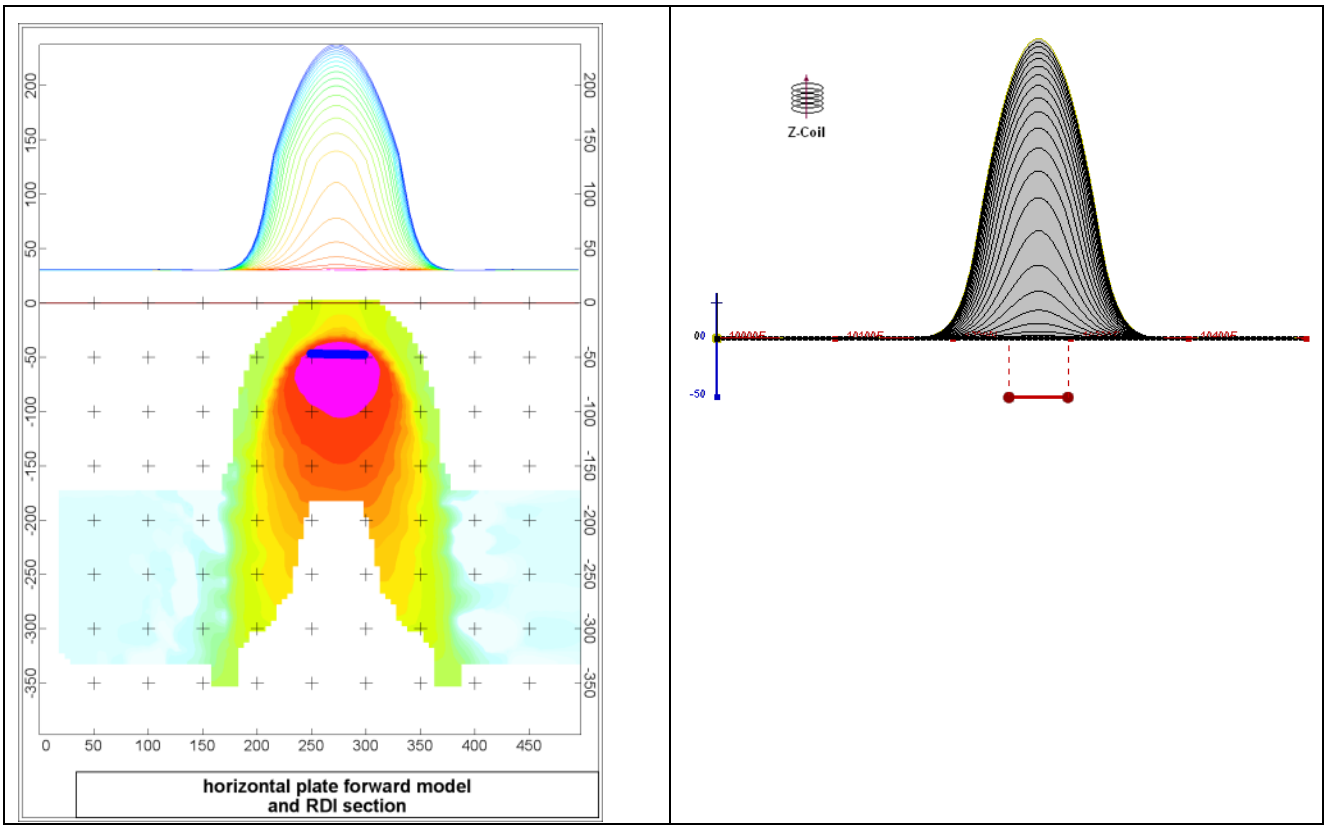

Figure K-5. Maxwell plate model and RDI from the calculated response for horizontal thin plate (depth 50 m, dim 50x100 m). 15-44 channels.

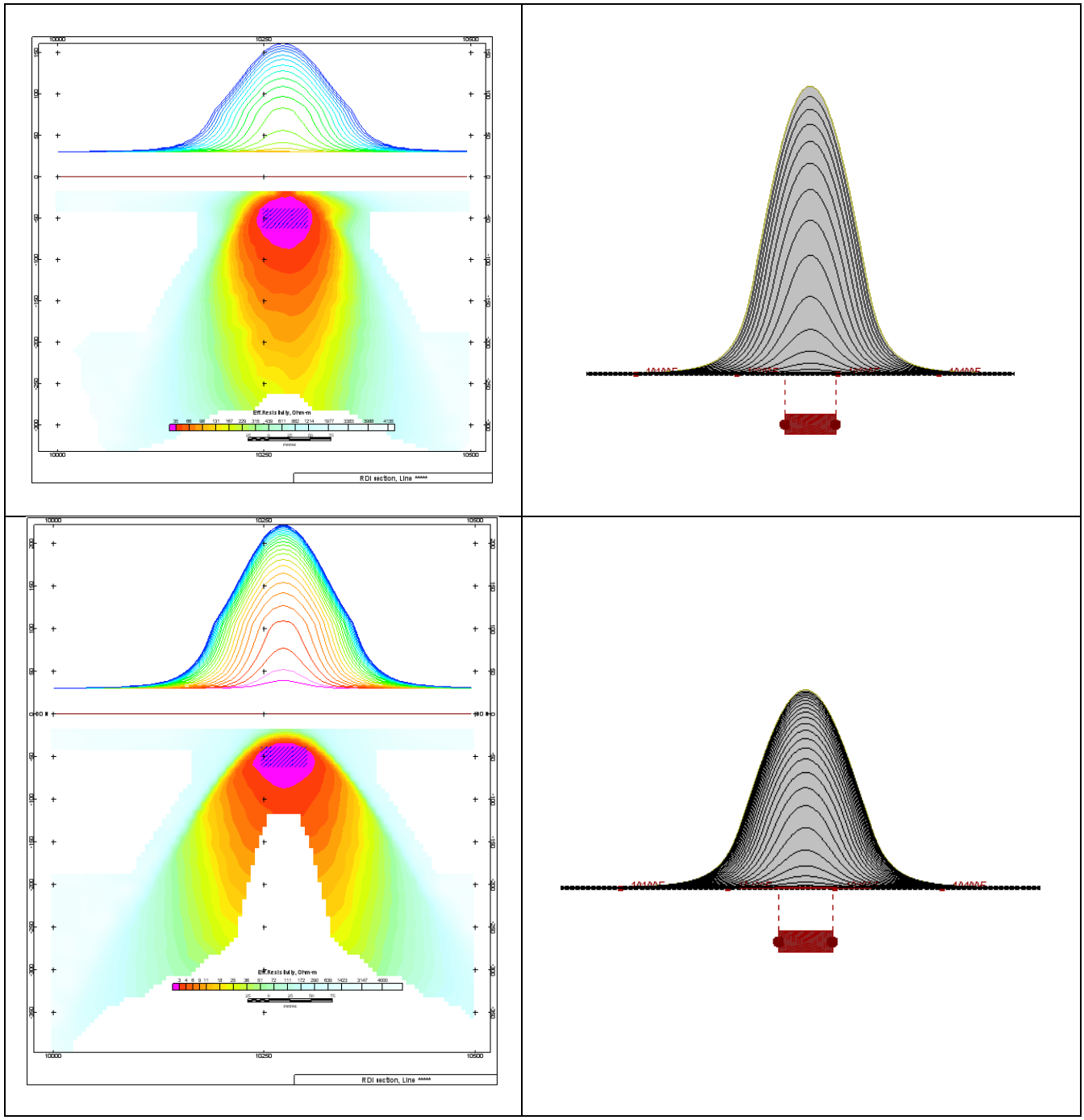

Figure K-6. Maxwell plate model and RDI from the calculated response for horizontal thick (20m) plate – less conductive (on the top), more conductive (below)

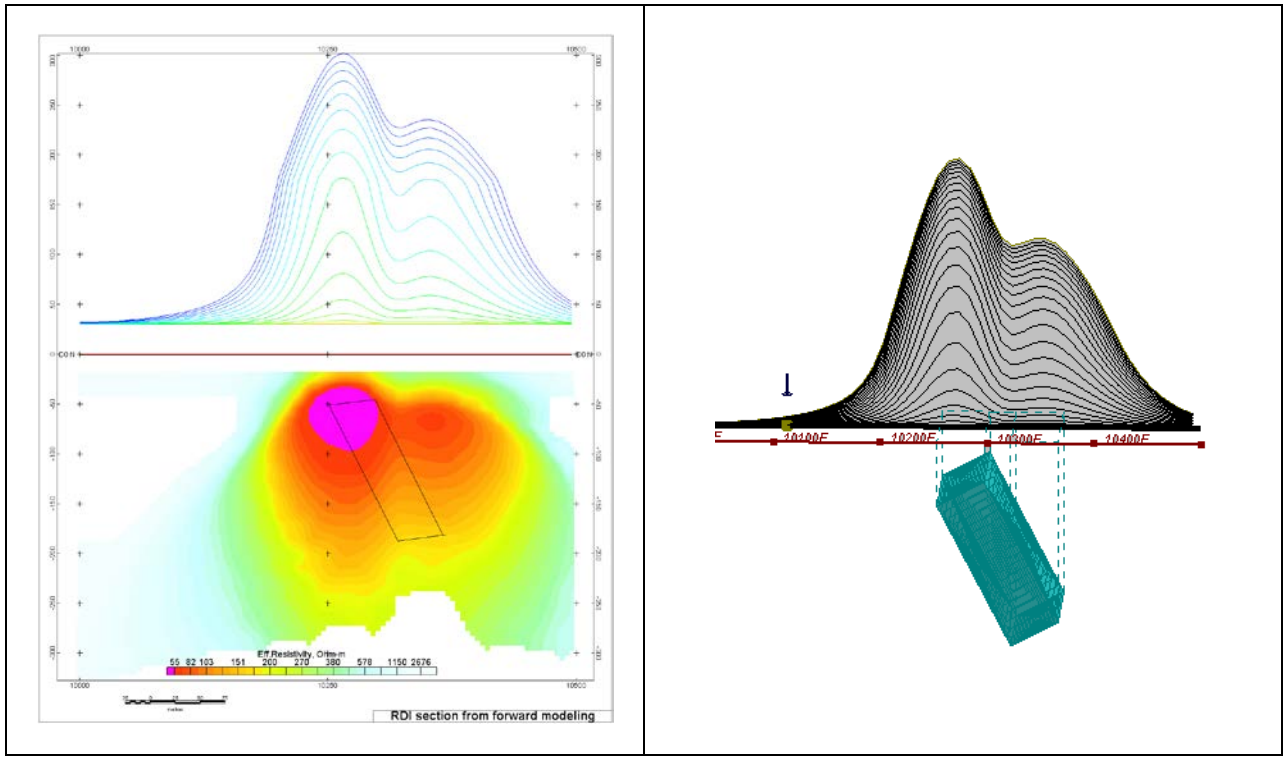

Figure K-7. Maxwell plate model and RDI from the calculated response for inclined thick (50m) plate. Depth extends 150 m, depth to the target 50 m.

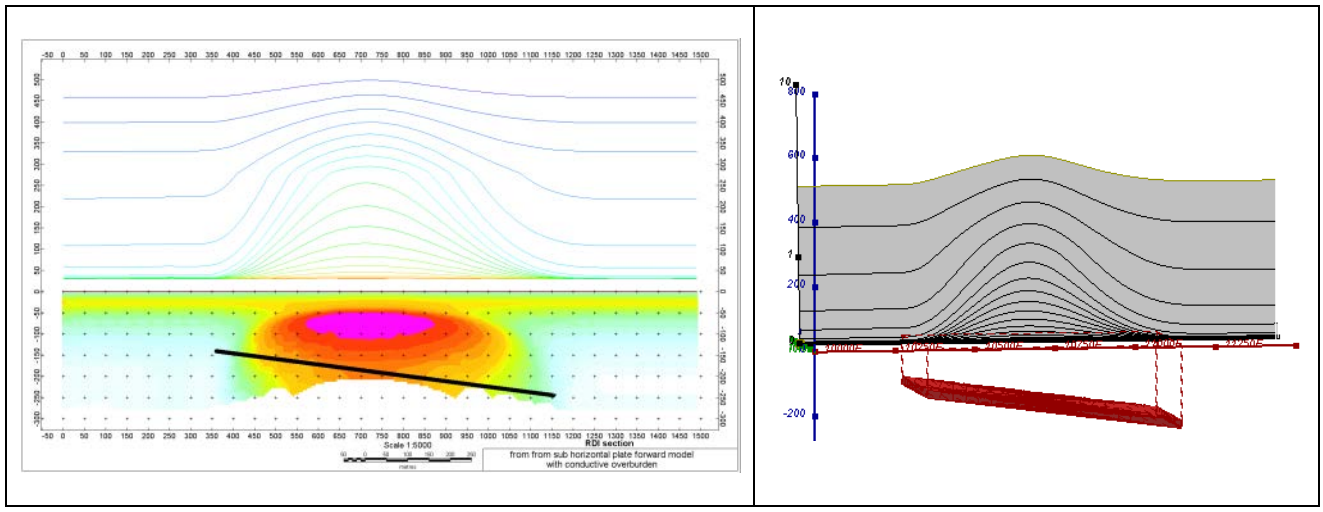

Figure K-8. Maxwell plate model and RDI from the calculated response for the long, wide and deep sub-horizontal plate (depth 140 m, dim 25x500x800 m) with conductive overburden.

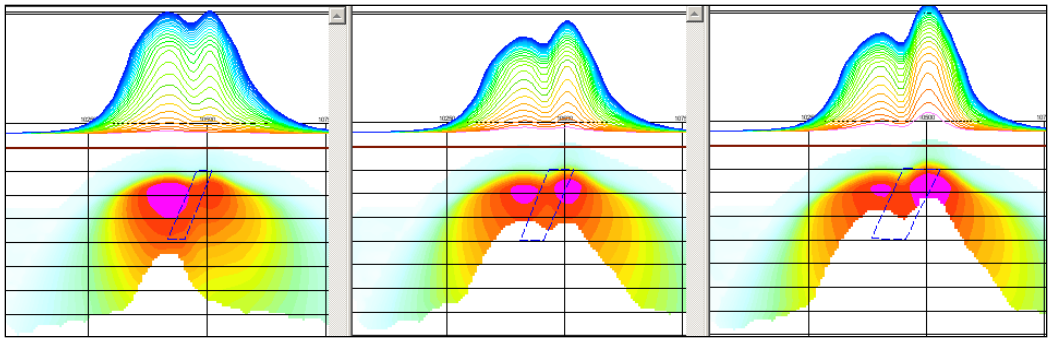

Figure K-9. Maxwell plate models and RDIs from the calculated response for "thick" dipping plates (35, 50, 75 m thickness), depth 50 m, conductivity 2.5 S/m.

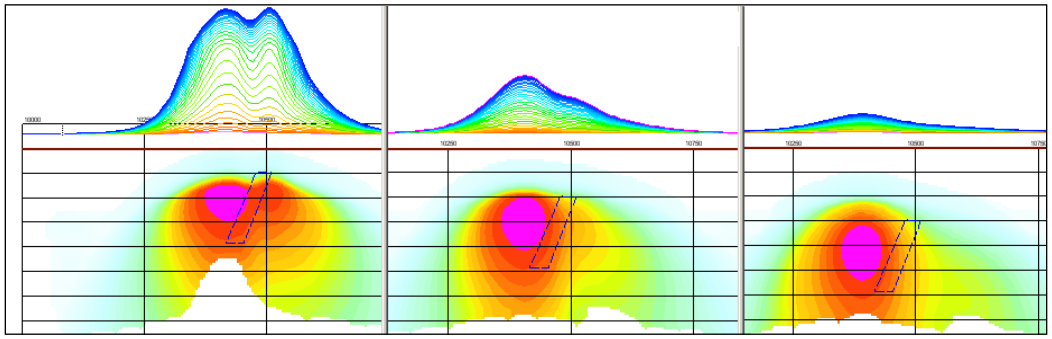

Figure K-10. Maxwell plate models and RDIs from the calculated response for "thick" (35 m thickness) dipping plate on different depth (50, 100, 150 m), conductivity 2.5 S/m.

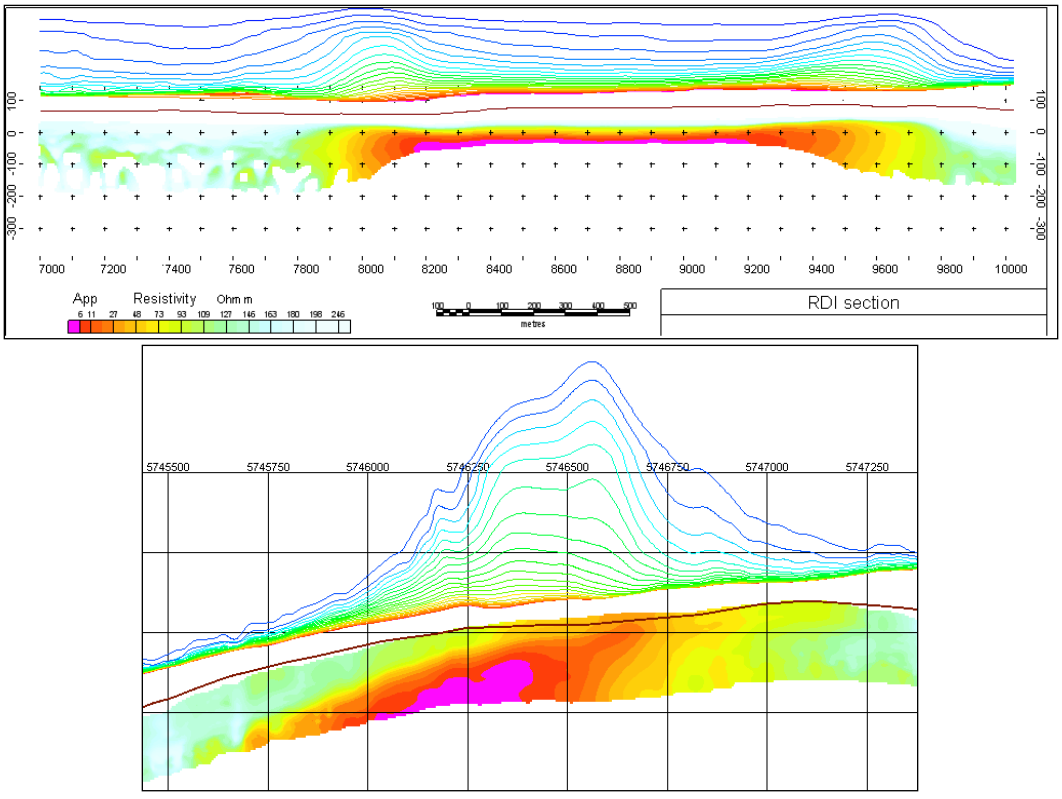

Figure K-11. RDI section for the real horizontal and slightly dipping conductive layers.

FORMS OF RDI PRESENTATION

Presentation of series of lines

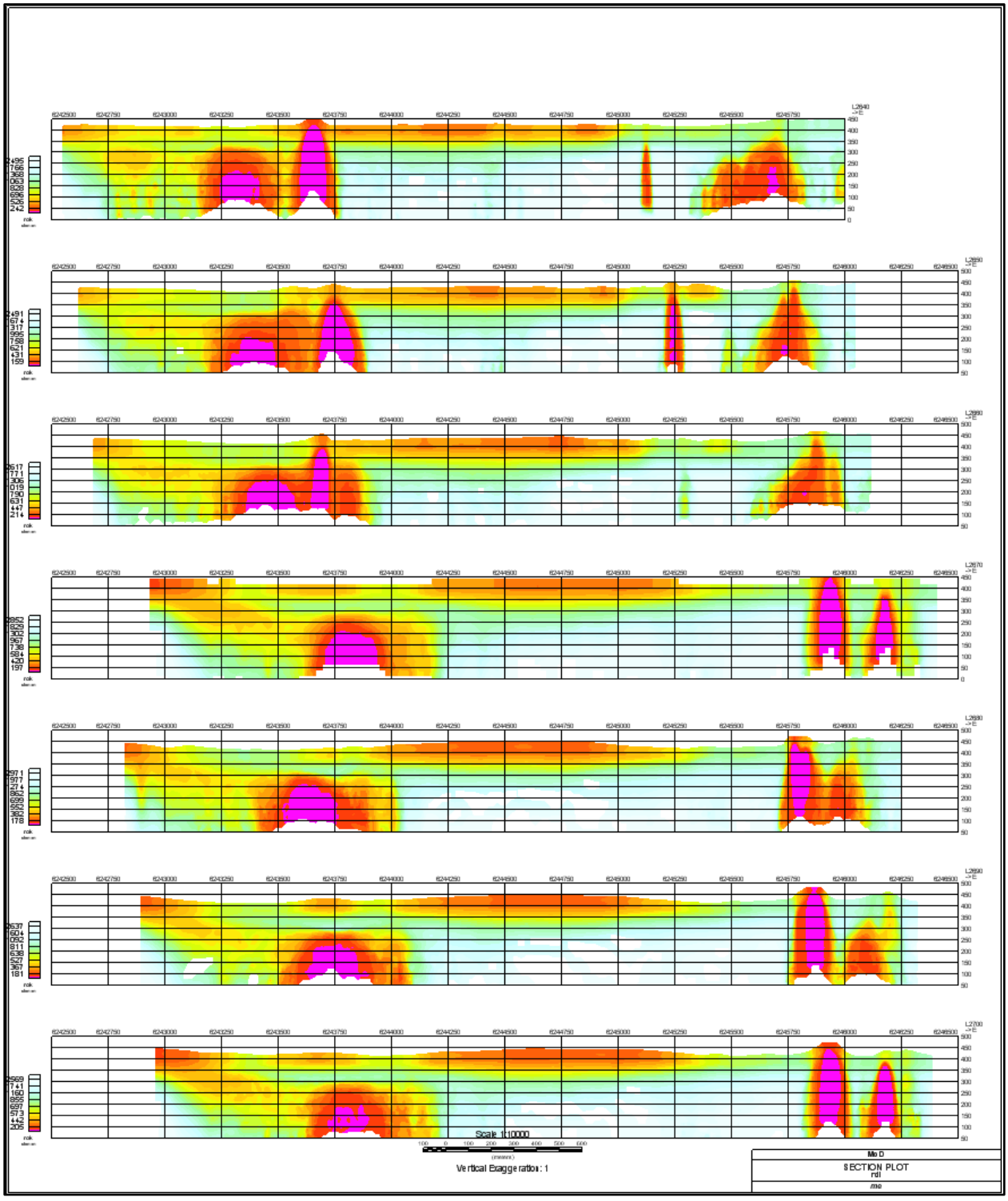

3D presentation of RDIs

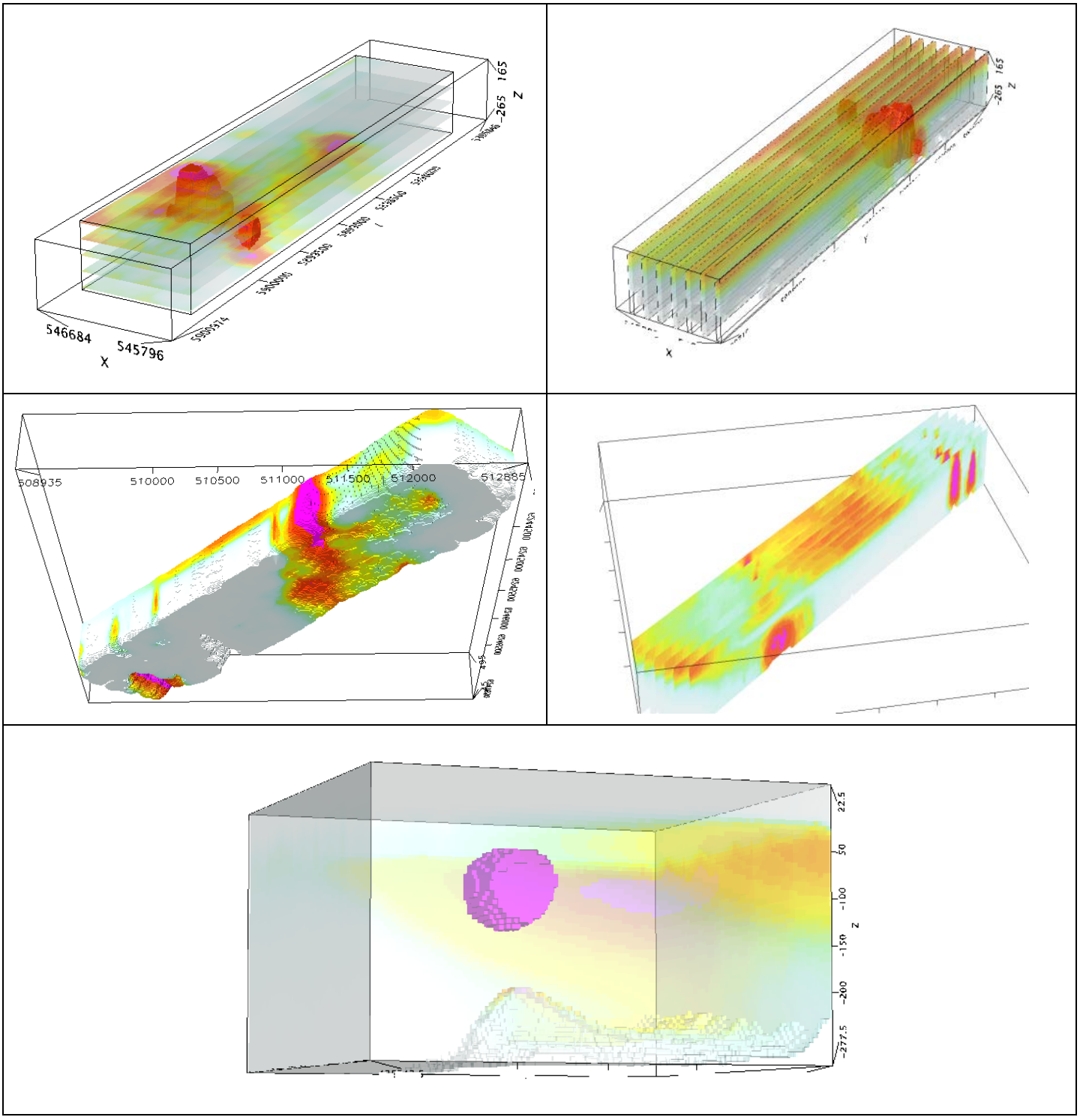

Apparent Resistivity Depth Slices plans

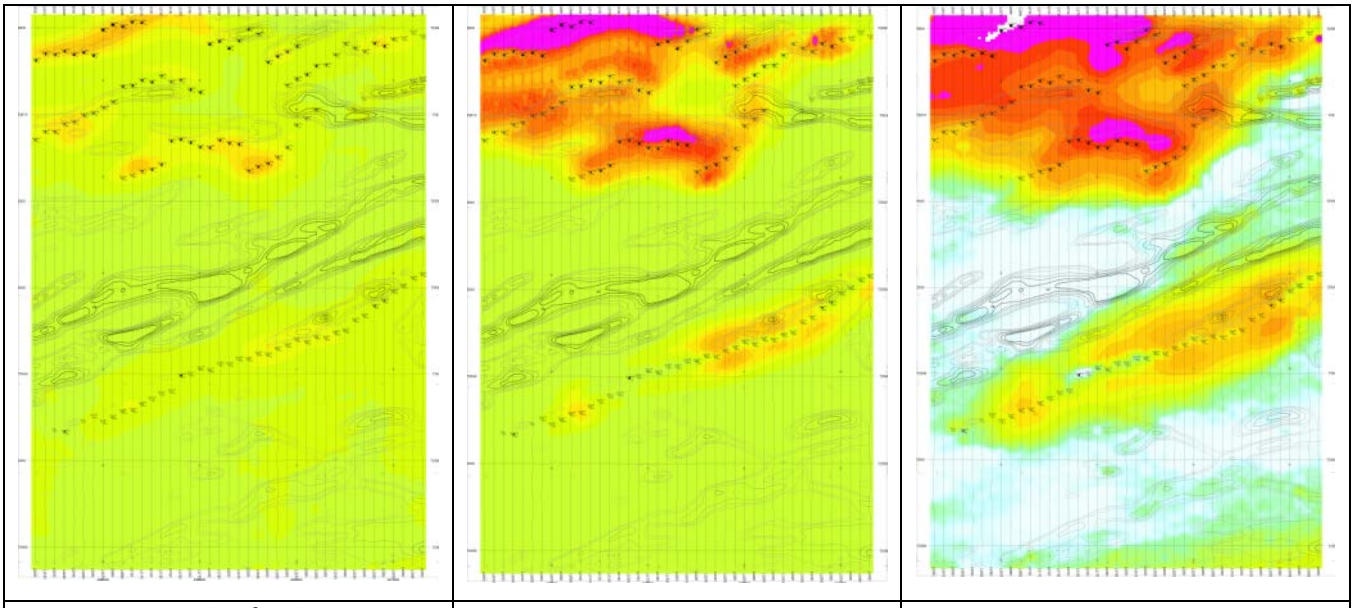

0 m (surface)	-100 m	-200 m

3d views of apparent resistivity depth slices

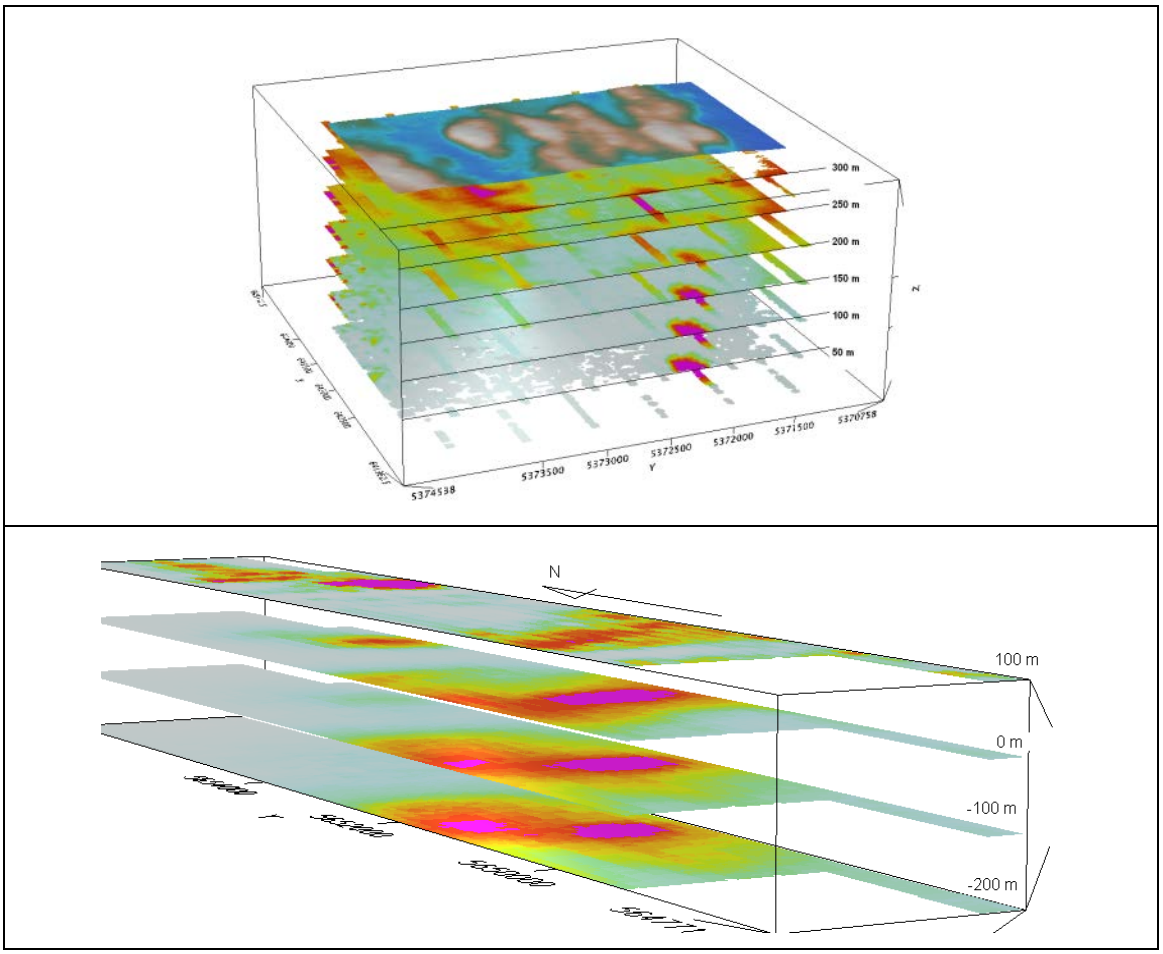

Real base metal targets in comparison with RDIs:

RDI section of the line over Caber deposit (“thin” subvertical plate target and conductive overburden).

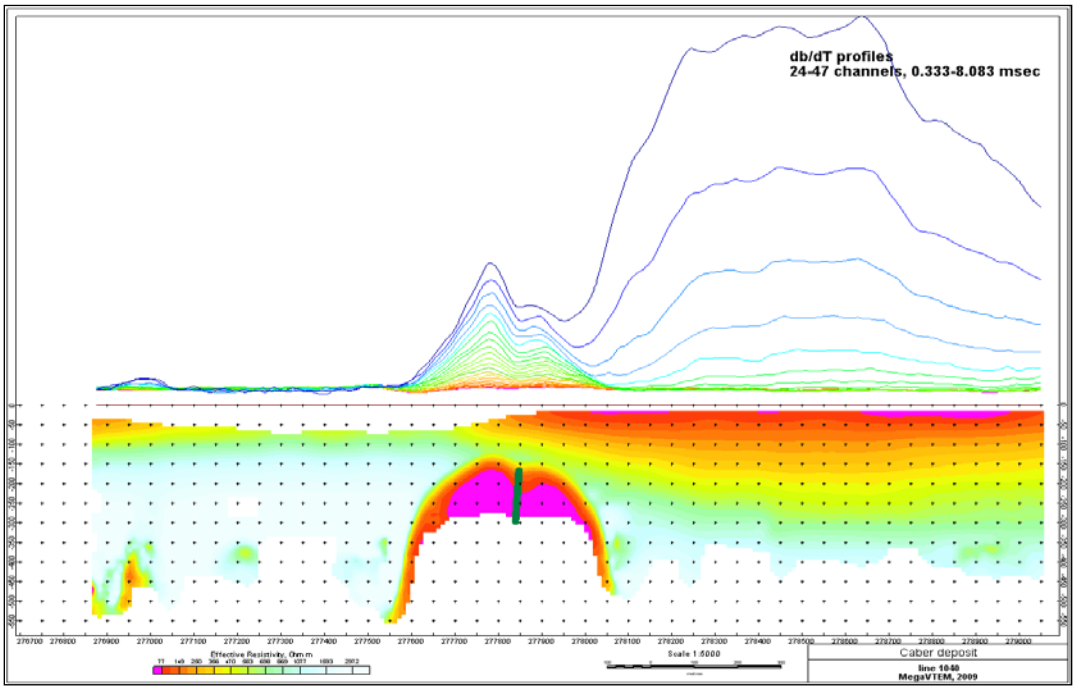

3-D RDI voxels with base metals ore bodies (Middle East):

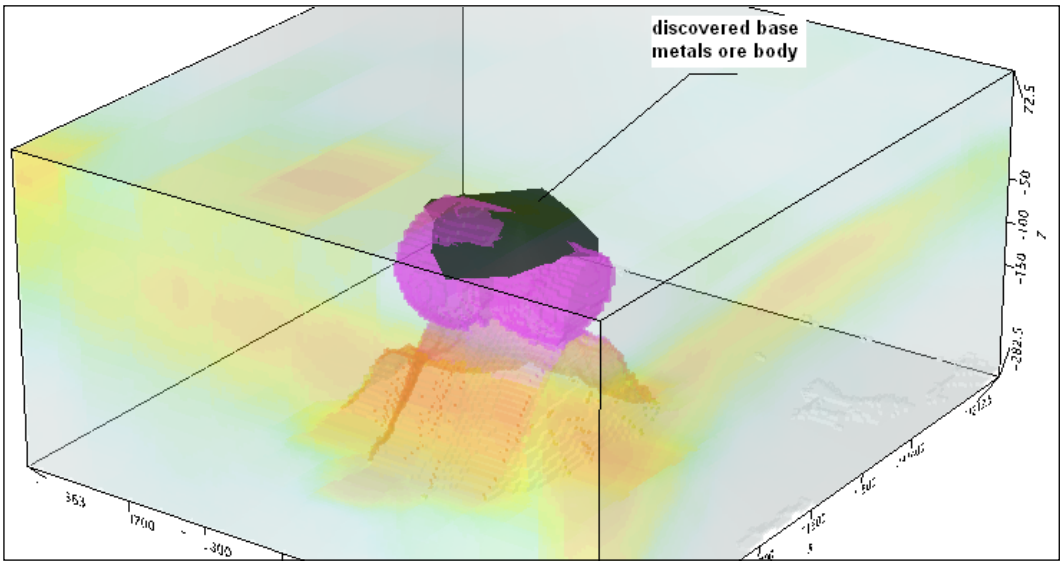

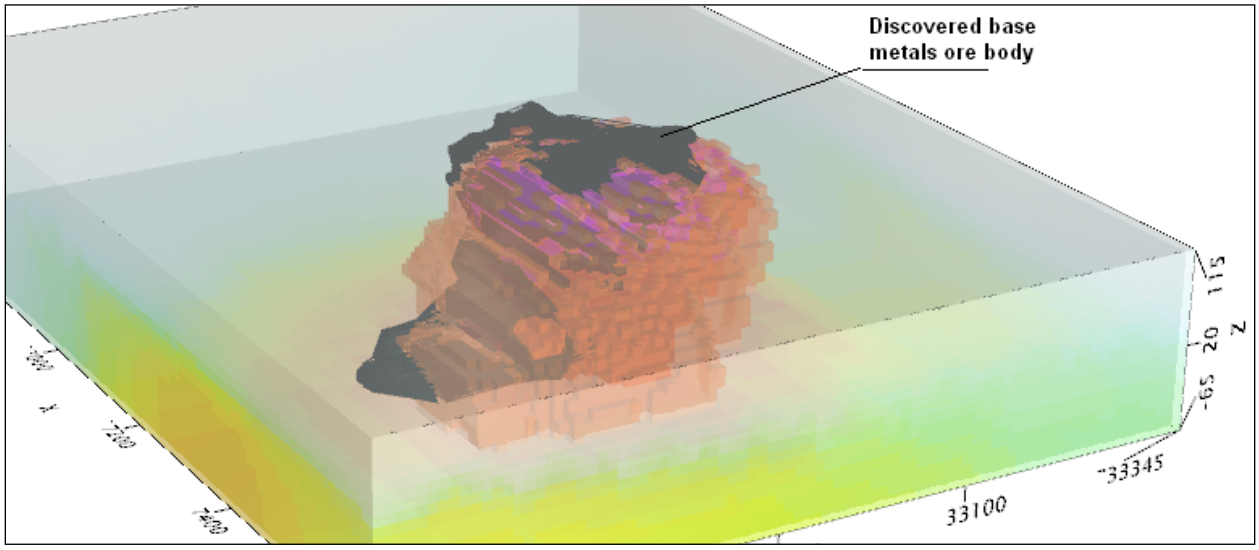

Alexander Prikhodko, PhD, *P.Geo.*
Geotech Ltd.
April 2011

Appendix L. TEST SITES AND CALIBRATIONS

7.4.1. BOURGET TEST SITE

The Bourget test was flown to ensure that the aeromagnetic system measures the total field values with an absolute accuracy of 10 nT or less after the aircraft has been compensated. This test requires that data is recorded coincidentally with the data from the nearby Ottawa magnetic observatory.

With the magnetic sensor at 1000 feet, the 4 cardinal headings are flown, repeating the entire test twice for a total of 8 passes. The test was performed on July 20, 2014 as presented in Figure L-1.

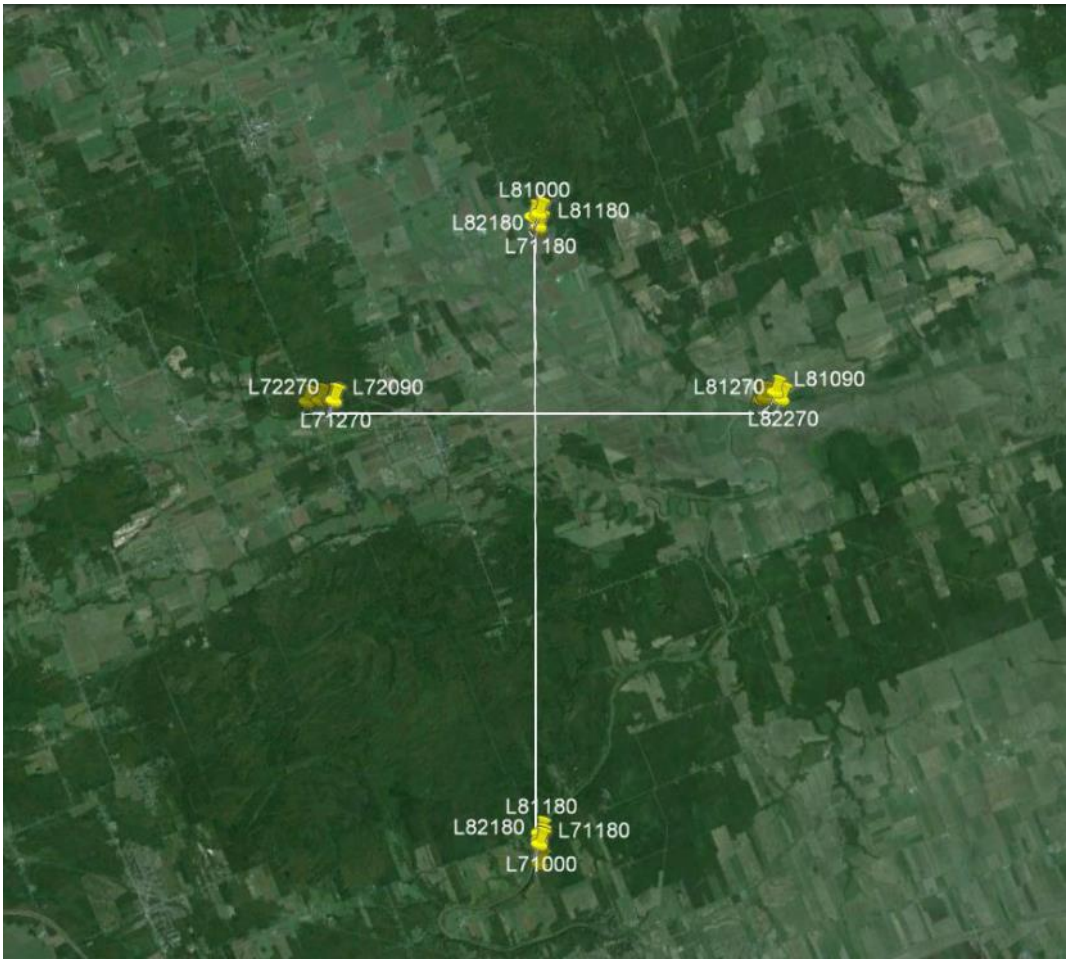

Figure L-1. Bourget Test lines on Google Earth™ (July 20, 2014).

AEROMAGNETIC SURVEY SYSTEM CALIBRATION TEST RANGES AT BOURGET, ONTARIO

AIRCRAFT TYPE AND REGISTRATION: AS 350 B3E C-GEOC
ORGANIZATION (COMPANY): Geotech Ltd/Geotech Aviation
MAGNETOMETER TYPE: Geometrics G-823A Caesium Vapour
MAGNETOMETER SERIAL NUMBER: C2202 s/n 75373
COMPILED BY: Nick Venter

DATE: July 20th 2014
HEIGHT FLOWN: 1000 FEET
SAMPLING RATE: 10 samples / SECOND
DATA ACQUISITION SYSTEM: Geotech DAQ

Direction of flight across the Crossroads	Time that Survey Aircraft was over the Crossroads (HH/MM/SS) Greenwich Mean Time	Total Field Value (nT) Recorded in Survey Aircraft over Crossroads (T1)	Observatory Diurnal Reading at Previous Minute i.e. Hours + Minutes (T2) from Printout	Observatory Diurnal Reading at Subsequent Minute i.e. H hours + (M + 1) mins. (T3) from Printout	Interpolated Observatory Diurnal Reading at Time H hours + M mins + S sec T4 = T2 + S (T3 – T2) ----- 60	Calculated Observatory Value T5 = T4 - C*	Error Value T6 = T1 - T5
EXAMPLE	20:34:40 Z	56840.4 nT	57397.5 nT	57398.3 nT	57398.0 nT	56842.0 nT	-1.6 nT
NORTH	18:58:47.4	54009.07 nT	54555.03	54555.23	54555.18 nT	54005.18 nT	3.88 nT
SOUTH	18:44:05.6	54005.79 nT	54553.35	54553.54	54553.36 nT	54003.36 nT	2.42 nT
EAST	18:08:30.6	54001.93 nT	54549.63	54549.91	54549.77 nT	53999.77 nT	2.16 nT
WEST	18:16:46.0	54002.62 nT	54550.35	54550.58	54550.52 nT	54000.52 nT	2.09 nT
NORTH	19:19:15.4	54009.59 nT	54557.10	54557.42	54557.18 nT	54007.18 nT	2.41 nT
SOUTH	19:04:54.4	54009.29 nT	54555.91	54556.31	54556.27 nT	54006.27 nT	3.02 nT
EAST	18.24.27.2	54004.14 nT	54551.41	54551.56	54551.47 nT	54001.47 nT	2.66 nT
WEST	18:32:44.0	54003.93 nT	54551.67	54551.79	54551.75 nT	54001.75 nT	2.17 nT

*C is the difference in the total field between the Blackburn or Meanook Observatory value (O) and the value (B) at the point above the crossroads at a given height.
Blackburn Observatory: 1000 Feet, C = (O-B) = 550 nT; 500 Feet, C = 556 nT
Meanook Observatory: 1000 Feet, C = (O-B) = 0 nT; 500 Feet, C = 0 nT
Total = 20.81 nT

Average North-South Heading Error (T6 North - T6 South) = 0.42 nT
Average East-West Heading Error (T6 East - T6 West) = 0.28 nT
Number of Passes for Average = 8 2.60 nT

The completed document must be forwarded to the GSC Project Leader prior to the start of field operations and a copy must be attached to the next weekly report.

7.4.2. REID–MAHAFFEY TEST SITE

The Reid–Mahaffey test, located near Timmins, is flown as a prerequisite to all surveys for the Government of Ontario Ministry of Northern Development and Mines (MNDM) to ensure that the airborne electromagnetic system is operational and responds to a broad range of electromagnetic responses at different depths below surface.

Sixteen (16) traverse lines are flown at 200 m line spacing and north-south oriented, similar to the survey specifications of Block 1. Four (4) tie-lines are flown perpendicular to traverse lines, as indicated in the tables below and figure L-2. The test was performed with EM bird terrain clearance of 30 m. These lines were flown on August 5, 2014.

Line orientation for the Reid–Mahaffey Test.

Traverse lines

Traverse lines	Direction
10	N to S
20	S to N
30	N to S
40	S to N
50	N to S
60	S to N
70	N to S
80	S to N
90	N to S
100	S to N
110	N to S
120	S to N
130	N to S
140	S to N
150	N to S
160	S to N

Tie lines

Tie lines	Direction
9010	W to E
9020	E to W
9030	W to E
9040	E to W

On the location of line 40, six additional lines are flown in north-south direction at different level of EM bird terrain clearance: 50 m, 75 m, 100 m, 125 m, 150 m and 200m, as indicated in table below. These lines were flown on August 5, 2014.

EM bird terrain clearance on line 40, Reid–Mahaffey Test

Location of L40	EM bird altitude (m)
4050	50
4075	75
4100	100
4125	125
4150	150
4200	200

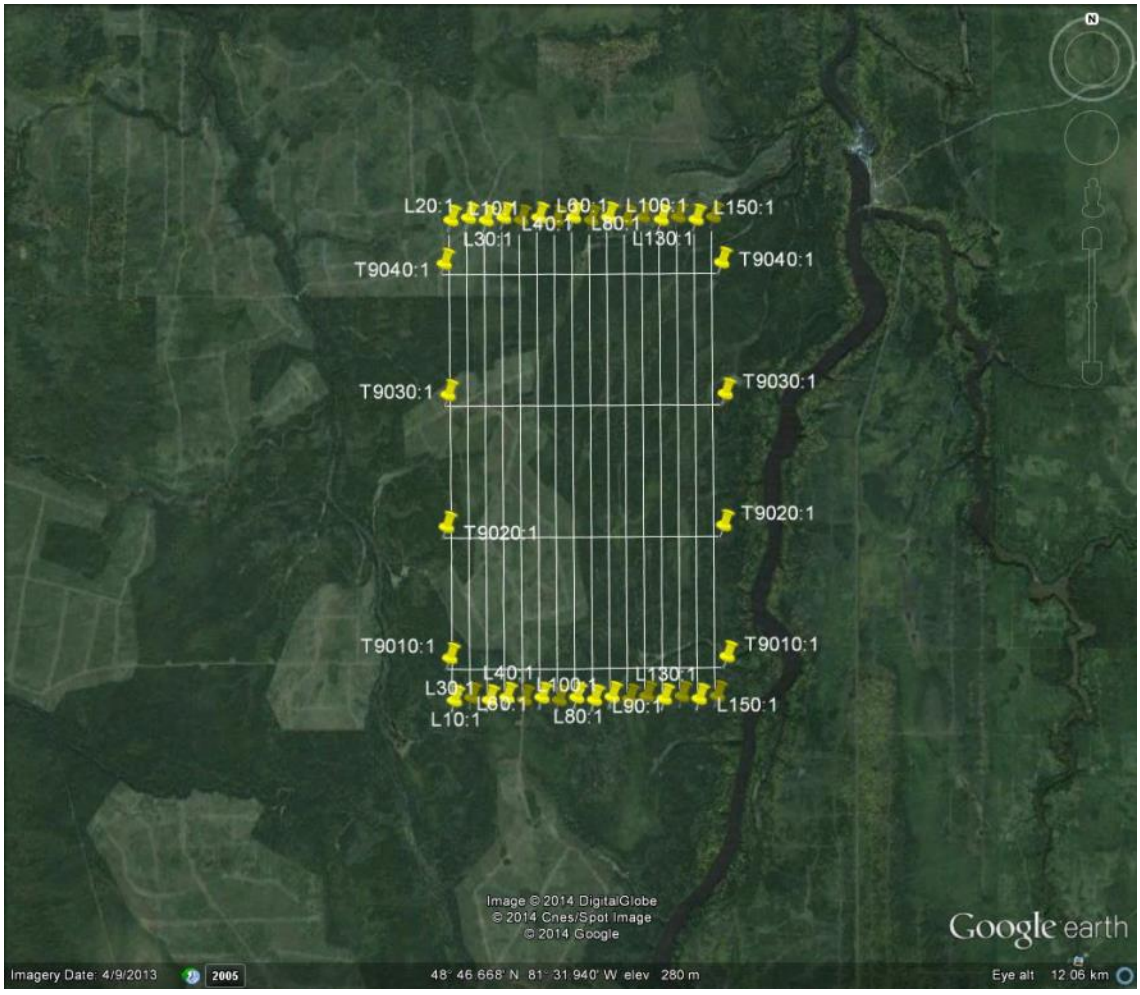

Figure L-2. Reid–Mahaffey Test lines on Google Earth™ (August 5, 2014).

Data acquired in Reid–Mahaffey was processed and presented in a Geosoft database and grids. Additional products include the selection of anomalies, resistivity-depth images (RDI) and apparent conductivity depth slices.

7.4.3. FULL WAVEFORM VTEM CALIBRATION

The calibration is performed with the completely assembled VTEM system connected to the helicopter at the survey site on the ground. Measurements of the half-cycles are collected and used to calculate a sensor calibration consisting of a single stacked half-cycle waveform. The purpose of the stacking is to attenuate natural and man-made magnetic signals, leaving only the response to the calibration signal. The stacked half-cycle allows the transfer functions between the receiver and data acquisition system, $H_D(\omega)$, and current sensor and data acquisition system, $H_R(\omega)$, to be determined. These transfer functions are used as a part of the system response correction during processing to correct the half-cycle waveforms and data acquired on a survey flight to a common transfer function:

$$D(\omega) = [H_C(\omega)/H_D(\omega)]\, D_R(\omega)$$

$$A(\omega) = [H_C(\omega)/H_R(\omega)]\, A_R(\omega)$$

where $H_C(\omega)$ is the common transfer function, and $D_R(\omega)$ and $A_R(\omega)$ are the FFT's of the raw receiver and current sensor responses recorded by the data acquisition system.

This process allows for the receiver response, $R(\omega)$, to become independent of the sensor characteristics determined by the transfer functions $H_D(\omega)$ and $H_R(\omega)$ and acts similar to a deconvolution of the data.

$$R(\omega) = \frac{D(\omega)I(\omega)}{A(\omega)}$$

where, $D(\omega)$ is the FFT of the actual receiver data sample $D(t)$, $I(\omega)$ is the FFT of a reference or "Ideal waveform" and $A(\omega)$ is the FFT of the actual waveform.

7.4.4. HIGH ALTITUDE CALIBRATION

The high altitude calibration is conducted on each survey flight. At the beginning and at the end of each flight the helicopter climbs at 1000 feet above ground to check the EM "zero level". When at the required altitude, at least 60 seconds of data were acquired in normal operation mode.

Reference transmitter current and receiver voltage waveforms, each sampled at 192 kHz, were also recorded at high altitude for all survey flights. The recorded waveforms were transformed into an ideal form, having zero current at the beginning of the off-time, by the Full Waveform calibration (see Full Waveform VTEM Calibration).

The final delivered dataset contains these processed windowed high altitude data for the one hundred and eight (108) survey flights in Geosoft database format (Appendix G). A graphical representation of a VTEM waveform is shown in Figure 5.

7.4.5. ALUMINIUM PLATE TEST

This test is performed on ground to verify the sensitivity of the system. An aluminium plate of known conductive response is positioned in alternated positions (vertical and horizontal) for about 10 seconds for 3 time measurements. Response of corresponding dB/dt and B-field data is then verified.

Result of the test performed on July 25, 2014 is presented in a Geosoft database view below. When the aluminum plate is horizontal with respect to the loop, measured signal will show positive response, indicating a proper polarity (*see* H1, H2, H3, H4 in Figure L-3).

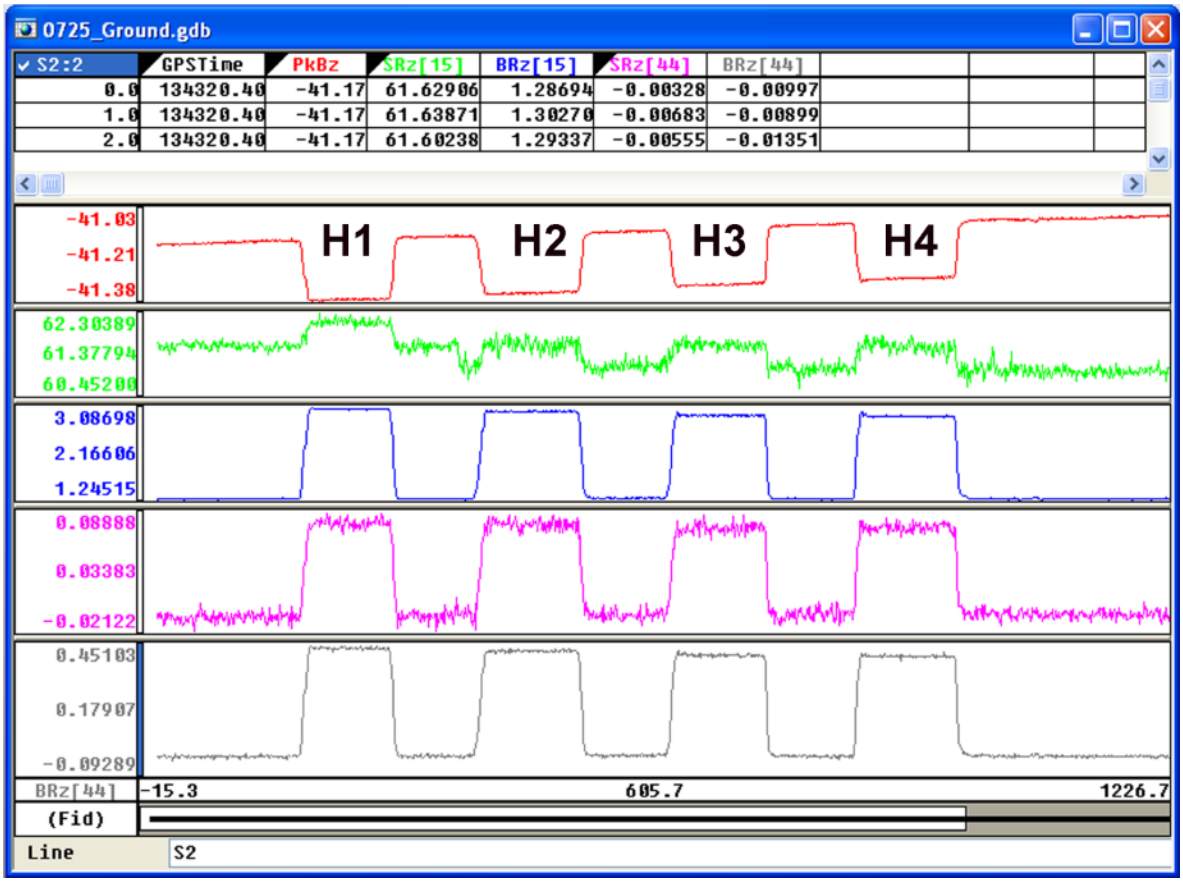

Figure L-3. Plate test results performed on July 25, 2014.

7.4.6. TEST LINES

Daily test lines were acquired to ensure that the airborne system is operating repeatability and as expected. Three test line locations were selected, two of them were flown in an east-west direction and one was flown in a north-south direction, as presented in figure below (Figure L-4).

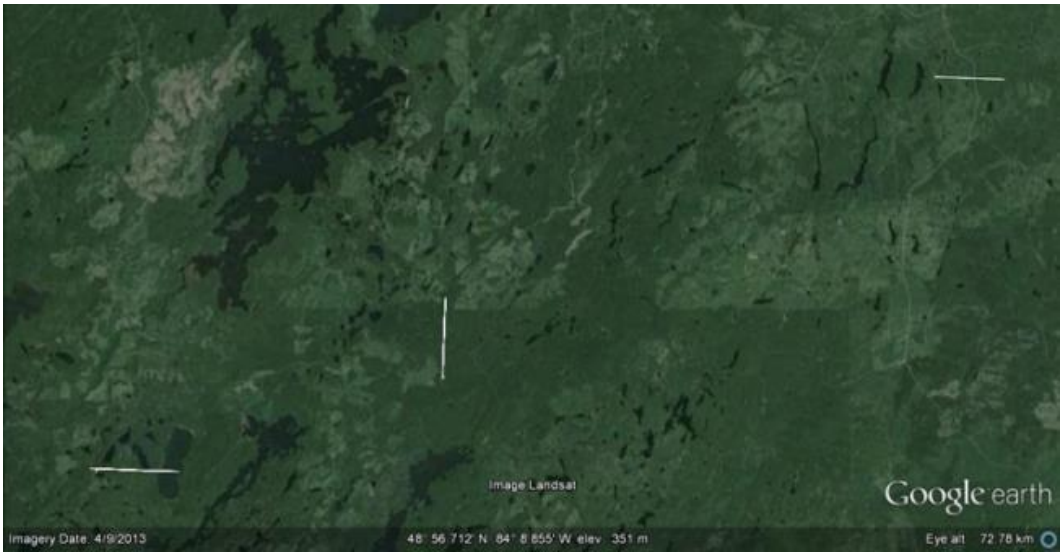

Figure L-4. Location of test lines flown in a daily basis.

7.4.7. RADAR ALTIMETER CALIBRATION TEST

The purpose of the radar altimeter calibration is to verify the performance of radar altimeter readings using the GPS elevation data as the reference.

The calibration is performed flying over the same spot at various altitudes, ranging from 85 m (283 feet) to 150 m (500 feet). The selected spot has known elevation and flat terrain. This test was performed on August 8, 2014 at the beginning of the survey (Figure L-4) and at the end of the survey on October 23, 2014.

As observed in the graphical results presented below, where the GPS elevations versus radar readings are plotted, the relationship between radar and GPS readings are linear, and the radar readings are very accurate (R^2~1.0), for the range of flying heights to be expected for the survey.

Radar checks were preformed once per day. These checks consisted of the ground crew communicating with the operator/pilot via radio when the tail of the system would leave the ground.

Nominal Altitude above ground (m)	Radar Altitude Raw Data (m)	DGPS Altitude Ellipsoidal Height (m)	DTM = DGPS - Radar Alt Ellipsoidal Height WGS84 (m)	DGPS Altitude (ALT) ALT=DGPS - AVERAGE(DTM) (m)
86.89	89.6	443	353.40	90.06
89.94	90.6	443.8	353.20	90.86
100.61	101	454.1	353.10	101.16
120.43	120.5	473	352.50	120.06
150.91	150.3	502.8	352.50	149.86

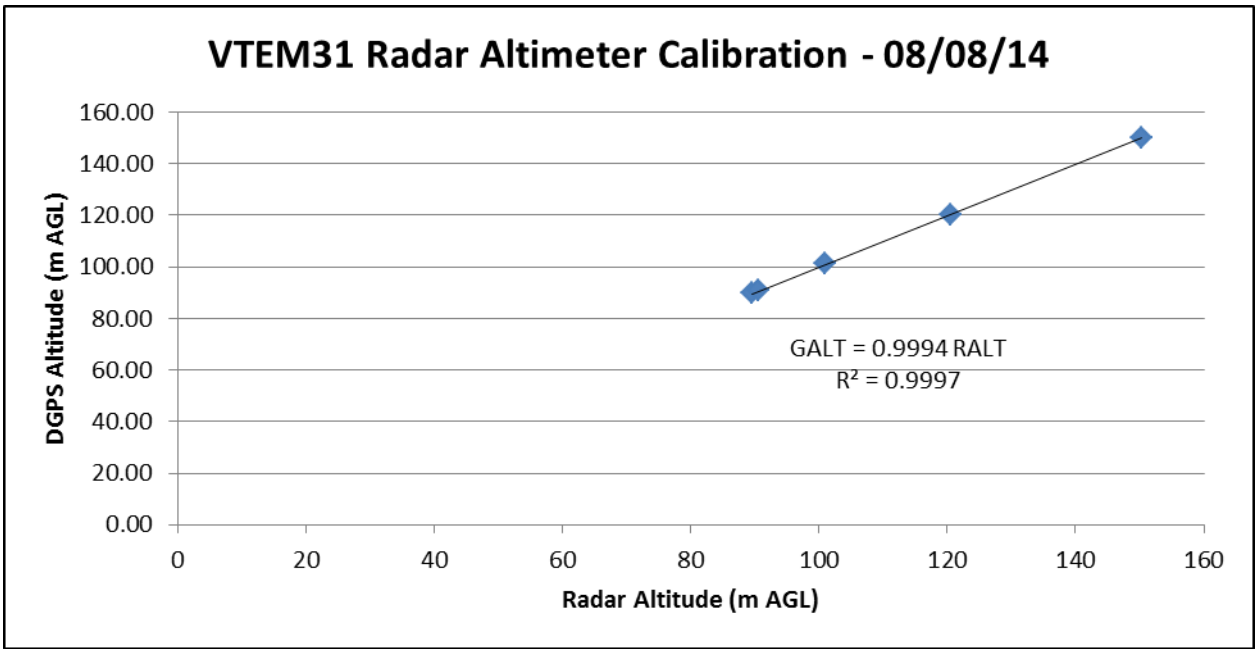

Figure L-5. Radar altimeter test results performed on August 8, 2014.

7.4.8. MAGNETOMETER CLOVERLEAF TESTS

Calibration flights are performed to verify the heading errors of the magnetometer in the 4 cardinal directions. The TDEM data is analyzed during this process as well to confirm data quality in terms of response to turns and varying wind conditions.

This test is performed once per month. Three tests were performed during this survey: August 9, September 14 and October 23, 2014 (Figures L-6 and L-7).

Test Date: August 9, 2014

Figure L-6. Flight path of Heading test performed on August 9, 2014.

Raw Heading Data (Mag channel is diurnally corrected and lagged)

	Direction	Line #	Fiducial	Mag
pass 1	90	90	10599.0	56456.6
	180	180	14784.0	56456.7
	270	270	7598.0	56456.6
	360	360	18131.0	56456.4
pass 2	90	90	10599.0	56456.6
	180	180	14784.0	56456.7
	270	270	7598.0	56456.6
	360	360	18131.0	56456.4

Heading Effect Coefficients

Direction	Heading Correction
90	-0.02
180	-0.13
270	-0.02
360	0.17

Heading corrected data

Direction	Line #	Fiducial	Mag Corr
90	90	10599.0	56456.6
180	180	14784.0	56456.6
270	270	7598.0	56456.6
360	360	18131.0	56456.6
90	90	10599.0	56456.6
180	180	14784.0	56456.6
270	270	7598.0	56456.6
360	360	18131.0	56456.6

Test Date: October 23, 2014

Figure L-7. Flight path of Heading test performed on October 23, 2014.

Raw Heading Data (Mag channel is diurnally corrected and lagged)

	Direction	Line #	Fiducial	Mag1
pass 1	90	90	53243.5	56460.3
	180	180	54083.4	56458.8
	270	270	52922.4	56460.8
	360	360	54414.4	56462.6
pass 2	90	90	53243.5	56460.3
	180	180	54083.4	56458.8
	270	270	52922.4	56460.8
	360	360	54414.4	56462.6

Heading Effect Coefficients

Direction	Heading Correction
90	0.30
180	1.84
270	-0.16
360	-1.97

Heading corrected data

Direction	Line #	Fiducial	Mag Corr
90	90	53243.5	56460.6
180	180	54083.4	56460.6
270	270	52922.4	56460.6
360	360	54414.4	56460.6
90	90	53243.5	56460.6
180	180	54083.4	56460.6
270	270	52922.4	56460.6
360	360	54414.4	56460.6